License 2005/16

Prospecting licence issued to NunaMinerals A/S

PGE Exploration in the Fiskefjord License,

Southern West Greenland, 2008

Compiled by:
Paul Armitage
Senior Geologist
NunaMinerals A/S
Issortarfimmut 1
P.O. Box 790
DK–3900 Nuuk
Greenland

24 March, 2009

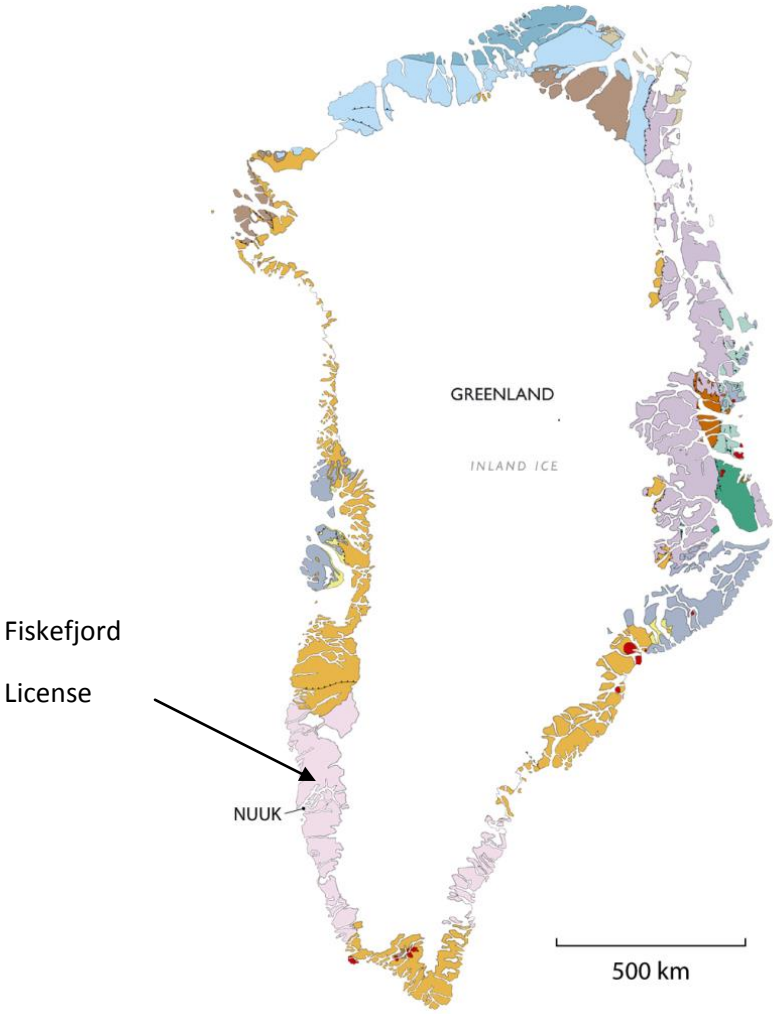

License no:	2005/16
Area:	Fiskefjord
Year:	2008
Field Period:	13.06.2008 – 19.06.2008
Operator:	NunaMinerals A/S

PGE exploration in the Fiskefjord licence, southern West Greenland, 2008

Compiled by:

Paul Armitage
Senior Geologist
NunaMinerals A/S
Issortarfimmut 1
P.O. Box 790
DK–3900 Nuuk
Greenland

24 March, 2009

CONTENTS

Introduction

NunaMinerals holds an exclusive exploration licence (no. 2005/16, with 100% ownership) covering an area of 824.25 km^2 in the Fiskefjord area. The Fiskefjord project was initiated in the summer of 2005, when limited sampling was carried out. Based on encouraging initial results the program was significantly expanded in 2006. The licence expires at the end of 2009.

Location

Fiskefjord is located in southern West Greenland, and the licence includes sub-areas north and south of the fjord (Fig. 1). Since January 2008, the Amikoq area that is situated mostly south of the fjord has been part of an Option Agreement between NunaMinerals and Impala Platinum Holdings Ltd. Exploration at Amikoq in 2008 is reported separately (Armitage 2009 and later status reports).

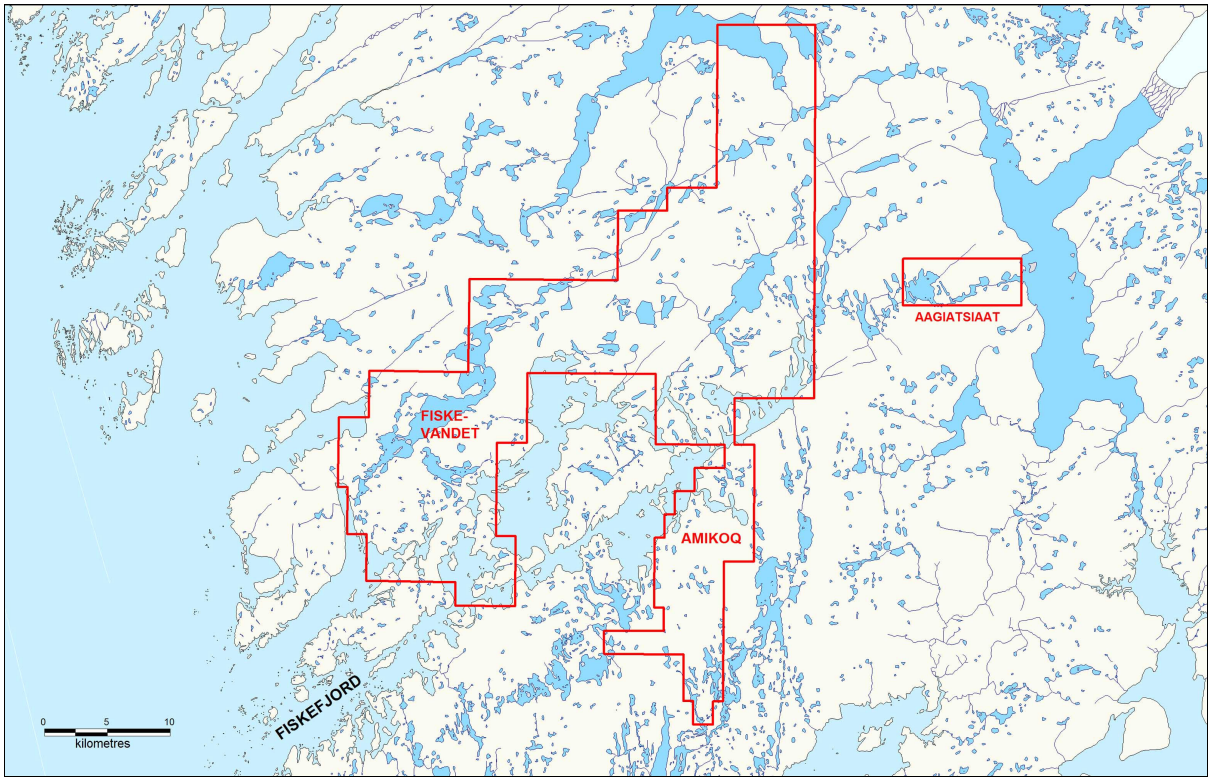

Fig. 1. Map of the Fiskefjord licence (no. 2005/16) naming the main sub-areas.

Physiography and climate

The terrain of Fiskefjord is a mixture of gently undulating lowland and rolling hills. Towards the northeast, the hills rise up to 400 m above sea level with an average elevation of about 200 m. Except for a few steep cliffs, particularly where the land meets Fiskefjord, the area is accessible on foot. Geological structures are very conspicuous from the air or viewed from elevated positions, with generally good bedrock exposure. East of Amikoq, a north-south lineament marks a transition to a mountain range to the east with elevations of up to 700 m.

The climate is moderate Arctic with a mean temperature of +7^{o}C in July and -7^{o}C in February. In most areas of Fiskefjord, the flora is limited to lowland tundra and consists of mosses, grasses and low scrub. On the north shores of Fiskefjord, small areas sheltered from the wind with favourable sun conditions are remarkably fertile with dense vegetation and larger bushes.

Fieldwork was carried out in the periods 14–19 June and 4th September. The weather was bright and dry on all but one of the days and allowed a satisfactory amount of fieldwork to be carried out.

Accessibility

Amikoq and much of Fiskefjord is accessed from Nuuk by helicopter (*c.* 30 minutes) or by boat from Nuuk or Atammik at the mouth of Fiskefjord. Daily flights link Nuuk with Kangerlussuaq, one of two international airports. Flights between Kangerlussuaq and Copenhagen (Denmark) operate daily in the summer months and 5 times a week during winter. During the summer, there are 3 weekly flights from Copenhagen to Narsarsuaq in South Greenland and from there flights connect to Nuuk. There are also 3 weekly flights direct from Reykjavik (Iceland) to Nuuk between May and September. The former route from Baltimore (USA) to Kangerlussuaq has been suspended.

The mouth of Fiskefjord is located along the coast of West Greenland *c.* 70 km north of Nuuk. Fiskefjord extends for *c.* 50 km inland and can be navigated by ocean-going ships for much of its length. Nuuk is the capital of Greenland and is also the largest town with *c.* 15,000 inhabitants and a modern harbour, which is open and ice-free all year round. In 2005, the Seqi olivine mine opened on the north shore of Fiskefjord, operated by the Swedish company Minelco A/S. This is a low-cost open pit mine close to the shore of the fjord, allowing a deep port that accommodates ships of unlimited size (Fig. 2).

Fig. 2. Seqi olivine mine on the north shore of Fiskefjord, with immediate access to a deep water port.

Aims

Historical data indicate the potential for platinum group element (PGE) mineralisation in the Fiskefjord area. Whole rock samples have returned up to 4.5 g/t combined platinum and palladium. The results of fieldwork conducted in 2005 and 2006 supported the historical data. A few samples from 2005 were analysed for all PGE metals and were shown to be enriched in all PGE including rhodium. One or more layered mafic to ultramafic complexes have been identified in the region (e.g. Garde 1997) and previous work has also indicated a potential for economic deposits of nickel and tungsten. Where mafic/ultramafic dykes transgress mafic-ultramafic country rocks, there is a PGE potential analogous to deposits such as Voisey's Bay in Labrador, Canada.

The northern part of the licence is underexplored and considered prospective for Cu and Ni. The main purpose of the 2008 field season is to follow up the historical exploration along mafic/ultramafic dykes in the Fiskevandet area and begin more detailed exploration of the Miaggoq intrusion.

Fieldwork

Fieldwork was carried out in 3 areas within the Fiskefjord licence: Fiskevandet South, Fiskevandet North, and Miaggoq (east of Fiskevandet). One flight camp were established near an NNE-SSW striking ultramafic dyke at Fiskevandet South, and another camp near a similar dyke at Fiskevandet North (Fig. 3). These may be continuations of the same dyke. Prospecting in the period 14-19 June involved rock and sediment sampling of dyke rocks and associated ultramafic country rocks that potentially host PGE mineralisation. At Miaggoq, a sequence of mafic and ultramafic intrusive rocks occurs. Fieldwork here was carried out for only a few hours on 4th September, and involved mapping the extent of the intrusive rocks and collecting *in situ* rock samples.

Personnel

The personnel working in the licence in 2008 are named in Table 1. Daily safety procedures are set out in the NunaMinerals field manual, which is updated annually prior to the field season. The manual covers common procedures such as helicopter approach and signalling, regular VHF radio communications between field personnel, and daily safety calls by satellite telephone to basecamp or NunaMinerals HQ.

Table 1. Field personnel in the Fiskefjord licence (excluding Amikoq) in 2008.

Name	**Position**	**Company**	**Field Period(s) (day/month)**
Claus Østergaard	Senior geologist	NunaMinerals	13/6-19/6
Paul Armitage	Senior geologist	NunaMinerals	14/6-18/6, 04/9
Niels Glahn-Berthelsen	Junior geologist	NunaMinerals	13/6-19/6
Mimmi Nilsson	Junior geologist	NunaMinerals	13/6-19/6
Jakob Kløve Jakobsen	Geologist	NunaMinerals	14/6-18/6
Hans Jakob Frederiksen	Assistant	NunaMinerals	13/6-19/6
Malik Ljungdahl	Assistant	NunaMinerals	13/6-19/6
Flint Heilmann	Assistant	NunaMinerals	14/6-18/6
James Thomsen	Assistant	NunaMinerals	14/6-18/6

Camp positions

Below are the camp positions in long/lat decimal degrees (see also Fig. 3).

Camp 1: 51.91985 W 64.92086 N (Fiskevandet South)
Personnel: Claus Østergaard, Niels Glahn-Berthelsen, Mimmi Nilsson, Hans Jakob Frederiksen, Malik Ljungdahl.

Camp 2: 51.87793 W 64.98696 N (Fiskevandet North)
Personnel: Paul Armitage, Jakob Kløve Jakobsen, Flint Heilmann, James Thomsen.

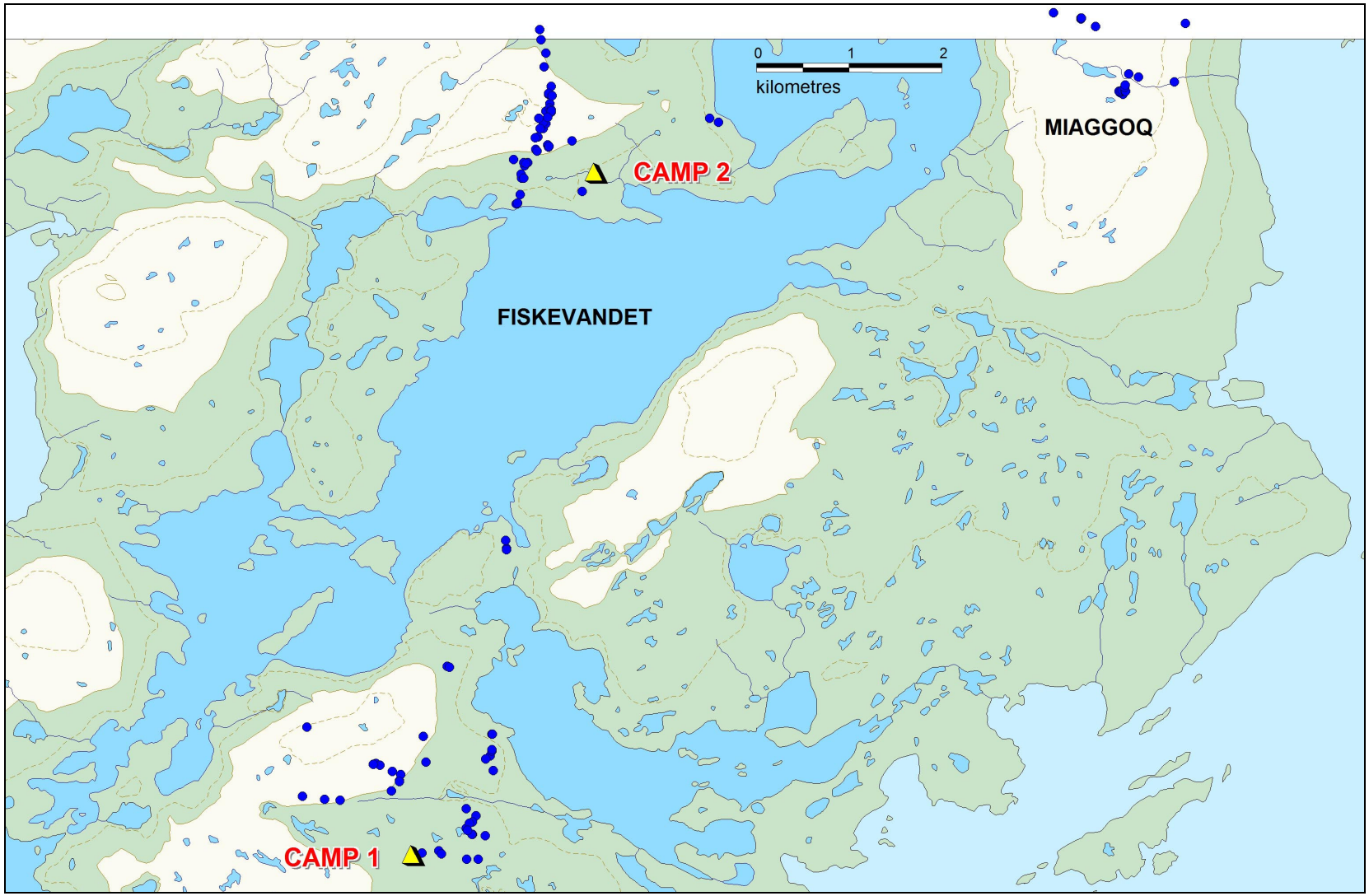

Fig. 3. Topographic map of Fiskevandet area (contour interval 50 m) showing location of camps (yellow triangles) and sample positions (blue circles). Note that a thin strip of the adjoining map sheet is missing at the top of the figure.

Laboratory methodology

ActLabs

All samples were analysed at the ActLabs laboratory housed within the NunaMinerals headquarters in Nuuk. Samples were dried at 60^{o}C and crushed, split and pulped in a tungsten carbide pulveriser to 85% passing 75μm. The pulps were analysed for Pt, Pd and Au concentrations by PbS fire assay with an ICP-OES finish. Detection limits were: Pt 5 ppb, Pd 4 ppb and Au 2 ppb. For most samples, the concentrations of 37 major and trace elements were determined by Aqua regia digestion with an ICP-OES finish. The positional and descriptive data for samples are given in Appendix 1 and the geochemical data in Appendix 2.

Cardiff University

A number of samples were analyses for major, trace and rare earth elements by Dr Iain McDonald of Cardiff University, as part of a regional comparative study involving samples from several locations in the Fiskefjord area, particularly the Amikoq prospect. The raw data are presented in Appendix 3 and the analyses are addressed in relevant sections of this report.

Bulk analysis for major element and trace elements was carried out using a JY Horiba Ultima 2 inductively coupled plasma optical emission spectrometer (ICP-OES) and Thermo X7 series inductively coupled plasma mass spectrometer (ICP-MS). Samples were first ignited at 900^{o}C to determine loss on ignition and then fused with Li metaborate on a Claisse Fluxy automated fusion system to produce a melt that could be dissolved in 2% HNO_3 for analysis. Full details of the standard ICP analysis procedures and the instrumental parameters are given in McDonald & Viljoen (2006).

Regional geology

The Amikoq intrusion in the Fiskefjord area is part of the Akia tectono-stratigraphic terrane. The accretion and evolution of this high grade grey gneiss-amphibolite complex has been comprehensively researched by Garde (1997), and relevant parts of his report are reproduced in this section. Areas referred to are shown in Fig. 4.

To date, the Nuuk region has been subdivided into six different Archaean terranes, amalgamated in the period *c.* 2950 to 2700 Ma (Hollis *et al.* 2004). In order of decreasing antiquity these are the Isukasia and Færingehavn (*c.* 3850 to 3300 Ma), Akia (*c.* 3200 to 2975 Ma), Kapisillit (*c.* 3075 to 2960 Ma), Tasiusarsuaq (*c.* 3000 to 2800 Ma) and Tre Brødre (*c.* 2826 to 2750 Ma). The Akia terrane is located north of the Akulleq terrane which in turn lies to the north of the Tasiusarsuaq terrane (Fig. 5).

The Akia terrane is the largest of several tectono-stratigraphic terranes in the Nuuk region and has undergone a complex history of volcanic and plutonic igneous activity, deformation and metamorphism (e.g. Berthelsen 1960; Taylor *et al.* 1980; Wells 1980; Riciputi *et al.* 1990; McGregor *et al.* 1991; Garde 1997, and references therein). The terrane comprises two continental crustal complexes: a dioritic core dated at *c.* 3220 Ma that forms most of the Akia peninsula (Fig. 1), and a larger block dated at 3.05-2.97 Ga, mainly tonalitic orthogneiss with enclaves of supracrustal rocks between Fiskefjord and Nuuk Fjord (formerly known as Godthåbsfjord) and farther north. The bulk of the orthogneisses consist of tonalite that was intruded into, or was tectonically intercalated with supracrustal rocks and associated mafic intrusive complexes. The supracrustal rocks between Fiskefjord and Nuuk Fjord are older than *c.* 3.05 Ga (the age of the oldest orthogneisses that intrude them). They consist largely of heterogeneous, compositionally banded metavolcanic amphibolite, and metagabbroic and ultramafic rocks that represent disrupted layered intrusive complexes including olivine-rich cumulate rocks. Garde (1997) also reported local leucocratic amphibolite of andesitic affinity. The supracrustal rocks were interpreted as remnants of oceanic crust, into which the precursors of the orthogneisses were intruded, presumably in a convergent plate-tectonic setting (Garde 1990, 1997; Garde *et al.* 2000). Komatiites or other plume-related supracrustal lithologies have not been reported from the Akia terrane (Garde 2007).

Intense deformation and metamorphism accompanied the 3000 Ma magmatic accretion. Thrusts along amphibolite-orthogneiss contacts were succeeded by large recumbent isoclines, upright to overturned folds,

and local domes with granitic cores. Syntectonic granulite facies metamorphism is thought to be due to heat accumulation by repeated injection of tonalitic magma. Strong ductile deformation produced steep linear belts before the thermal maximum ceases, whereby folds were reoriented into upright south-plunging isoclines. Two large tonalite-trondhjemite-granodiorite (TTG) complexes were then emplaced, followed by granodiorite and granite.

Post-kinematic diorite plugs with unusually high MgO, Cr and Ni, and low LIL and immobile incompatible element contents, terminated the 3000 Ma accretion. Hybrid border zones and orbicular textures suggest rapid crystallisation from superheated magma. The diorites most likely formed from ultramafic magma contaminated with continental crust.

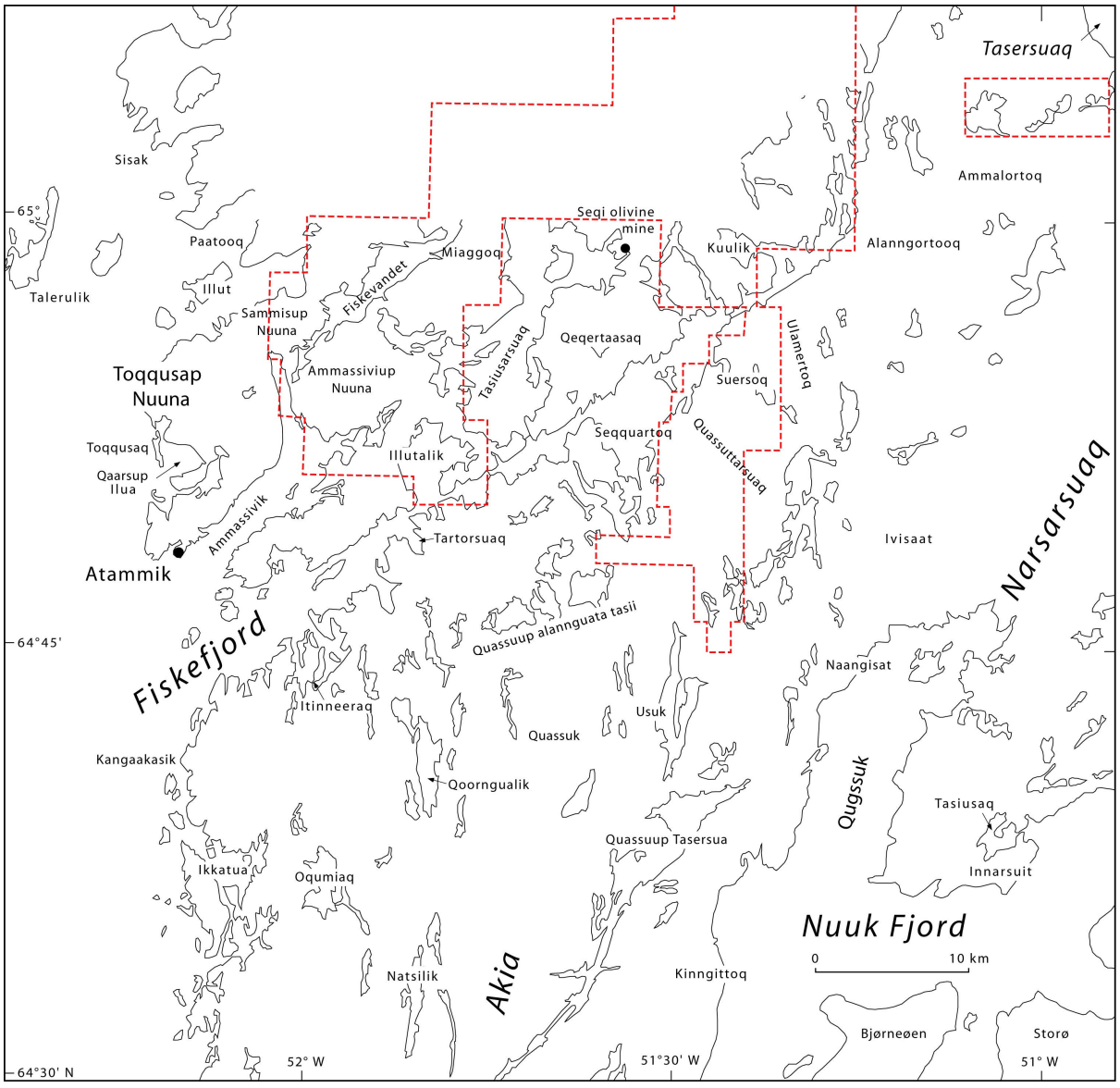

Fig. 4. Outline map of the Fiskefjord area showing place names referred to in the text (modified from Garde 1997). The Fiskefjord licence area is demarcated by a stippled red border. The northernmost part is outside the map area.

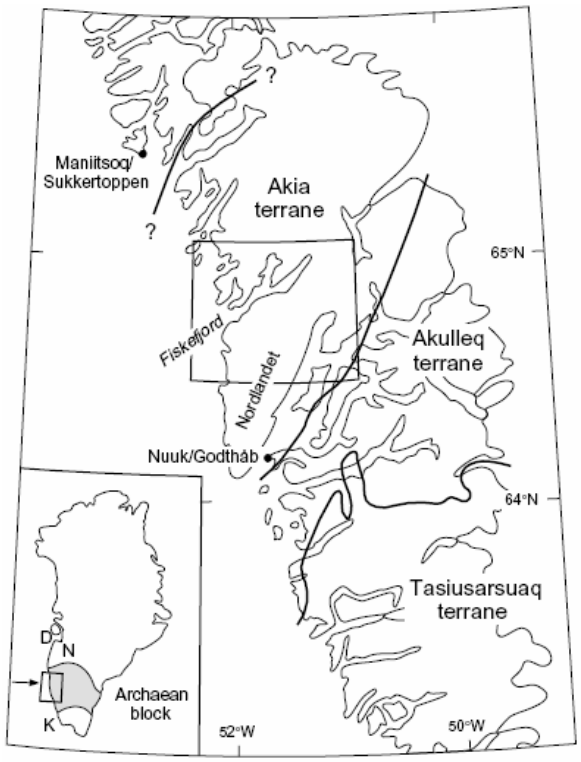

Fig. 5. Positions of three Archaean tectonostratigraphic terranes: Akia, Akulleq and Tasiusarquaq in the northern part of the Archaean block of southern West Greenland (inset map), with frame showing locations of the Fiskefjord area in the southern part of the Akia terrane. D = Disko Bugt. N and F mark the position of the Proterozoic Nagssugtoqidian and Ketilidian orogens.

Widespread high-grade retrogression preserved a granulite facies core in the southwest of the Akia terrane. To the east, the retrogressed gneiss grades into amphibolite facies gneiss unaffected by granulite facies metamorphism and retrogression. LIL elements were depleted during granulite facies metamorphism and reintroduced during retrogression, probably transported in anatectic silicate melts and in fluids. Rb-Sr isotope data, and relationships between retrogression, high-strain zones and granite emplacement, show that retrogression took place shortly after the granulite facies metamorphism, before terrain assembly at *c.* 2720 Ma, probably by movement of melts and fluids into the upper, marginal zone of granulite facies rocks from deeper crust still being dehydrated. Retrogression during Late Archaean terrane assembly was in narrow reactivated zones of ductile deformation. In the Proterozoic, it occurred with faulting and dyke emplacement.

Layered complexes with stratiform ultrabasic and noritic rocks

Two large layered complexes consisting of ultrabasic, noritic and metagabbroic rocks are embedded within supracrustal rocks. One complex, defining the Amikoq prospect, extends for *c.* 25 km in a N–S direction across central Fiskefjord, from west/southwest of Quassuttarsuaq through Suersoq and northwards to the embayment Kuulik (Fig. 4, Fig. 6). Another occurs at Sammisup Nunaa, northeast of Toqqusap Nunaa, and another at Miaggoq, east of Fiskevandet. These km-scale bodies of ultrabasic rocks may be fragments of larger layered complexes. During a day's reconnaissance at Miaggoq, the present author found the igneous sequence to be identical to Amikoq.

The Amikoq complex consists of elongate lenses and layers of olivine-rich ultrabasic rocks which either pass laterally or grade upwards into norite, which in turn is overlain by homogeneous amphibolite. The ultrabasic and noritic rocks together form discontinuous, 10–50 m (locally *c.* 150 m) thick sheets along the base of a major unit of massive, homogeneous amphibolite. This amphibolite outlines an elongate, doubly plunging synform with a southern closure south of Quassuttarsuaq and a northern closure north of Suersoq and at Kuulik. The ultrabasic and noritic rocks occur both along the flanks and in the two hinge zones of this fold. The longest noritic sheet can be traced for at least 15 km.

Most of the exposed lower boundary of the layered complex comprises intrusive or tectonic contacts with grey orthogneiss, and both the orthogneiss and ultrabasic-noritic rocks are often appreciably deformed along them. In places, a *c.* 10 m thick layer of flaggy, strongly schistose, biotite and garnet-rich pelitic sediment occurs along the lower contact of the layered complex (Garde 1997; note: this protolith interpretation is questioned

later in the present report). Bengaard (1988) observed little-deformed norite cutting compositional banding in the metasediments, suggesting an intrusive relationship (note: this is another observation that is questioned). At Suersoq, steep isoclinal folds occur in the layered complex and adjacent supracrustal rocks, including thin horizons of 'infolded' metasediments. These folds pre-date the emplacement of the surrounding orthogneiss.

In the field the norite typically occurs as a sugary, light grey, generally homogeneous rock, but igneous layering consisting of metre-thick orthopyroxene-rich horizons alternating with norite has also been noted. Whereas contacts between dunitic and noritic rocks are sharp or gradational over less than *c.* 5 m, the boundaries between the noritic rocks and overlying homogeneous amphibolite is typically very gradual, with transitions over several tens of metres marked by increasing hornblende (Garde 1997; note: the present report documents conflicting evidence, but it is local evidence and does not rule out a gradual, possibly tectonised, contact elsewhere).

The norite has metamorphic textures. Orthopyroxene mostly forms equidimensional, *c.* 2–5 mm anhedral grains, commonly replaced by up to 1–2 mm green hornblende in rounded embayments. Matrix calcic plagioclase (about An_{75}) forms large anhedral grains up to 10 mm with frequent tiny hornblende inclusions. Metamorphic equilibrium is suggested by common triple junctions between plagioclase, orthopyroxene or hornblende, and by the absence of mineral zoning.

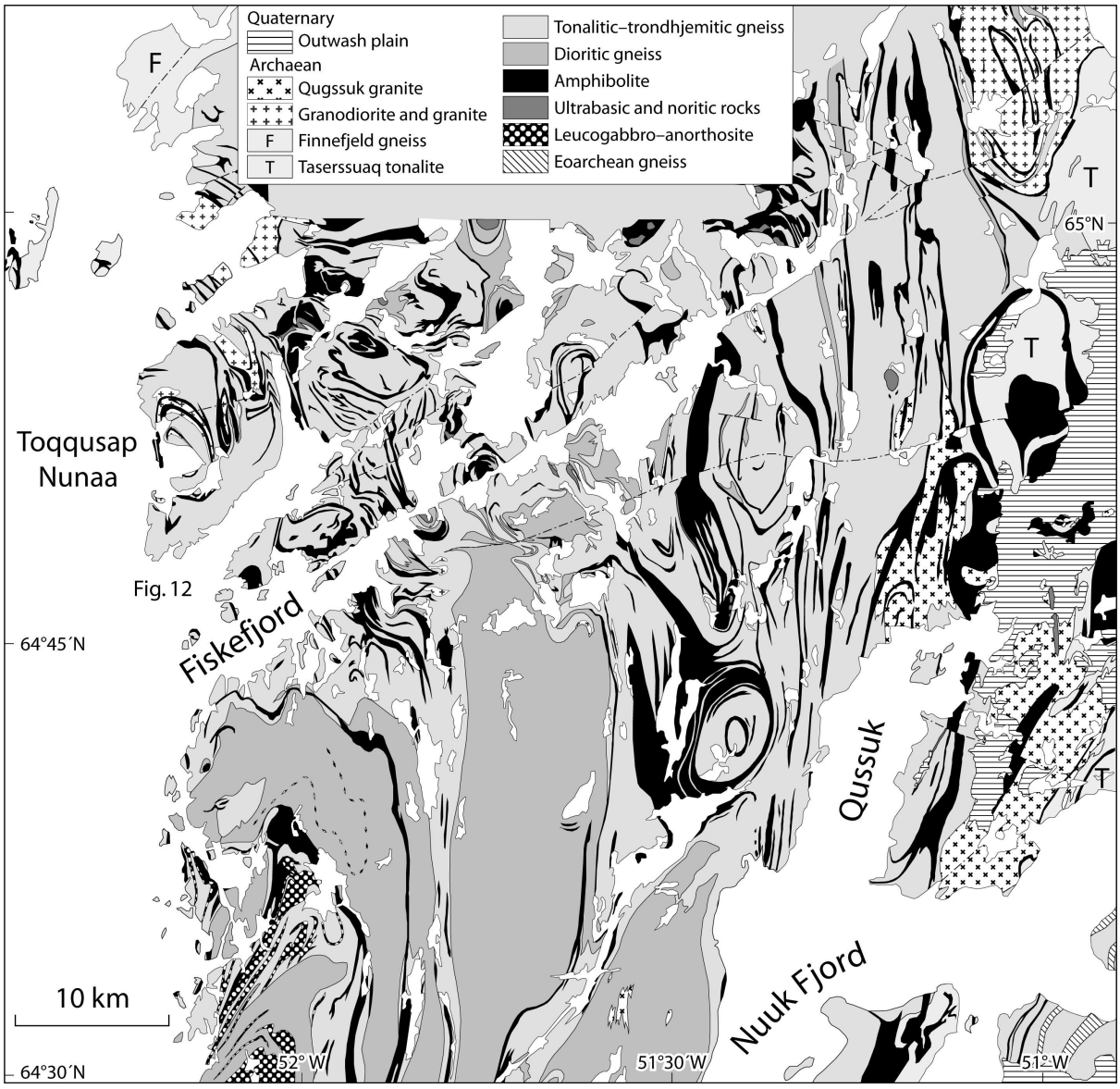

Fig. 6. Simplified geological map of the Fiskefjord region, southern West Greenland (modified from Garde 1997).

The deformed margins of the noritic bodies contain a distinct schistosity. Elongate, poikiloblastic orthopyroxene crystals up to 10 mm, intergrown with hornblende and subordinate pale brown phlogopite, are oriented parallel to schistosity and surrounded by a mosaic of equant to elongate plagioclase grains. The orthopyroxene grains are commonly composite, consisting of smaller lensoid domains with slightly different optical orientations.

Origin of the ultrabasic and noritic rocks

All the larger ultrabasic bodies in the Fiskefjord area predominantly consist of granular, medium-grained, olivine-rich, locally chromite-bearing dunitic rocks, in which magmatic layering and orthocumulus textures are fairly common features. There is a common association with noritic cumulates and, at Quassuttarsuaq, there is a thick overlying sequence of homogeneous amphibolite. Despite strong deformation and flattening which has disrupted the ultrabasic bodies (e.g. south and west of Quassuttarsuaq) some of them retain thicknesses in the order of 1 km. The available observations from the Fiskefjord area suggest that the large ultrabasic bodies are cumulate rocks that were formed at the bases of large magma chambers (Garde 1997).

Plate tectonic scenario of the Fiskefjord area

Around central and outer Fiskefjord, interleaved supracrustal rocks and grey orthogneiss define well-exposed interference patterns between two or three sets of superimposed folds. In other parts of the area, interference patterns have been modified by prominent younger, N–S trending high strain zones, and by domes with cores of younger granites. Those parts of the area underlain by the Tasersuaq tonalite and Finnefjeld gneiss complexes have not been subject to strong penetrative deformation.

The structural elements in the Fiskefjord area may be representative of the entire Akia terrane. The northwestern, northeastern and southeastern parts of the area are all characterised by complex, multiply folded outcrop patterns, frequent changes in the orientation of structural elements, and structures up to *c.* 10 km in size (Berthelsen 1960; Lauerma 1964; Garde 1986; Garde *et al.* 1987). These structures appear to have formed during the early phases of the *c.* 3000 Ma continental crustal accretion. The central and southern parts are dominated by somewhat larger structures in the lithologically very homogeneous, granulite facies areas of *c.* 3220 Ma Nordlandet dioritic gneiss.

Several other tracts are characterised by prominent, N–S trending structures with distinct steeply dipping schistosity, subhorizontal linear elements and large isoclinal folds. Some of these N–S trending high strain zones occur along the margins of dioritic gneiss units in the southern part of the area. Another, major high strain zone follows the west coast of inner Nuuk Fjord and continues northwards through the head of Fiskefjord. This is the Qussuk-Ulamertoq zone, and was established before or during the *c.* 3000 Ma granulite facies event.

This and related N–S trending structures are believed to have formed principally in response to E–W compression. Subhorizontal elongation is indicated by the common mineral lineation and shallow south-plunging fold axes. It is possible that this elongation was also related to a transcurrent component, but no direct evidence for this has been observed.

McGregor *et al.* (1991) and McGregor (1993) suggested that the high-strain zone along the western part of outer Nuuk Fjord and Nuuk town is continuous with the Qussuk-Ulamertoq zone, and that both developed after the assembly of the Akia and Akulleq terranes at approx. 2700 Ma. While the Qussuk-Ulamertoq zone appears to have been reactivated in connection with the terrane assembly, the available field evidence suggests that it came into existence at approx. 3000 Ma under granulite facies metamorphic conditions.

Several dome shaped structures developed late in the structural evolution. Most have cores of leucocratic tonalite, trondhjemite or granite. Lauerma (1964) described the almost 10 km wide Ipernat dome west of Naangisat, and Berthelsen (1950) mapped a smaller dome around Qaarsup Ilua in the western part of Toqqusap Nunaa. Other domes or partial domes with cores of leucocratic orthogneiss occur at Qeqertaasaq, south of Quassuup Tasersua, at Quassuttarsuaq, and north of Narsarsuaq. The Igaanaanguit granodiorite forms a *c.* 20 km long, NNE-trending composite dome *c.* 10 km northeast of the head of Fiskefjord.

The field relations, compositions, ages and structural evolution of most orthogneiss and related rock units in the Fiskefjord area are compatible with and suggestive of a convergent plate-tectonic environment. These rocks (tonalitic-trondhjemitic grey gneiss and tonalite complexes) have compositions which are consistent with an origin from subducted oceanic crust by melting of hydrated basaltic rocks and modified by subsequent crystal fractionation in the lower crust; mantle components are only likely to have been directly involved in the genesis of the Nordlandet dioritic gneiss and the Qeqertaasaq diorite precursors, but in different ways.

The early structures in the grey gneiss, subhorizontal(?) thrusts and two or several phases of recumbent isoclinal folds, would comply with conditions formed by lateral stress fields which might be expected in progressively deeper levels of a convergent plate margin. Possible directions of plate motion and subduction would be broadly east-west during the two main phases of deformation (Smalledal and Paakitsoq phases). The succeeding emplacement of large dome-shaped plutonic complexes and development of vertical structures, broadly contemporaneously with and succeeding the peak of metamorphism, may have been achieved at a stage when subduction was ceasing, the production of new continental crust had culminated, and the accumulation of heat in the middle part of the new crust reached its maximum and declined.

Remobilisation of part of the earlier formed orthogneisses and emplacement of localised granitic rocks then took place, perhaps associated with contemporary redistribution of mobile elements in the deeper part of the crust. The narrow linear high-strain zones with horizontal structures, which comprise a long-lived structural element in the evolution of the Fiskefjord area, may have developed in response to a gradual change from convergence of the inferred plates to transcurrent motion along an approximately north-south path where the crust was still sufficiently ductile.

The intrusion of post-kinematic diorite plugs is not interpreted as directly related to plate-tectonic processes but was more likely due to subsequent underplating by ultramafic magma and apparently linked to the formation of the norite belt in the adjacent area to the north.

While the plate-tectonic scenario outlined above for the orthogneisses in the Fiskefjord area and their structural evolution is in part based on positive evidence (especially referring to the geochemistry of the TTG suites), the origin of the supracrustal association is much more speculative. The heterogeneous and homogeneous amphibolites, partially preserved layered noritic-ultrabasic rocks, and sporadic metasediments may represent fragments of one or more ophiolite sequences, but remnants of a sheeted dyke complex have not been identified, and cherty layers are so far not known. There may have been more than one group, separated in time by the accretion of the Nordlandet dioritic gneiss. Further, it has not been firmly established how much of the homogeneous amphibolite has been derived from extrusive volcanic rocks, subvolcanic sills, sheeted dyke complexes, layered complexes, or combinations of these possibilities.

The homogeneous amphibolite was probably chemically altered during or after its emplacement, but important geochemical similarities with better preserved Archaean tholeiitic metabasalts from neighbouring regions can still be recognised. However, even the origin of the latter rocks has not been proven – partly because of their likely contamination and metasomatic alteration, and partly because the detailed composition of a hypothetical Archaean MORB is not known. Nevertheless, Garde (1997) favours the opinion that the supracrustal rocks in the Fiskefjord area represent relict oceanic crust, due to: (a) the fact that no basement of continental crust has been identified (coupled with widespread evidence that the supracrustal rocks have been intruded by the orthogneiss precursors); and (2) the nature and in particular great scarcity of metasediments.

The simple plate-tectonic model presented above requires that early intrusions of orthogneiss precursors would have to be emplaced into oceanic crust. Xenoliths and fragments of mafic supracrustal rocks are actually present both in dioritic and tonalitic grey gneiss, but the picture is complicated by the fact that some of the dioritic gneiss represents an earlier continental nucleus. Furthermore, in the absence of age determinations of the supracrustal units, still more complicated tectonic scenarios could easily be advanced.

Terrane assembly

The Archaean crust in the Nuuk Fjord region consists of several terranes with different ages, lithologies and tectonic and metamorphic histories (Friend *et al.* 1988a). The Akia and Akulleq terranes and their common tectonic boundary were first described by Friend *et al.* (1988b). Their assembly is the latest Archaean event

known to have affected the Akia terrane. The Ivinnguit fault that forms the terrane boundary is a NE-trending, subvertical to moderately WNW-dipping, 10–15 m thick mylonite zone.

The timing of the terrane assembly is poorly constrained but occurred in the interval between approx. 2800 Ma (age of the Ikkatoq gneisses in the Akulleq terrane which are cut by the Ivinnguit fault) and approx. 2720 Ma (ages of granite sheets that cut several terrane boundaries: McGregor *et al.* 1991; Friend *et al.* 1996). However, no such sheets/dykes have so far been observed in the Fiskefjord area, and it is uncertain how far the effects of the terrane assembly can be traced northwest of the terrane boundary itself.

McGregor *et al.* (1991) and McGregor (1993) described a NNE–SSW zone of strong ductile deformation continuous with the Qussuk-Ulamertoq high strain zone along western Nuuk Fjord, which according to these authors postdates the juxtaposition of the Akia and Akulleq terranes. However, as discussed above, at least the Qussuk-Ulamertoq zone itself was established prior to the assembly of the two terranes.

Granulite facies metamorphism and retrogression

Granulite facies metamorphism extends over the southwestern part of the Akia terrane, including Nordlandet and a large part of the Fiskefjord area, whereas the easternmost part of the Fiskefjord area (and of the Akia terrane) consists of upper amphibolite facies rocks that have not experienced granulite facies metamorphism. Large tracts between these two areas are variably retrogressed. Whole-rock Pb-Pb ages of 3000 $\pm$ 70 Ma (Taylor *et al.* 1980) and 3112 $\pm$ 40 Ma (Garde 1989a) obtained from orthogneiss in Nordlandet and the eastern part of the Fiskefjord area have been interpreted to date the granulite facies metamorphism. A 2999 $\pm$ 4 Ma SHRIMP age of metamorphic zircon overgrowth in a garnet-sillimanite bearing metasediments from Nordlandet just south of the Fiskefjord area (Friend & Nutman 1994) firmly establishes that the peak of granulite facies metamorphism occurred at approx. 3000 Ma, i.e. it culminated during or just after emplacement of the main phase of grey tonalitic-trondhjemitic gneiss. SHRIMP zircon data from Nordlandet dioritic gneiss suggest that this unit experienced an earlier thermal event at approx. 3180 Ma. The approx. 3000 Ma granulite facies metamorphism outlasted two phases of isoclinal folding and a phase of upright, more open folding named the Paakitsoq phase by Berthelsen (1960) in the western and central parts of the Fiskefjord area. Granulite facies metamorphism appears to have overlapped with doming, and was succeeded by localised ductile deformation and emplacement of small granodiorite and granite plutons and granite sheets in the northern and eastern parts of the area.

Physical conditions of metamorphism

According to Pillar (1985) and Riciputi *et al.* (1990) granulite facies metamorphism took place without free fluids, and fluid inclusion data from grey gneiss in the Fiskefjord area seem to support this (Garde 1990). However, some aspects of the granulite facies rocks may be ascribed to fluid activity during the granulite facies event, for instance hornblende-bearing mafic pegmatites on Nordlandet in which 'high-grade' hornblende partially replaces orthopyroxene (McGregor *et al.* 1986; McGregor 1993). Further, the geochemistry of granulite facies biotite may suggest the presence of metamorphic fluids (Garde 1997).

Phases of metamorphism

Dymek (1978, 1984) studied metamorphism of supracrustal rocks from several parts of the Nuuk Fjord region and described a regional upper amphibolite to hornblende granulite facies metamorphic event *M1* and a regional retrogressive event *M2*, the latter within the stability field of kyanite. Although his study was carried out before it was recognised that the Nuuk Fjord region consists of several terranes with different magmatic, tectonic and metamorphic histories, his observations regarding the *M2* metamorphic phase are pertinent to the Fiskefjord area. Dymek (1978, 1984) noted that the *M2* event was very variably developed within a given outcrop or even within a single thin section. When Dymek (1978) first described the *M2* event, no source for the thermal input or water necessary for hydration was proposed. In a subsequent paper, Dymek (1984) suggested a possible correlation for the *M2* event with shear heating and hydration along predominantly subvertical high-grade shear zones of local and regional extent.

Cause of granulite facies metamorphism

Garde (1990) discussed several possible mechanisms of the approx. 3000 Ma granulite facies metamorphism in the Fiskefjord area: emplacement of originally dry magma; dehydration by CO_2 streaming; thermal

metamorphism; and in agreement with other workers cited above concluded that the approx. 3000 Ma granulite facies metamorphism was probably caused by heat accumulated during continuous injection of tonalitic magma into the growing continental crust. This mechanism of thermal metamorphism by over-accretion had previously been described in detail by Wells (1979, 1980) and applied to the approx. 2800 Ma granulite facies metamorphism in the Buksefjorden area south of Nuuk Fjord.

Retrogression

The widespread retrogression in the central and eastern parts of the Fiskefjord area had several causes. Some Late Archaen and Proterozoic retrogression unrelated to granulite facies metamorphism is readily visible at small scale along late shear zones, faults, and at the margins of the Proterozoic dykes. However, Garde (1997) contends that much of the retrogression is best explained as related to approx. 3000 Ma granulite facies thermal metamorphism. There is strong geochemical evidence that both granulite facies metamorphism and retrogression were accompanied by mobility of LIL elements. The presence of granulite facies quartz-feldspathic veins and syn- and post-granulite facies I-type granites suggest that dehydration melting of grey gneiss took place. Fluid activity at granulite facies conditions is indicated from Rb geochemistry of biotite. Petrography and mineral chemistry suggest that retrogression took place under a range of upper to lower amphibolite facies *P-T* conditions, and that there were perhaps two or more episodes of retrogression in some areas. Rb-Sr isotope geochemistry of grey gneiss in the Qussuk area indicates that a large part of the retrogression took place not later than approx. 2950 Ma ago. There is field evidence that also Late Archaean and Proterozoic retrogression not related to granulite facies metamorphism took place, but Garde (1997) has not found evidence of *widespread, Late* Archaean deformation along the Qussuk-Ulamertoq zone or other high strain zones in the Fiskefjord area, or of accompanying fluid activity and retrogression with regional importance.

Early Proterozoic events

The Early Proterozoic geological events in the Fiskefjord area may be cratonic expressions of the contemporary Nagssugtoqidian, Ammassalikian and Ketilidian orogenic events at the northern and southern margins of the Archaean block (e.g. Watterson 1978; Kalsbeek *et al.* 1987, 1990; Chadwick & Garde 1996). Proterozoic igneous, structural and metamorphic modification of the Archaean crust at the exposed level in the Fiskefjord area was very limited. As elsewhere in the Archaean block of southern West Greenland, several generations of mafic dykes were emplaced in the Fiskefjord area, and a contemporaneous system of wrench faults was developed. A weak regional thermal event caused resetting of epidote and biotite Rb-Sr and biotite K-Ar ages in this and other parts of the Archaean craton (Garde 1986). Stronger local heating also occurred, evidenced by intrusion of granitic dykes of continental crust origin at Qussuk (Kalsbeek *et al.* 1980; Kalsbeek & Taylor 1983).

Faults

The Fiskefjord area contains a number of prominent dextral, NE- to ENE-trending faults and a few conjugate sinistral, WNW-trending faults which are best developed in the eastern part of the area (Fig. 7). The faults are Early Proterozoic in age and are younger than the earliest, *c.* 2200 Ma old, N–S trending high-Mg and related dykes (Bridgwater *et al.* 1995; Nutman *et al.* 1995) which they offset, approximately comtemporaneous with NE-trending metadolerite dykes, and apparently older than a *c.* 2085 Ma old granitic dyke at Qussuk.

The largest fault is the NE-trending Fiskefjord fault with a dextral displacement of *c.* 5 km in the outer part of Fiskefjord. The displacement diminishes towards the northeast, and at the head of the fjord the fault dissolves into a conjugate system of smaller NE- and WNW-trending dextral and sinistral faults (Garde 1987). Their senses of displacement indicate that the maximum stress vector had an approximately E–W orientation. Towards Tasersuaq, a new dextral fault reappears along the line of the Fiskefjord fault and probably continues under the lake and the glacier Sermeq northeast of the Fiskefjord area (Garde 1987). Other NE-trending faults occur north and south of Fiskefjord, displaying local ductile deformation expressed by flaggy, variably chloritised rocks. Displacement of mafic marker horizons in the country rocks indicate dextral movement in the order of 1–2 km.

Most of the Proterozoic faults are bounded by narrow zones up to a few tens of metres wide, where movement of hydrous fluids has caused low-temperature retrogression with growth of chlorite and muscovite, oxidation of iron sulphides and reddening of feldspar.

Mafic dykes

Detailed field and geochemical accounts of mafic dykes in the southern Sukkertoppen, Isukasia and Fiskefjord areas are given by Berthelsen & Bridgwater (1960), Bridgwater *et al.* (1985, 1995), Hall *et al.* (1985) and Hall & Hughes (1986, 1987). The dykes comprise several groups. An older N–S trending group of high-Mg and related dykes predates the main period of faulting (this group apparently also includes some NE-trending dykes; Hall & Hughes 1987). Two younger tholeiitic groups trending *c.* 050° and 085° are contemporary with, or postdate faulting and belong to the tholeiitic metadolerite dykes of southern West Greenland (Rivalenti 1975; Bridgwater *et al.* 1976). One of the earliest dykes, the N–S trending Paakitsoq dyke through Toqqusap Nunaa (Berthelsen & Bridgwater 1960), has been dated at 2110 ± 85 Ma by the whole-rock Rb-Sr method (Bridgwater *et al.* 1995), and an early, likewise N–S trending high-Mg dyke from the adjacent Isukasia area has yielded a SHRIMP zircon U-Pb age of 2214 ± 10 Ma (Nutman *et al.* 1995).

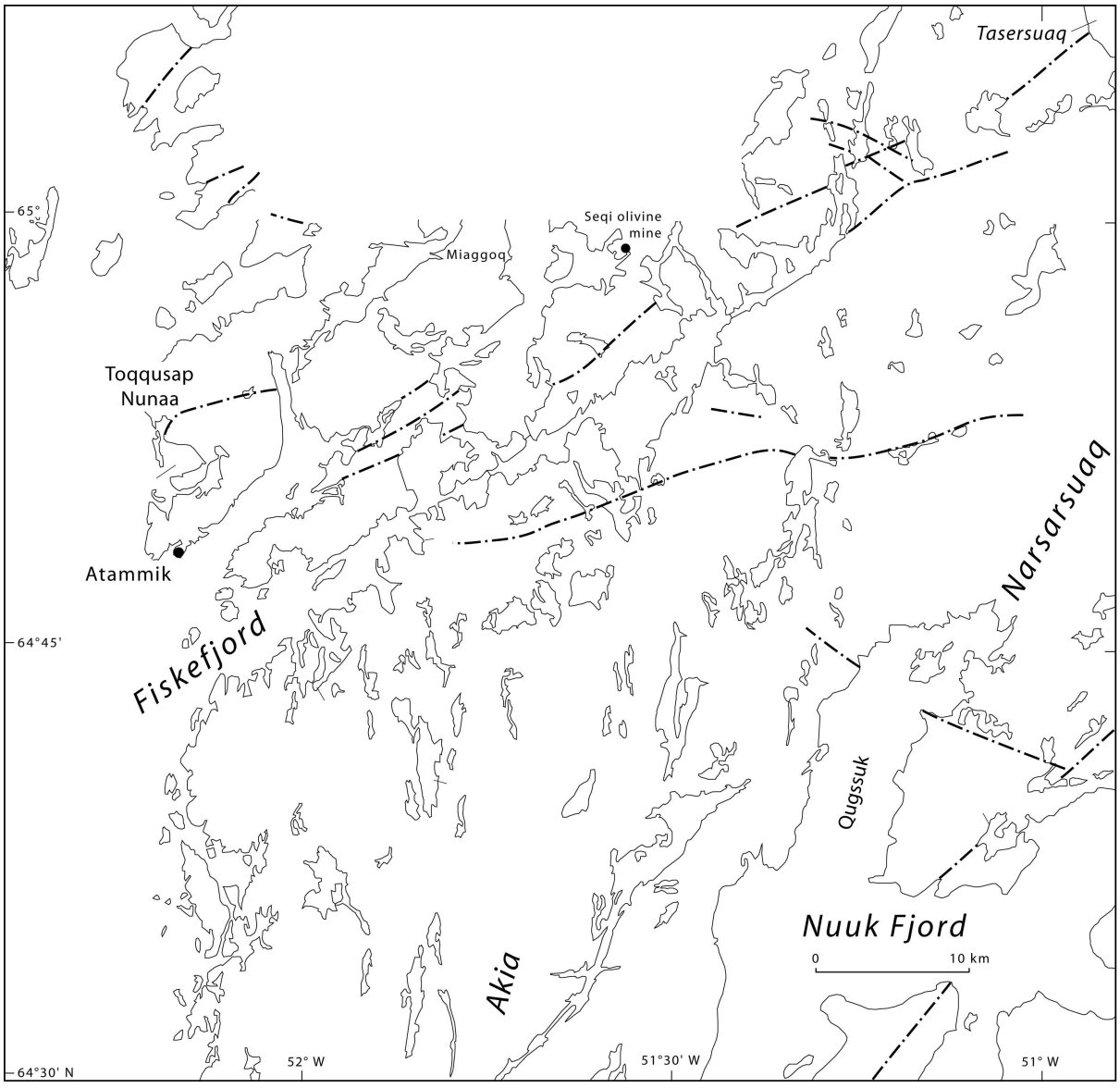

Fig. 7. Proterozoic faults in the Fiskefjord area (modified from Garde 1997).

The high-Mg dykes were first described by Berthelsen & Bridgwater (1960). Geochemical, mineral-chemical and isotopic data from these dykes have been published by Bridgwater *et al.* (1985, 1995), Hall *et al.* (1985) and Hall & Hughes (1986, 1987). The dykes are shown on the Isukasia and Fiskefjord 1:100 000 scale maps (Garde 1987, 1989b). Most of the dykes consist of variably altered pyroxene and plagioclase and have doleritic textures and tholeiitic compositions, but several of the N–S trending ones are olivine- or orthopyroxene-bearing or both and boninitic to noritic in composition, with up to 21% MgO, high Cr and Ni, high Mg/Fe ratios, and also relatively high silica contents (Hall & Hughes, 1987; Bridgwater et al., 1995).

The high-Mg dykes only rarely show evidence of interaction with their local wall rock, and for this and other reasons Hall & Hughes (1987) argued that they represent a distinct boninitic magma type and were derived from depleted harzburgitic mantle which had been metasomatised in the Late Archaean prior to melt extraction. Contrary to this interpretation, Bridgwater *et al.* (1985, 1995) suggested that the high-Mg dykes were derived from a primitive high-Mg magma, which was contaminated shortly before dyke emplacement with components selectively extracted from the lower crust. In this context it is interesting to note that post-kinematic Archaean diorites south of outer Fiskefjord have most likely obtained their apparent boninitic character by strong contamination with wall rock orthogneiss (see previous section and Garde, 1991), which may lend support to the second of the above interpretations of the origin of the high-Mg dykes by Bridgwater *et al.* (1985, 1995).

According to Hall & Hughes (1987), two major swarms of Early Proterozoic (ca. 2.1 Ga) basic dykes occur within the Archaean craton of southern West Greenland. One swarm comprises ophitic and sub-ophitic tholeiitic dolerites (MD dyke swarm), while the other (the BN dyke swarm) constitutes mainly norites in which the pyroxenes and olivines are enclosed by plagioclase oikocrysts. The close geochemical similarity between a quenched norite and the coarser grained varieties indicates that the composition of the latter type has not been significantly modified by crystal accumulation. The BN dykes are geochemically distinctive, most having high MgO (ca. 16%), Cr and Ni contents in conjunction with relatively high SiO_2, light rare earth (REE) and large ion lithophile (LIL) element concentrations. The texture, mineral chemistry and petrochemistry of the quenched noritic dyke all bear strong resemblances to those features in modern boninitic lavas. The BN dykes also correspond to proposed parental liquids of the Bushveld Complex and other major layered basic igneous intrusions. The two dyke swarms are petrogenetically distinct. The tholeiitic dolerites were derived from a relatively undepleted, primordial mantle while the noritic dykes originated from a metasomatised harzburgitic source. The widespread distribution of similar Proterozoic intrusions suggests crustal underplating by harzburgitic mantle on a worldwide scale at this time.

HISTORICAL EXPORATION

Exploration by other parties

The Fiskefjord area was explored by Kryolitselskabet Øresund from 1967 to 1975. They conducted ground geophysics over rusty showings and drilled a number of targets. Falconbridge carried out reconnaissance exploration for nickel and copper in the early 1990's, and Cominco conducted nickel exploration in the mid 1990's. The licence held by Cominco was transferred to Platinova A/S, which together with Aber Resources and Lexam continued with diamond exploration. A small segment of Cominco's licence around a dunite complex was transferred to Ujarak Minerals ApS. NunaOil A/S had an option agreement with Ujarak Minerals in 1997-1998. They assessed the dunite potential and carried out reconnaissance for PGE. Falconbridge has more recently continued with nickel exploration, and New Millennium Resources has looked at the niobium potential at Qaqarssuk. South Norseman Resources has carried out diamond exploration, and Crew recently explored for gold and platinum in the eastern part of Fiskefjord, but surrendered the licence in 2005.

A study on PGE distribution in nickel-mineralised samples from the norite belt in the northern part of the Fiskefjord region has been conducted by the Geological Survey of Denmark and Greenland (Secher 2001). In 2005, two smaller areas within Fiskefjord were studied in detail, and included MSc theses on sulphides and PGE's (Hollis *et al.* 2006; Kristensen 2006).

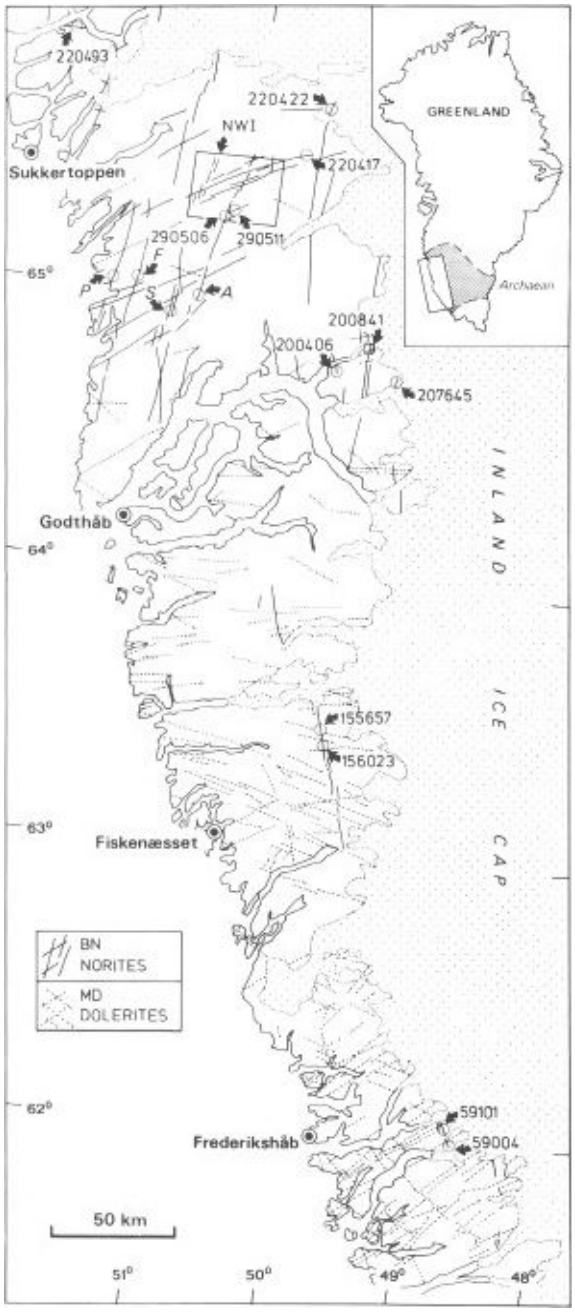

Fig. 8. Sketch map showing the distribution of Early Proterozoic basic dykes in the Archaen craton of southern West Greenland (from Hall & Hughes 1987 – numbers indicate sites of noritic dyke samples collected by those authors). *P, S, F* and *A* are the Pakitsoq, Sister, Feeder and Aornit noritic dykes described by Berthelsen & Bridgwater (1960).

NunaMinerals exploration

Pre-2008 activities

Following positive results from 2005, NunaMinerals intensified regional exploration in 2006. A regional sediment sampling programme collected more than 1,000 samples, and 4 stratigraphic drill holes were completed to increase the understanding of the potential for platinum group element (PGE) mineralisation.

The company focussed on 4 magmatic intrusions: the Amikoq, Fiskevandet, Miaggoq and Ulamertoq intrusions, all separated by several kilometres and which may or may not be related. NunaMinerals initiated a joint project with GEUS (Geological Survey of Denmark and Greenland) with the aim of identifying the origin of these mafic-ultramafic complexes. Preliminary results suggest that the majority of the studied rocks represent layered intrusive complexes, which amplifies the possibility that they host PGE.

Several point samples from the ultramafic complexes returned 500-800 ppb Pt+Pd. During the same period, a minor geophysical survey was completed in order to define potential drill targets.

Fiskevandet

Geological overview

A NNE-SSW striking ultramafic dyke crops out on the north shore of Fiskevandet (Fig. 9) and can be followed indefinitely northwards (along the linear trail of sample annotations in Fig. 20). Around 51.89360 W 64.98890 N, the dyke meets an ENE-SSW striking dolerite dyke (Fig. 10), but their relative age cannot be observed as the entire intersection is covered (Fig. 11). The two main dykes correspond to Hall & Hughes' (1987) boninitic (BN) dykes that strike NNE-SSW and tholeiitic metadolerite (MD) dykes that strike ENE-SSW. The BN dyke at Fiskevandet is named the Feeder dyke in Berthelsen & Bridgwater (1960) (Fig. 8).

On the Fiskefjord 1:100,000 geological map, the BN dyke is not shown to continue southwards beyond a limited globular body by the south shore of Fiskevandet (Fig. 20). However, sampling in the area in 2008 and a helicopter reconnaissance trip did succeed in following the dyke at least a few kilometres southwards. The reconnaissance noted that sulphides occur in considerable volume in ultramafic country rocks at their margins to the dyke.

At several locations the BN dyke is offset by a few metres along covered dextral shear zones; e.g. just north of 51.89022 W 64.99179 N. However, there is larger offset along a few sinistral shear zones; e.g. 40 m offset across a steep topographic cleft just south of 51 89174 W 64.99027 N. There are still larger shear zones represented by deep, linear valleys that are parallel to Fiskefjord (the dextral Fiskefjord fault).

Foliation in the country rock strikes east-west to ENE-SSW in the immediate area of the dykes (Fig. 17). The BN dyke has a high angle to this foliation, while the MD dyke is parallel or subparallel to it (Fig. 13). A large, apparent 'finger' or apophysis of the BN dyke protrudes into the country rock at 51.89109 W 64.99237 N (Fig. 12). The country rocks have various compositions: at 51.89214 W 64.99054 N, for example, the lithology adjacent to the BN dyke is a foliated amphibolite with magnetite-rich bands and exhibits dextral shear folding along the dyke margin (Fig. 14). The amphibolites alternate with quartz-feldspathic biotite gneiss (Fig. 15) displaying occasional boudins of more mafic composition (Fig. 16). The alternation of mafic and felsic country rocks is reflected to some extent on the Fiskefjord geological map (Fig. 20). Plagioclase-rich diopsidic gneisses are also common (Fig. 17).

A small, very fine grained basalt dyke cuts the BN dyke and its country rock, observed at 51.89022 W 64.99179 N (Fig. 18). This cross-cutting dyke is also offset along minor, rusty dextral shear zones. West and southwest of the Camp 2 position, a wider (4-5 m), approximately NE-SW striking dolerite dyke cuts the country rock foliation (Fig. 19). At one locality the dyke transgresses and offsets a shear zone, presumably by intrusive dilation, while at other localities the dyke is itself offset by shear zones.

Fig. 9. Northward view of east margin of BN dyke. Note high angle of dyke margin to country rock foliation seen on right, and possible steep flow foliation or later overprint in dyke, parallel to margin. Jakob Kløve Jakobsen for scale. Location: 51.89174 W 64.99027 N

Fig. 10. Southwestward view along ENE-SSW striking dolerite dyke (resistant, dark, low ridge in right half of photo). Photo taken from 51.86300 W 64.99200 N

Fig. 11. WSW-ward view from outcrop of dolerite over covered area where it intersects the NNE-SSW striking BN dyke. Location: approx. 51.89361 W 64.98872 N.

Fig. 12. Possible 'finger' (apophysis) of BN dyke protruding into quartz-feldspathic biotite country gneiss. Location: 51.89109 W 64.99237 N just west of main BN dyke body. Jakob Kløve Jakobden for scale.

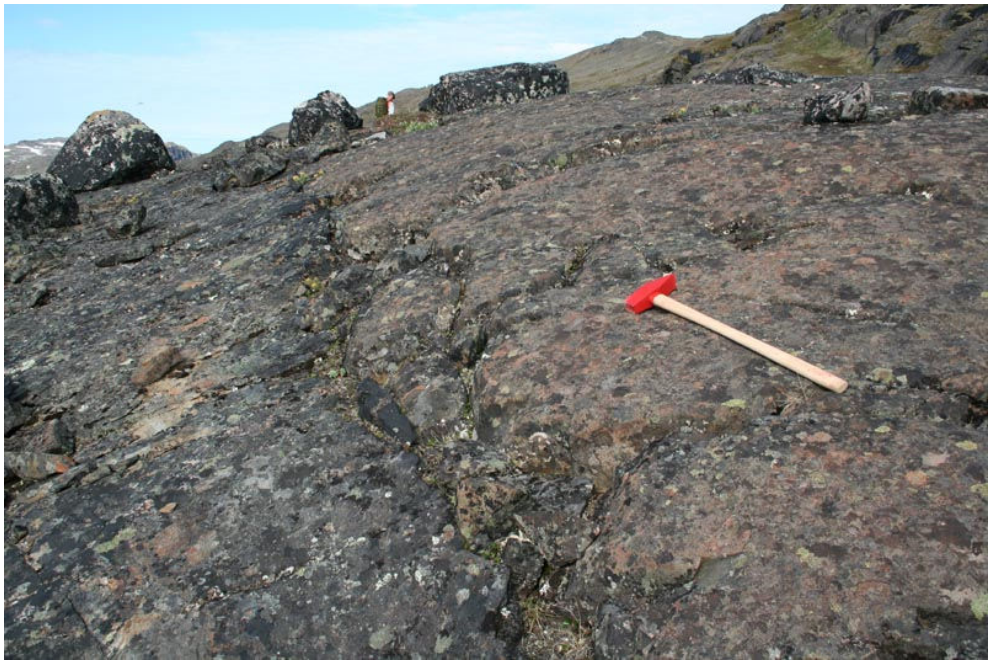

Fig. 13. Westward view of sharp contact between MD dyke (right) and quartz-feldspathic biotite country gneiss (left). Contact is slightly irregular, subparallel to country rock foliation.

Fig. 14. Prominent magnetite-rich bands in amphibolite country rock with dextral shear folding (which is more prominent beyond the photo) against west margin of BN dyke. Location: 51.89214 W 64.99054 N

Fig. 15. Quartz-feldspathic biotite gneiss with tight to isoclinal folding and partly deformed (syntectonic?) granitoid dyke- and vein-like intrusions.

Fig. 16. Boudin-like amphibolitic(?) xenolith or dyke in quartz-feldpathic biotite gneiss.

Fig. 17. NW'ward view of west contact of BN dyke (right) to plagioclase-rich diopsidic gneiss (left) with foliation-conformable rusty zones. Photo taken from 51.88870 W 64.99334 N

Fig. 18. Approx. northward view of thin, very fine grained basalt/dolerite(?) dyke cutting country rock foliation and BN dyke (not in photo). James Thomsen for scale. Location: 51.89022 W 64.99179 N

Fig. 19. Southwestward view of 4-5 m wide dolerite dyke cutting E-W striking country rock foliation. Location is west of Camp 2 position seen in lower left (51.87793 W 64.98696 N). Note minor dextral offset of dyke. Relation to BN and MD dykes is unknown.

Sampling and results

All sample positions and their ranges of Pt+Pd grades are shown in Fig. 20. In the Fiskevandet South area (detailed in Fig. 21), sulphide pods were sampled along the hangingwall of the dyke. At Fiskevandet North (detailed in Fig. 22), the BN and MD dykes were sampled along their axis and at the margins at several localities. Country rocks adjacent to the dyke margins were also sampled. The BN dyke was particularly difficult to sample due to its extreme hardness.

Positional and descriptive data for all samples are given in Appendix 1. Fire assay results and major and trace elements concentrations for all samples are presented in Appendix 2. The most significant results, which are all from Fiskevandet South, are given in Table 2 below.

Table 2. The five highest assays among all collected samples. The Pt+Pd grades of these samples stand out above the remainder, which carry below 50 ppb Pt+Pd.

Sample ID	Type	Elevation (m)	Westing	Northing	Pd (ppb)	Pt (ppb)	Au (ppb)	Pt+Pd (ppb)
195067	RGB	146	51.90180	64.93108	860	195	103	1055
183257	SSC	64	51.90176	64.93259	710	189	37	899
12901	RGB	155	51.90217	64.93055	597	143	74	741
195068	RGB	144	51.90181	64.93115	438	100	44	538
181756	RGB	67	51.90179	64.93257	266	16	32	282

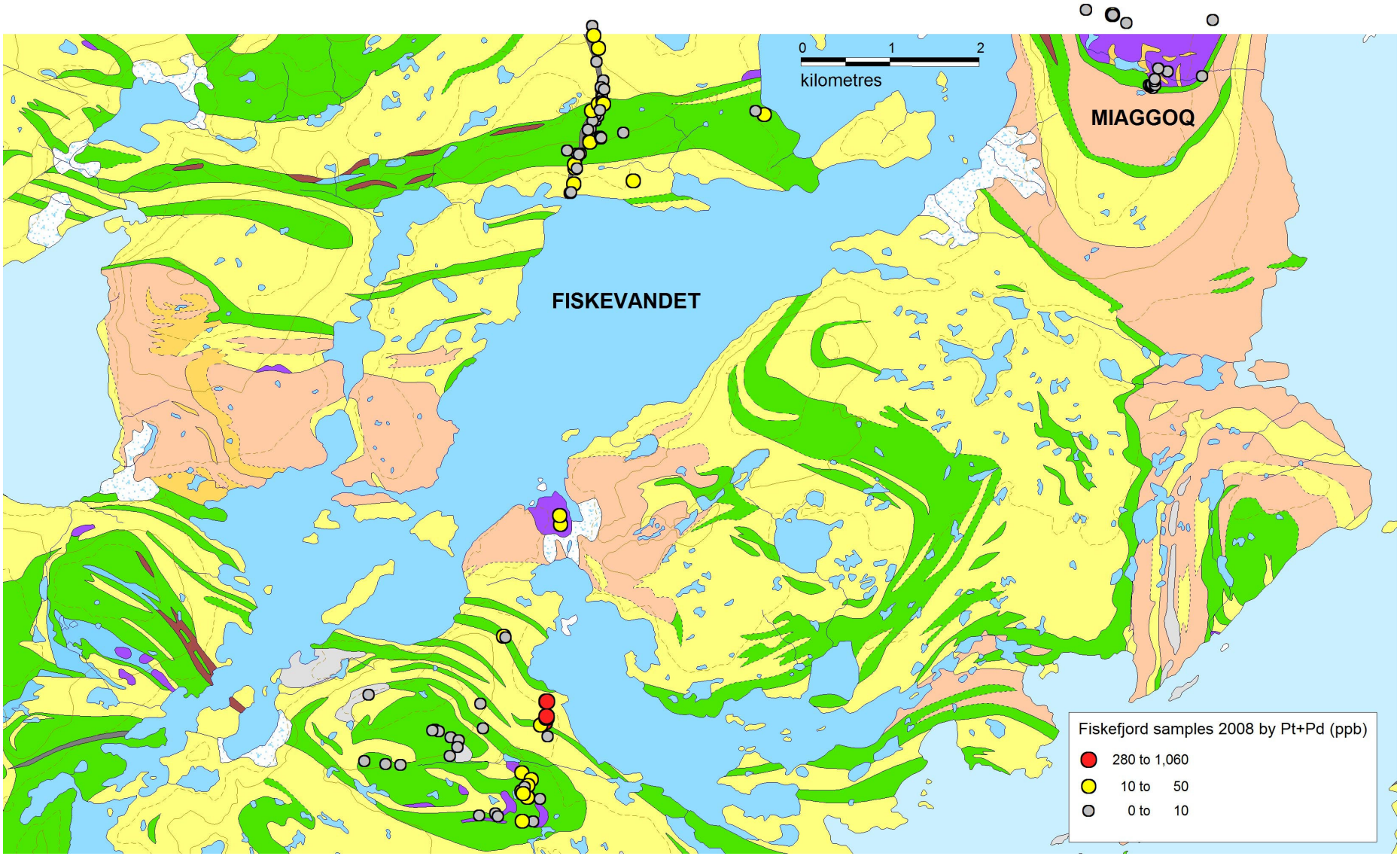

Fig. 20. Geological map of Fiskevandet area showing samples by combined Pt+Pd in ppb. Lithological legend: yellow/pink = 'basement' gneisses, green = amphibolite, pale blue = norite (slightly darker blue than lakes), purple = ultramafics, maroon = metasediments, dark grey = mafic/ultramafic dykes, pale grey = cover.

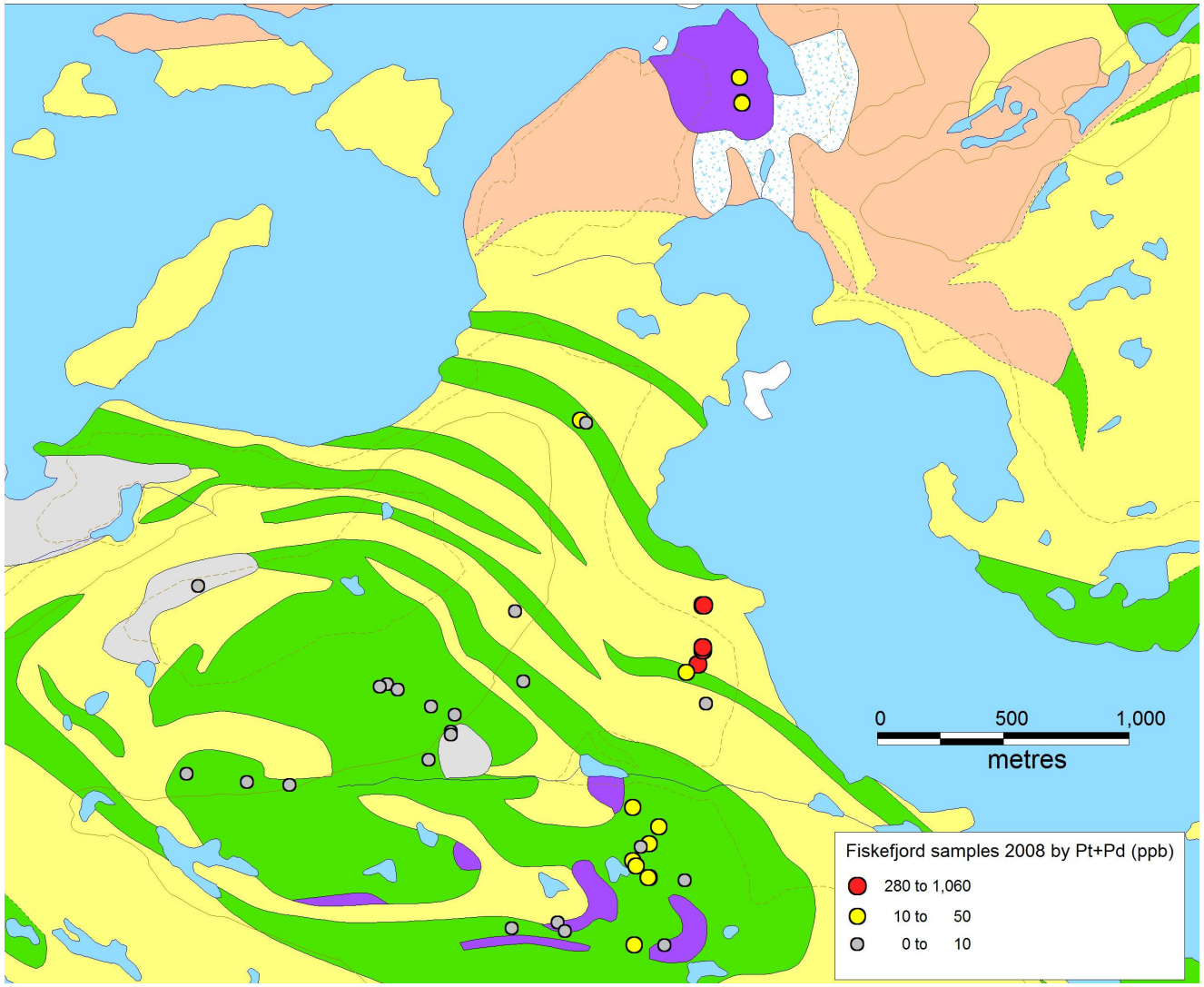

Fig. 21. Geological map of Fiskevandet South area showing samples by Pt+Pd grade (thematic legend in lower right). Lithological legend: yellow/pink = 'basement' gneisses, green = amphibolite, purple = ultramafics, blue = lakes.

Fig. 22. Geological map of Fiskevandet North area showing samples by Pt+Pd grade (thematic legend in lower right). Lithological legend: yellow = 'basement' gneisses, green = amphibolite, purple = ultramafics, maroon = metasediments, dark grey = boninitic dyke, blue = lakes. Trace of tholeiitic metadolerite (MD) dyke added to original map.

Geochemistry

At Fiskevandet North, one sample from the middle of the BN dyke and one sample from the middle of the MD dyke were analysed for major, trace and rare earth elements at Cardiff University, as part of a regional comparative geochemical study. Historical samples from country rock ultramafics in the Fiskevandet West area were also analysed. The spidergrams (large ion lithophile and high field strength elements) and rare earth element charts are presented below. The local data are given here for comparison with published regional data. The raw data are given in Appendix 3.

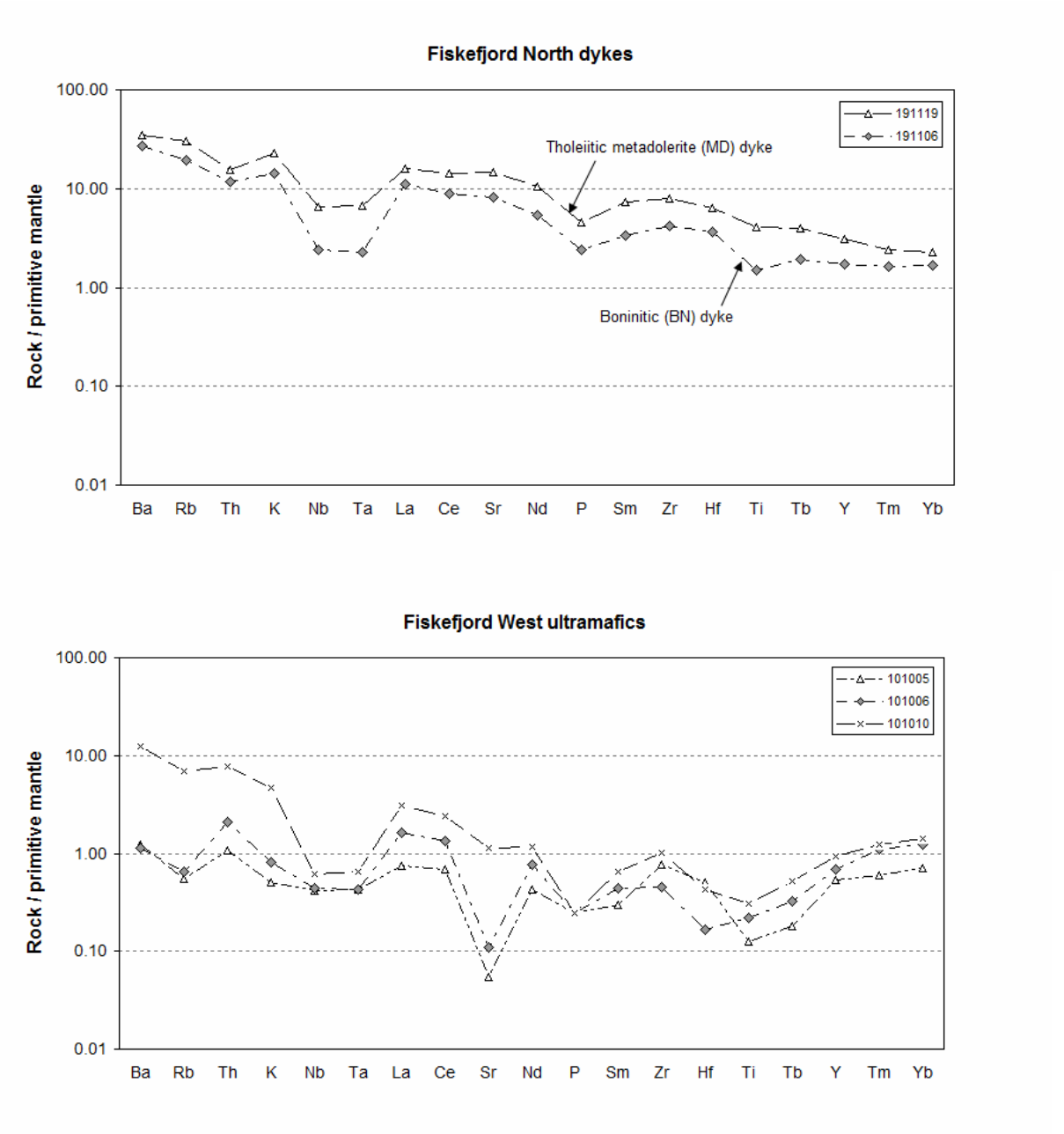

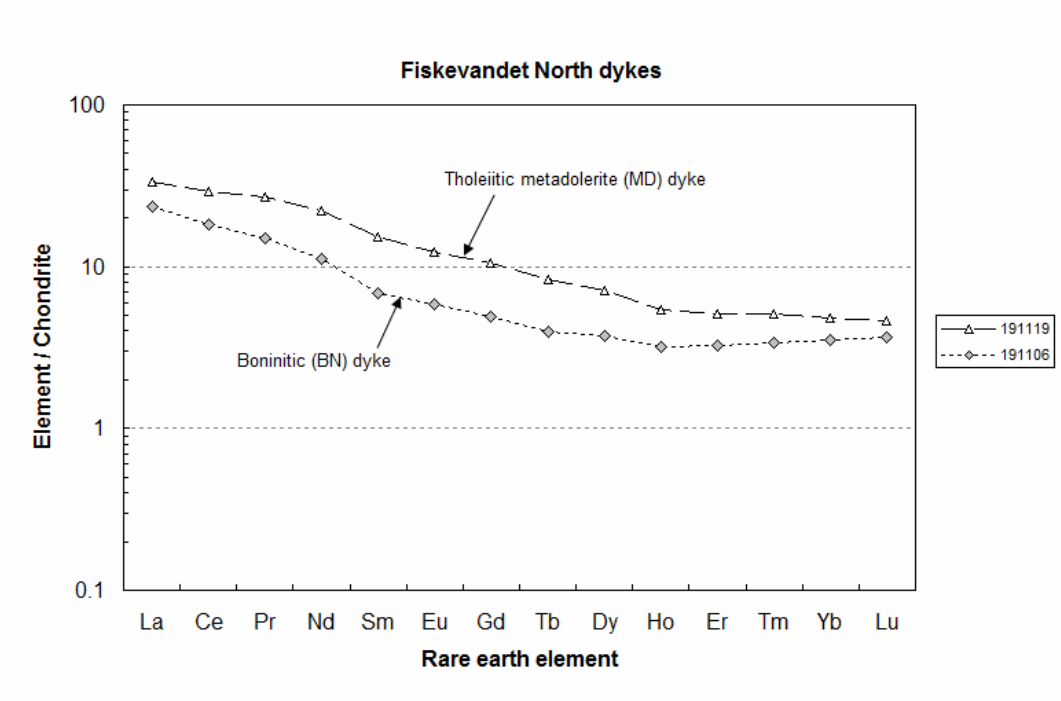
Fiskevandet North dykes
100
10
1
0.1
Element / Chondrite
Tholeiitic metadolerite (MD) dyke
Boninitic (BN) dyke
191119
191106
La
Ce
Pr
Nd
Sm
Eu
Gd
Tb
Dy
Ho
Er
Tm
Yb
Lu
Rare earth element

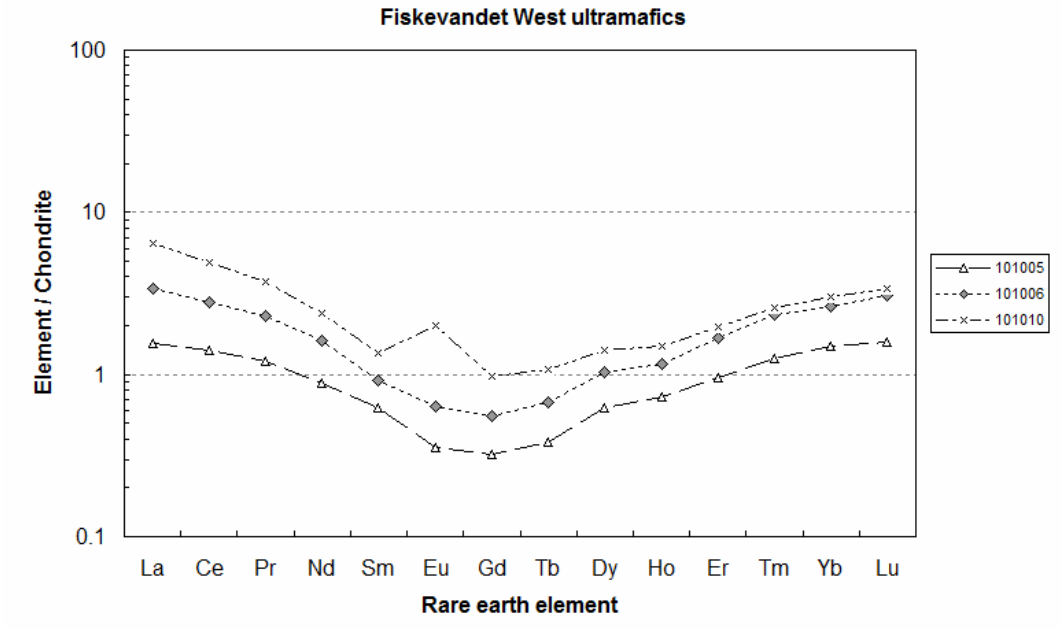
Fiskevandet West ultramafics
100
10
1
0.1
Element / Chondrite
101005
101006
101010
La
Ce
Pr
Nd
Sm
Eu
Gd
Tb
Dy
Ho
Er
Tm
Yb
Lu
Rare earth element

Miaggoq

Geological overview

The existing 1:100,000 Fiskefjord map shows Miaggoq to be a roughly oval body of ultramafics underlain by amphibolite which in turn overlies basement gneiss (southern half of Miaggoq shown in Fig. 29), all intruded by granitoid pegmatites. In the present work, however, the Miaggoq area was found to be a sequence of moderately, locally steeply, north-dipping to north-northwest dipping units of 'basement' gneiss, norites, ultramafics and amphibolites (Fig. 23) that are visually identical to the Amikoq sequence (Armitage 2009). Miaggoq differs from Amikoq in having a far thicker unit or sequence of ultramafic (mainly dunitic) rocks, thinner units of leuconorites, and a large volume of irregular, apparently syntectonic granitoid intrusions. The granitoids appear to be limited to the ultramafics, but the reason for this requires investigation.

In similarity to other occurrences of mafic-ultramafic intrusive sequences in the region, Miaggoq appears to be a fragment of a former, possibly coherent layered igneous intrusion. The basement rocks were not observed in the time available. A synform may be present in the area that repeats the basement-norite-ultramafic-amphibolite sequence to the north (Fig. 24) but in reverse.

Igneous layering is very well developed in the ultramafics, which are mostly of yellow-green, medium to coarse grained, sugary, dunitic composition. The extent of the visually distinct ultramafics was mapped at 1:2,500 scale. However, time did not allow the full outline to be mapped and there is little purpose in presenting the map until more detail can be added. The lower part of the Miaggoq sequence was found to be a relatively thin sheet of leuconorite and metanorite (weakly to moderatly tectonised leuconorite) similar to those observed at Amikoq. A garnetiferous gneiss that is always associated with metanorite at Amikoq, and is thought to be a product of extreme metamorphism of the leuconorite, has not yet been observed at Miaggoq.

A thin (10-12 m) sheet of coarse grained leuconorite overlies the ultramafics and is in turn overlain by amphibolites comprising the roof of the Miaggoq sequence (Fig. 25, Fig. 26). The leuconorite is more foliated than the main noritic units at Amikoq, probably due to the presence of shear zones along the lower and upper contacts (Fig. 27, Fig. 28). Shear strain is concentrated along zones of rheological contrast, in particular the main lithological contacts. However, there is no obvious indication of the sense of movement. Other significant shear zones transgress and offset the Miaggoq sequence and are clearly visible in aerial view.

Fig. 23. Northward view of the Miaggoq ultramafics showing (in upward structural stratigraphy from foreground to background) leuconorite/metaleuconorite, ultramafics with granitoid intrusives, and roof amphibolites.

Fig. 24. Eastward view to Miaggoq area from Fiskevandet North. Note gently south-dipping, dark, assumed amphibolites overlying a pale lithology that is either basement gneiss or possible leuconorite, mirroring a sequence observed to the south (beyond right of photo where the dip is to the north). Thus, the view is roughly along the axis of an open synform.

Fig. 25. Westward along-strike aerial view of northern part of Miaggoq sequence showing leuconorite (pale rock in centre) overlying brown ultramafics (left) and underlying dark amphibolites (right). Ground view in Fig. 26 below.

Fig. 26. Westward view of steeply north-dipping, aprox. 10-12m thick, foliated leuconorite sheet overlying the ultramafics (left) and underlying the roof amphibolites (far right, just beyond photo).

Fig. 27. Westward view of steeply dipping shear zone in leuconorite overlying the ultramafics (left).

Fig. 28. Westward view of sheared southern contact between ultramafics (right) and assumed metanorite (left).

Sampling and results

Time allowed only 20 samples to be collected at Miaggoq (Fig. 29), many of them from the same lithologies that are known to contain PGE at Amikoq. The assay results (Table 3 below) are disappointing but should not be considered a representation of the PGE potential of the area. The PGE reef along the western flank of Amikoq is only 2-4 m thick and was revealed by channel sampling. The density of sampling at Miaggoq needs to be far greater to have any chance of revealing any stratiform or stratabound PGE mineralisation.

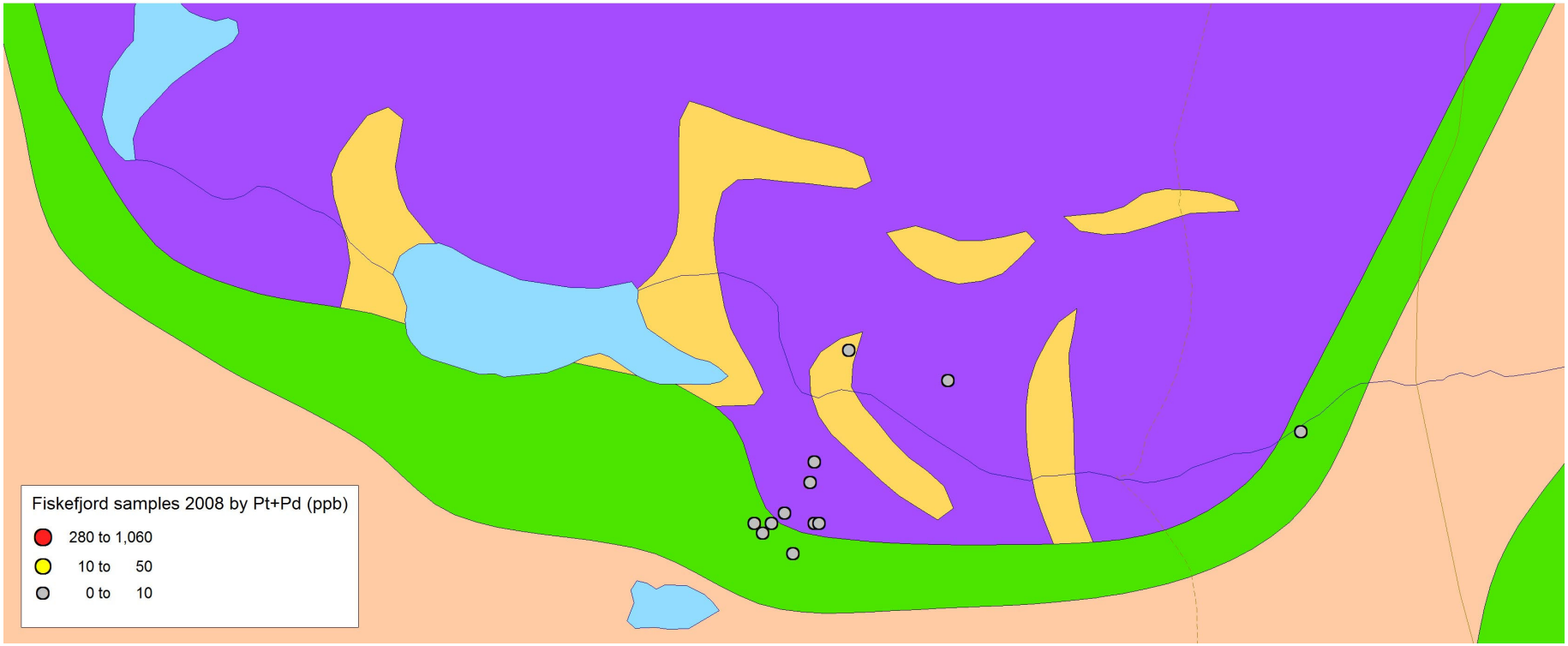

Fig. 29. Geological map of Miaggoq area showing samples by Pt+Pd grade (thematic legend in lower right). Lithological legend: pink = 'basement' gneiss, green = amphibolite, purple = ultramafics, yellow = granitoids, blue = lakes. Note: most of the amphibolite unit is actually noritic.

Table 3. Summary of assay results for Miaggoq samples collected in 2008. Complete data are given in Appendix 1. Abbreviation: RGB = rock grab.

Sample ID	Type	Westing	Northing	Elevation (m)	Lithology	Pd (ppb)	Pt (ppb)	Au (ppb)	Pt+Pd (ppb)
193040	RGB	51.74279	65.00156	255	Peridotite	< 4	< 5	< 2	0
193041	RGB	51.74531	64.99590	259	Amphibolite	< 4	< 5	< 2	0
193042	RGB	51.75714	64.99467	365	Amphibolite	< 4	< 5	< 2	0
193043	RGB	51.75778	64.99485	364	Metanorite	< 4	< 5	< 2	0
193044	RGB	51.75800	64.99493	364	Metanorite	< 4	< 5	< 2	0
193045	RGB	51.75763	64.99496	362	Leuconorite	< 4	< 5	< 2	0
193046	RGB	51.75729	64.99502	361	Leuconorite	< 4	< 5	< 2	0
193047	RGB	51.75658	64.99496	359	Leuconorite	< 4	< 5	< 2	0
193048	RGB	51.75647	64.99491	358	Metanorite	< 4	< 5	< 2	0
193049	RGB	51.75674	64.99535	342	Metanorite	< 4	< 5	< 2	0
193050	RGB	51.75658	64.99553	337	Dunite	< 4	< 5	< 2	0
088218	RGB	51.77304	65.00254	405	Metanorite	< 4	< 5	< 2	0
088219	RGB	51.77304	65.00255	405	Pyroxenite	< 4	6	< 2	6
088220	RGB	51.76673	65.00195	393	Pyroxenite	< 4	6	< 2	6
088221	RGB	51.76673	65.00196	393	Metanorite	6	17	< 2	23
088222	RGB	51.76673	65.00197	393	Metanorite	< 4	< 5	< 2	0
088223	RGB	51.76662	65.00202	393	Leuconorite	< 4	< 5	< 2	0
088224	RGB	51.76344	65.00127	380	Leuconorite	< 4	7	< 2	7
088225	RGB	51.75349	64.99634	335	Ol peridotite	< 4	< 5	< 2	0
088226	RGB	51.75581	64.99661	326	Granitoid	< 4	< 5	< 2	0

Geochemistry

Four leuconorite samples (one of which is historical), one dunite sample, one olivine peridotite sample and one roof amphibolite sample were analysed for major and trace elements at Cardiff University. The spidergrams (large ion lithophile and high field strength elements) and rare earth element graphs are presented below. The local data are given here for comparison with regional data. The raw data are given in Appendix 3.

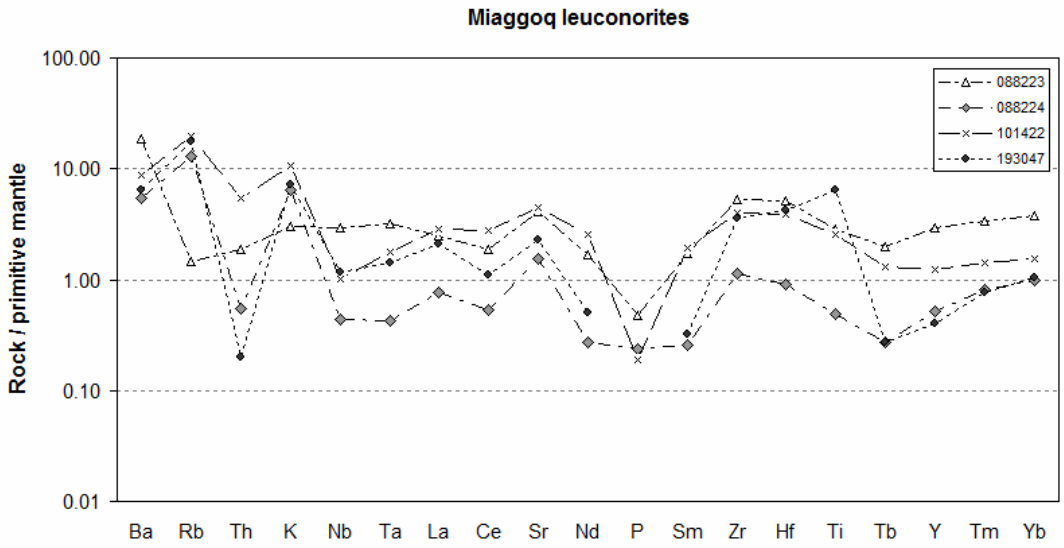
Miaggoq leuconorites
Rock / primitive mantle
100.00
10.00
1.00
0.10
0.01
088223
088224
101422
193047
Ba Rb Th K Nb Ta La Ce Sr Nd P Sm Zr Hf Ti Tb Y Tm Yb

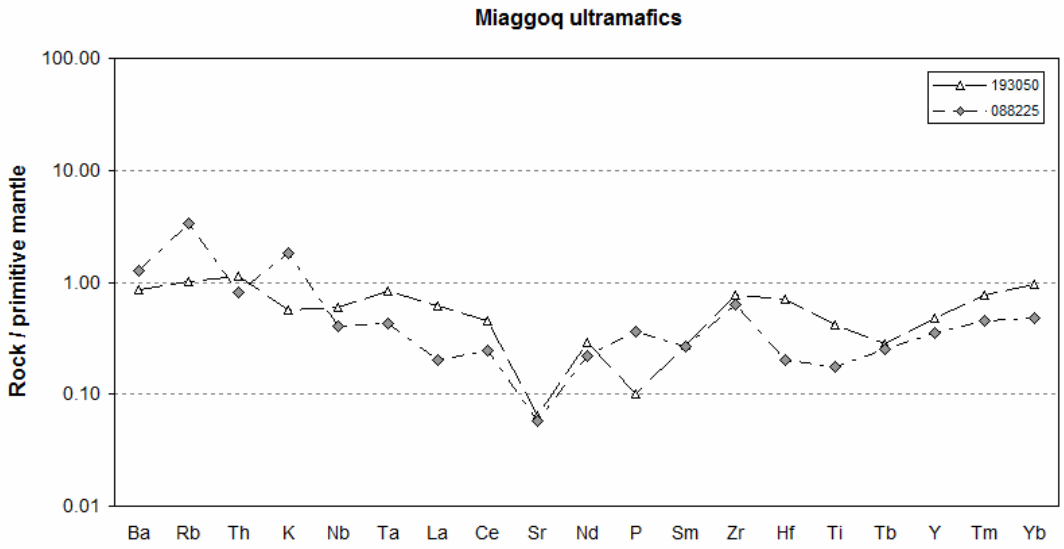
Miaggoq ultramafics
Rock / primitive mantle
100.00
10.00
1.00
0.10
0.01
193050
088225
Ba Rb Th K Nb Ta La Ce Sr Nd P Sm Zr Hf Ti Tb Y Tm Yb

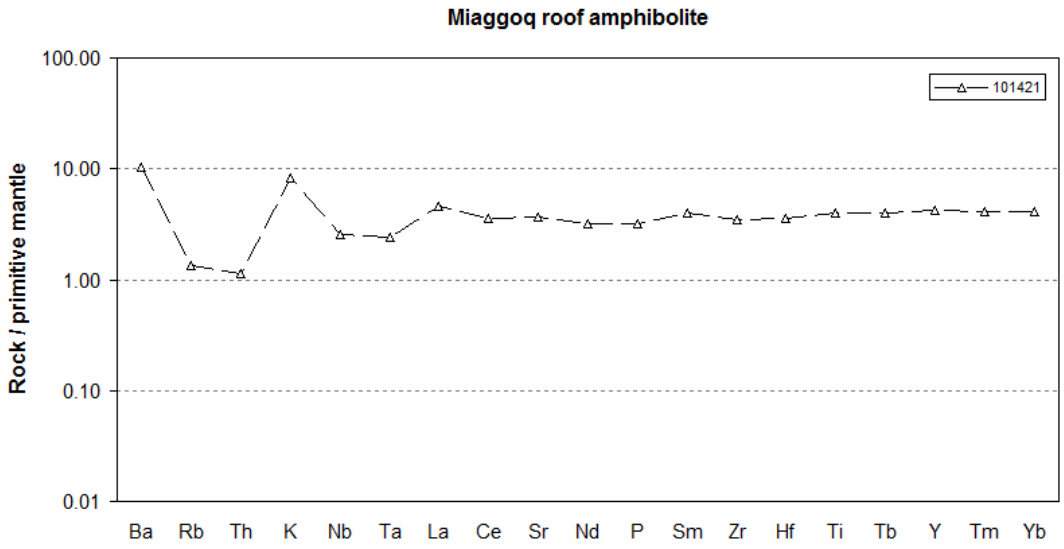
Miaggoq roof amphibolite
Rock / primitive mantle
100.00
10.00
1.00
0.10
0.01
101421
Ba Rb Th K Nb Ta La Ce Sr Nd P Sm Zr Hf Ti Tb Y Tm Yb

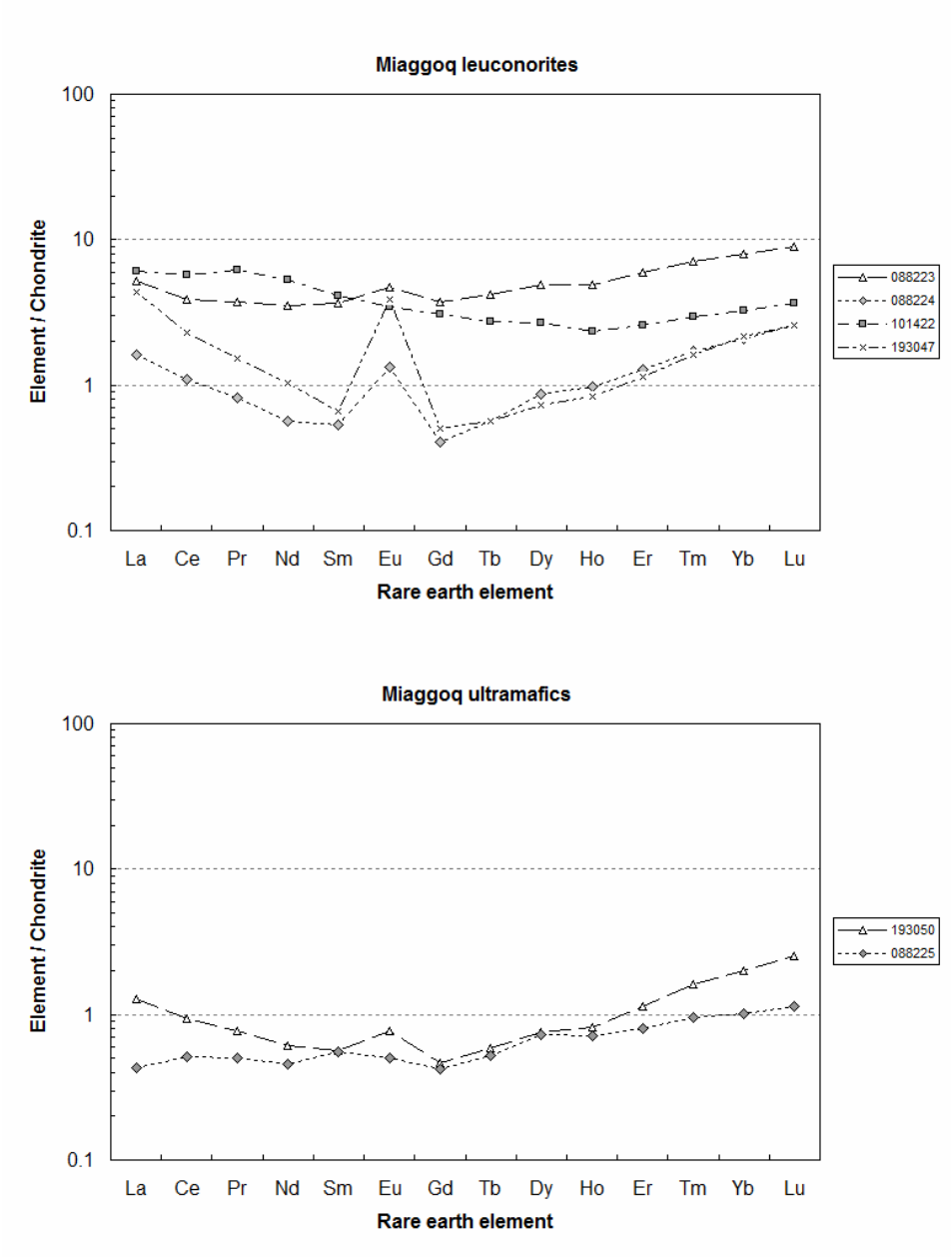
Miaggoq leuconorites
100
10
1
0.1
Element / Chondrite
La Ce Pr Nd Sm Eu Gd Tb Dy Ho Er Tm Yb Lu
Rare earth element
088223
088224
101422
193047
Miaggoq ultramafics
100
10
1
0.1
Element / Chondrite
La Ce Pr Nd Sm Eu Gd Tb Dy Ho Er Tm Yb Lu
Rare earth element
193050
088225

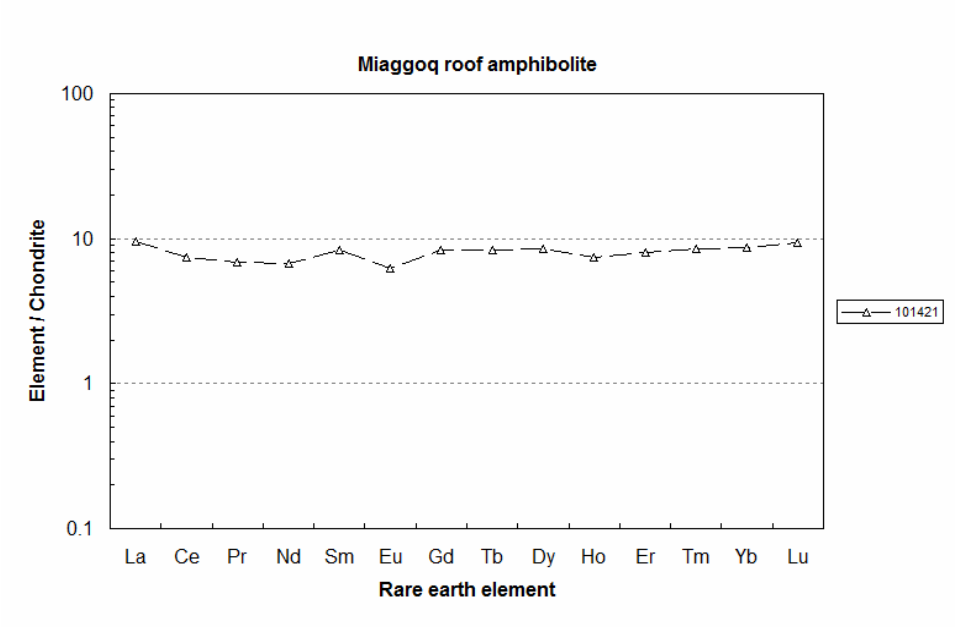
Miaggoq roof amphibolite
100
10
1
0.1
Element / Chondrite
La
Ce
Pr
Nd
Sm
Eu
Gd
Tb
Dy
Ho
Er
Tm
Yb
Lu
Rare earth element
101421

Recommendations

For Fiskevandet dykes:

1. Interpretation of historical data.
2. Identification and tracing of mafic-ultramafic dykes using existing maps, aeromagnetic, gravimetric and satellite imagery to plan a potential SkyTEM survey along the dykes. It is already known that some north-south striking dykes can be traced for up to 50km. As SkyTEM is an expensive technique, a survey area must be justifiably selected and include perhaps 3 flight lines at 50-75m spacing (depending on dip of dyke) along the strike of the dyke. SkyTEM could in theory progress the project but is not considered a vital activity until more substantial mineral grades and data can be acquired.
3. Fieldwork to include grab sampling and (where practical) channel sampling of contact zones in areas where (i) the dykes are shown to transgress ultramafic country rocks on existing geological maps; and (ii) where other ultramafic country rocks may be indicated by satellite, aeromagnetic or gravimetric imagery.

Resources: 1 relocating flight camp, 1 senior/project geologist, 2 junior geologists and 2 assistants. *Estimated time:* maximum 2 weeks but subject to findings of the desk study and initial ground truthing day (visiting several localities by helicopter to verify if remotely identified targets are ultramafic).

For Miaggog:

1. Interpretation of historical data.
2. Photography of the area from a helicopter for reconnaissance purposes.
3. Mapping of the main lithological contacts (an outline map is already commenced) and structures.
4. Channel sampling of the norite occurrences north and south of the central ultramafic core, with samples at 0.5 m or 1 m intervals. Two channel traverses are proposed in the south and at least two in the north as a minimum.
5. Additional grab sampling of any visually distinct zones in the norite and from contact zones.

Resources: 1 static flight camp, 1 senior/project geologist and 3 assistants (alternatively 1 junior geologist and 2 assistants). *Estimated time:* 1 week. The aerial photography can be done during the flight camp drop-off.

For occurrences of norite southwest of Fiskevandet:

1. Interpretation of historical data.
2. Photography of the norite occurrences from a helicopter for reconnaissance purposes.
3. Mapping of the main norite contacts and identification of suitable areas for channel sampling.
4. Channel sampling across norite unit(s) and grab sampling along contact zones.

Resources: 1 relocating flight camp (2 positions as the norite appears to be spread over a distance of approx. 3 km),1 senior/project geologist, 2 junior geologists and 2 assistants. *Estimated time:* 1 week. The aerial photography can be done during the flight camp drop-off.

References

Armitage P.E.B. 2009. PGE exploration in the Amikoq prospect, Fiskefjord region, West Greenland: 1 January – 31 December 2008. NunaMinerals A/S company report, 30 January 2009.

Bengaard, H.-J. 1988: Basic rocks of the inner Fiskefjord area, southern West Greenland. *Rapport Grønlands Geologiske Undersøgelse* **140**, 55–56.

Berthelsen, A. 1950: A Pre-Cambrian dome structure at Tovqussaq, West Greenland. *Meddelelser fra Dansk Geologisk Forening* **11**, 558–572.

Berthelsen, A. 1960: Structural studies in the pre-Cambrian of western Greenland. II. Geology of Tovqussap nunâ. *Bulletin Grønlands Geologiske Undersøgelse* **25**, 223 pp. (Also *Meddelelser om Grønland* **135**(6)).

Berthelsen, A. & Bridgwater, D. 1960: On the field occurrence and petrography of some basic dykes of supposed pre-Cambrian age from the southern Sukkertoppen District, western Greenland. *Bulletin Grønlands Geologiske Undersøgelse* **24**, 43 pp. (Also *Meddelelser om Grønland* **123**(3)).

Bridgwater, D., Keto, L., McGregor, V. R. & Myers, J. S. 1976: Archaean gneiss complex of Greenland. *In* Escher, A. & Watt, W. S. (ed.) *Geology of Greenland*, 18–75. Copenhagen: Geological Survey of Greenland.

Bridgwater, D., Fryer, B. & Gorman, B. E. 1985: Proterozoic basic dykes in southern Greenland and the coast of Labrador: tectonic setting, intrusion forms and chemistry. *Proceedings International Conference on Mafic Dyke Swarms*, 15–21. Toronto: University of Toronto Press.

Bridgwater, D., Mengel, F., Fryer, B., Wagner, P. & Hansen, S. C. 1995: Early Proterozoic mafic dykes in the North Atlantic and Baltic cratons: field setting and chemistry of distinctive dyke swarms. *In* Coward, M. P. & Ries, A. C. (ed.) Early Precambrian processes. *Geological Society Special Publication* (London) **95**, 193–210.

Chadwick, B. & Garde, A. A. 1996: Palaeoproterozoic oblique plate convergence in South Greenland: a re-appraisal of the Ketilidian orogen. *In* Brewer, T. S. (ed.) Precambrian crustal evolution in the North Atlantic region. *Geological Society Special Publication* (London) **112**, 179–196.

Dymek, R. F. 1978: Metamorphism of Archaean Malene supracrustals, Godthåb district, West Greenland. *In* Smith, I. E. M. & Williams, J. G. (ed.) *Proceedings of the 1978 Archaean geochemistry field conference*, 339–342. Toronto: University of Toronto Press.

Dymek, R. F. 1984: Supracrustal rocks, polymetamorphism, and evolution of the SW Greenland Archaean gneiss complex. *In* Holland, H. D. & Trendall, A. F. (ed.) *Patterns of change in Earth evolution*, 313–343. Berlin: Springer-Verlag.

Friend, C. R. L., Nutman, A. P. & McGregor, V. R. 1988a: Late Archaean terrane accretion in the Godthåb region, southern West Greenland. *Nature* **355**, 535–538.

Friend, C. R. L., Nutman, A. P. & McGregor, V. R. 1988b: Significance of the late Archaean granulite facies terrain boundaries, southern West Greenland. *In* Ashwal, L. D. (ed.) Workshop on the deep continental crust of South India. *Lunar and Planetary Institute Technical Report* **88-06**, 46–48.

Friend, C. R. L. & Nutman, A. P. 1994: Two Archaean granulite-facies metamorphic events in the Nuuk–Maniitsoq region, southern West Greenland: correlation with the Saglek block, Labrador. *Journal of the Geological Society* (London) **151**, 421–424.

Friend, C. R. L., Nutman, A. P., Baadsgaard, H., Kinny, P. D. & McGregor, V. R. 1996: Timing of late Archaean terrane assembly, crustal thickening and granite emplacement in the Nuuk region, southern West Greenland. *Earth and Planetary Science Letters* **142**, 353–365.

Garde, A. A. 1986: Field observations around northern Godthåbsfjord, southern West Greenland. *Rapport Grønlands Geologiske Undersøgelse* **130**, 63–68.

Garde, A. A. 1987: Geological map of Greenland, 1:100 000, Isukasia 65 V.2 Syd. Copenhagen: Geological Survey of Greenland.

Garde, A. A., Jensen, S. B. & Marker, M. 1987: Field work in the Fiskefjord area, southern West Greenland. *Rapport Grønlands Geologiske Undersøgelse* **135**, 36–42.

Garde, A. A. 1989a: Retrogression and fluid movement across a granulite-amphibolite facies boundary in middle Archaean Nuuk gneisses, Fiskefjord, southern West Greenland. *In* Bridgwater, D. (ed.) *Fluid movements – element transport and the composition of the deep crust*, 125–137. Dordrecht: Kluwer

Garde, A. A. 1989b: Geological map of Greenland, 1:100 000, Fiskefjord 64 V.1 Nord. Copenhagen: Geological Survey of Greenland.

Garde, A. A. 1990: Thermal granulite-facies metamorphism with diffuse retrogression in Archaean orthogneisses, Fiskefjord, southern West Greenland. *Journal of Metamorphic Geology* **8**, 663–682.

Garde, A. A. 1991: Post-kinematic diorite intrusions in Archaean basement rocks around outer Fiskefjord, southern West Greenland. *Bulletin of the Geological Society of Denmark* **39**, 167–177.

Garde, A. A., 1997: Accretion and evolution of an Archaean high-grade grey gneiss-amphibolite complex: the Fiskefjord area, southern West Greenland. *Bulletin Grønlands Geologiske Undersøgelse* **177**, 115 pp.

Garde, A. A., Friend, C. R .L., Nutman, A. P. & Marker, M. 2000: Rapid maturation and stabilisation of middle Archaean continental crust: the Akia terrane, southern West Greenland. *Bulletin of the Geological Society of Denmark* **47**, 1–27.

Garde, A. A. 2007: A mid-Archaean island arc complex in the eastern Akia terrane, Godthåbsfjord, southern West Greenland. *Journal of the Geological Society* (London) **164**, 565-579.

Hall, R. P., Hughes, D. J. & Friend, C. R. L. 1985: Geochemical evolution and unusual pyroxene chemistry of the MD tholeiite dyke swarm from the Archaean craton of southern West Greenland. *Journal of Petrology* **26**, 253–282.

Hall, R. P. & Hughes, D. J. 1986: A boninitic dyke in the eastern Sukkertoppen region: geochemistry of the boninitic-noritic dyke swarm of southern West Greenland. *Rapport Grønlands Geologiske Undersøgelse* **130**, 44–52.

Hall, R. P. & Hughes, D. J. 1987: Noritic dykes of southern West Greenland: early Proterozoic boninitic magmatism. *Contributions to Mineralogy and Petrology* **97**, 169–182.

Hollis, J.A., van Gool, J.A.M., Steenfelt, A. & Garde, A.A. 2004: Greenstone belts in the central Godthåbsfjord region, southern West Greenland: Preliminary results from field work in 2004. *Rapport Danmarks og Grønlands Geologiske Undersøgelse* **110** , 110 pp. + 1 DVD.

Hollis, J.A., Schmid, S., Stendal, H., van Gool, J.A.M. & Weng, W.L. 2006: Supracrustal belts in the Godthåbsfjord region, southern West Greenland. Progress report on 2005 field work: geological mapping, regional hydrothermal alteration and tectonic sections. *Rapport Danmarks og Grønlands Geologiske Undersøgelse* **2006/7**, 171 pp. + 1 CD-ROM.

Kalsbeek, F., Bridgwater, D. & Boak, J. 1980: Evidence of mid-Proterozoic granite formation in the Isua area. *Rapport Grønlands Geologiske Undersøgelse* **100**, 73–75.

Kalsbeek, F. & Taylor, P. N. 1983: Anatectic origin of mid-Proterozoic granite dyke in the Isukasia area, West Greenland. Pb-Pb and Rb-Sr isotopic evidence. *Rapport Grønlands Geologiske Undersøgelse* **115**, 38–42.

Kalsbeek, F., Pidgeon, R. T. & Taylor, P. N. 1987: Nagssugtoqidian mobile belt of West Greenland: a cryptic 1850 Ma suture between two Archaean continents – chemical and isotopic evidence. *Earth and Planetary Science Letters* **85**, 365–385.

Kalsbeek, F., Larsen, L. M. & Bondam, J. 1990: Geological map of Greenland 1:500 000, Sydgrønland, sheet 1. Descriptive text. Copenhagen: Geological Survey of Greenland, 36 pp.

Lauerma, R. 1964: On the structure and petrography of the Ipernat dome, western Greenland. *Bulletin de la Commission géologique de la Finlande* **215**, 1–88 (Also *Bulletin Grønlands Geologiske Undersøgelse* **46**, 88 pp).

McDonlald, I. & Viljoen, K.S. 2006. Platinum-group element geochemistry of mantle eclogites: a reconnaissance study of xenoliths from the Orapa kimberlite, Botswana. *Applied Earth Science (Trans. Inst. Min. Metall. B)* **115**, 81-93.

McGregor, V. R., Nutman, A. P. & Friend, C. R. L. 1986: The Archaean geology of the Godthåbsfjord region, southern West Greenland. *In* Ashwal, L. D. (ed.) Workshop on early crustal genesis: The *World's oldest rocks. Lunar and Planetary Institute Technical Report* **86-04**, 113–169.

McGregor, V. R., Friend, C. R. L. & Nutman, A. P. 1991: The late Archaean mobile belt through Godthåbsfjord, southern West Greenland: a continent-continent collision zone? *Bulletin of the Geological Society of Denmark* **39**, 179–197.

McGregor, V. R. 1993: Geological map of Greenland, 1:100 000, Qôrqut 64 V. 1 Syd. Descriptive text. Copenhagen: Geological Survey of Greenland, 40 pp.

Nutman, A. P., Hagiya, H. & Maruyama, S. 1995: SHRIMP U-Pb single zircon geochronology of a Proterozoic mafic dyke, Isukasia, southern West Greenland. *Bulletin of the Geological Society of Denmark* **42**, 17–22.

Pillar, J. E. 1985: Geochemistry of high grade gneisses with examples from West Greenland and British Columbia. Unpublished Ph.D. thesis, University of Leicester, U.K.

Riciputi, L. R., Valley, J. W. & McGregor, V. R. 1990: Conditions of Archean granulite metamorphism in the Godthaab–Fiskenaesset region, southern West Greenland. *Journal of Metamorphic Geology* **8**, 171–190.

Rivalenti, G. 1975: Chemistry and differentiation of mafic dykes in an area near Fiskenaesset, West Greenland. *Canadian Journal of Earth Sciences* **12**, 721–730.

Secher, K. 2001: The Pd + Pt dispersion in noritic and undifferentiated mafic rocks of the Archean craton east of Maniitsoq, southern West Greenland. A study based on reanalysis of rock samples from sulphide mineralised sections of mafic rocks within the "Norite belt" collected by GGU 1982. *Rapport Danmarks og Grønlands Geologiske Undersøgelse* **2001/123**, 22 pp.

Sun, S.M. & McDonough, W.F. 1989. Chemical and isotopic systematics of oceanic basalts: implications for mantle composition and processes. In: Saunders, A.D. & Norry, M.J. (eds) Magmatism in the ocean basins. *Geological Society Special Publication* (London) **42**, 313–345.

Taylor, P. N., Moorbath, S., Goodwin, R. & Petrykowski, A. C. 1980: Crustal contamination as an indication of the extent of early Archaean continental crust: Pb isotopic evidence from the late Archaean gneisses of West Greenland. *Geochimica et Cosmochimica Acta* **44**, 1437–1453.

Watterson, J. 1978: Proterozoic intraplate deformation in the light of south-east Asian neotectonics. *Nature* **273**, 636–640.

Wells, P. R. A. 1979: Chemical and thermal evolution of Archaean sialic crust, southern West Greenland. *Journal of Petrology* **20**, 187–226.

Wells, P. R. A. 1980: Thermal models for the magmatic accretion and subsequent metamorphism of continental crust. *Earth and Planetary Science Letters* **46**, 253–265.

Appendix 1

Sample database.

Sample ID	Pt+Pd	Pd	Pt	Au	Ag	Cd	Cu	Mn	Mo	Ni	Pb	Zn	Al	As	B	Ba	Be	Bi	Ca	Co	Cr	Fe	Ga	Hg	K	La	Mg	Na	P	S	Sb	Sc	Sr	Ti	Tl	U	V	W
88218	0.00	-4	-5	< 2	N/A	N/A	N/A	N/A	N/A	N/A	N/A	N/A	N/A	N/A	N/A	N/A	N/A	N/A	N/A	N/A	N/A	N/A	N/A	N/A	N/A	N/A	N/A	N/A	N/A	N/A	N/A	N/A	N/A	N/A	N/A	N/A	N/A	N/A
88219	6.00	-4	6	< 2	N/A	N/A	N/A	N/A	N/A	N/A	N/A	N/A	N/A	N/A	N/A	N/A	N/A	N/A	N/A	N/A	N/A	N/A	N/A	N/A	N/A	N/A	N/A	N/A	N/A	N/A	N/A	N/A	N/A	N/A	N/A	N/A	N/A	N/A
88220	6.00	-4	6	< 2	N/A	N/A	N/A	N/A	N/A	N/A	N/A	N/A	N/A	N/A	N/A	N/A	N/A	N/A	N/A	N/A	N/A	N/A	N/A	N/A	N/A	N/A	N/A	N/A	N/A	N/A	N/A	N/A	N/A	N/A	N/A	N/A	N/A	N/A
88221	23.00	6	17	< 2	N/A	N/A	N/A	N/A	N/A	N/A	N/A	N/A	N/A	N/A	N/A	N/A	N/A	N/A	N/A	N/A	N/A	N/A	N/A	N/A	N/A	N/A	N/A	N/A	N/A	N/A	N/A	N/A	N/A	N/A	N/A	N/A	N/A	N/A
88222	0.00	-4	-5	< 2	N/A	N/A	N/A	N/A	N/A	N/A	N/A	N/A	N/A	N/A	N/A	N/A	N/A	N/A	N/A	N/A	N/A	N/A	N/A	N/A	N/A	N/A	N/A	N/A	N/A	N/A	N/A	N/A	N/A	N/A	N/A	N/A	N/A	N/A
88223	0.00	-4	-5	< 2	N/A	N/A	N/A	N/A	N/A	N/A	N/A	N/A	N/A	N/A	N/A	N/A	N/A	N/A	N/A	N/A	N/A	N/A	N/A	N/A	N/A	N/A	N/A	N/A	N/A	N/A	N/A	N/A	N/A	N/A	N/A	N/A	N/A	N/A
88224	7.00	-4	7	< 2	N/A	N/A	N/A	N/A	N/A	N/A	N/A	N/A	N/A	N/A	N/A	N/A	N/A	N/A	N/A	N/A	N/A	N/A	N/A	N/A	N/A	N/A	N/A	N/A	N/A	N/A	N/A	N/A	N/A	N/A	N/A	N/A	N/A	N/A
88225	0.00	-4	-5	< 2	N/A	N/A	N/A	N/A	N/A	N/A	N/A	N/A	N/A	N/A	N/A	N/A	N/A	N/A	N/A	N/A	N/A	N/A	N/A	N/A	N/A	N/A	N/A	N/A	N/A	N/A	N/A	N/A	N/A	N/A	N/A	N/A	N/A	N/A
88226	0.00	-4	-5	< 2	N/A	N/A	N/A	N/A	N/A	N/A	N/A	N/A	N/A	N/A	N/A	N/A	N/A	N/A	N/A	N/A	N/A	N/A	N/A	N/A	N/A	N/A	N/A	N/A	N/A	N/A	N/A	N/A	N/A	N/A	N/A	N/A	N/A	N/A
191101	0.00	-4	-5	< 2	< 4	< 5	< 2	< 0.2	< 0.5	25	262	2	445	< 2	15	1.86	< 2	< 10	87	< 0.5	< 2	0.79	40	430	2.94	< 10	< 1	0.27	< 10	4.45	0.332	0.012	0.02	< 2	2	49	0.04	< 10
191102	5.00	5	-5	< 2	5	< 5	< 2	< 0.2	< 0.5	34	374	< 1	469	< 2	25	1.24	< 2	< 10	47	< 0.5	< 2	0.93	39	186	2.87	< 10	< 1	0.18	< 10	3.85	0.353	0.018	0.02	< 2	2	56	0.06	< 10
191103	0.00	-4	-5	4	< 4	< 5	4	< 0.2	< 0.5	181	235	11	127	3	42	4.72	< 2	< 10	31	0.6	< 2	4.51	42	298	3.72	10	< 1	0.05	< 10	0.35	0.948	0.035	1.31	< 2	5	119	0.15	< 10
191104	0.00	-4	-5	< 2	< 4	< 5	< 2	< 0.2	< 0.5	31	307	< 1	357	< 2	20	0.92	< 2	< 10	57	< 0.5	< 2	0.76	30	217	2.4	< 10	< 1	0.15	< 10	3.24	0.285	0.017	0.02	< 2	2	44	0.06	< 10
191105	6.00	6	-5	< 2	6	< 5	< 2	< 0.2	< 0.5	34	348	3	408	< 2	23	1.77	< 2	< 10	58	< 0.5	< 2	1.38	35	262	2.7	< 10	< 1	0.2	< 10	3.5	0.512	0.016	0.03	< 2	3	83	0.06	< 10
191106	10.00	5	5	< 2	5	5	< 2	< 0.2	< 0.5	38	373	< 1	423	< 2	23	1.65	< 2	< 10	86	< 0.5	< 2	1.29	38	251	3.06	< 10	< 1	0.27	< 10	3.66	0.467	0.019	0.03	< 2	3	73	0.08	< 10
191107	20.00	12	8	< 2	12	8	< 2	< 0.2	< 0.5	28	325	3	427	< 2	22	1.67	< 2	< 10	49	< 0.5	< 2	1.28	35	245	2.55	< 10	< 1	0.15	< 10	3.56	0.507	0.014	0.02	< 2	2	83	0.05	< 10
191108	16.00	9	7	< 2	9	7	< 2	< 0.2	< 0.5	36	386	< 1	419	< 2	25	1.17	< 2	< 10	50	< 0.5	< 2	1.01	38	192	3.13	< 10	< 1	0.13	< 10	3.69	0.364	0.016	0.03	< 2	3	58	0.06	< 10
191109	0.00	-4	-5	< 2	< 4	< 5	< 2	< 0.2	< 0.5	37	316	3	312	< 2	21	1.72	< 2	< 10	56	< 0.5	< 2	1.37	29	317	2.49	< 10	< 1	0.23	< 10	2.8	0.493	0.025	0.03	< 2	3	84	0.09	< 10
191110	0.00	-4	-5	< 2	< 4	< 5	< 2	< 0.2	< 0.5	23	344	< 1	484	< 2	21	0.67	< 2	< 10	51	< 0.5	< 2	0.57	37	181	2.61	< 10	< 1	0.11	< 10	4.32	0.212	0.013	0.02	< 2	2	30	0.05	< 10
191111	12.00	6	6	< 2	6	6	< 2	< 0.2	< 0.5	41	368	2	341	< 2	25	1.79	< 2	< 10	56	< 0.5	< 2	1.55	33	311	2.84	< 10	< 1	0.19	< 10	3.25	0.535	0.019	0.03	< 2	4	82	0.07	< 10
191112	0.00	-4	-5	< 2	< 4	< 5	< 2	< 0.2	< 0.5	33	395	< 1	495	< 2	27	1.43	< 2	< 10	71	< 0.5	< 2	1.16	41	259	3.04	< 10	< 1	0.19	< 10	4.44	0.429	0.015	0.02	< 2	3	66	0.06	< 10
191113	0.00	-4	-5	< 2	< 4	< 5	< 2	< 0.2	< 0.5	31	374	2	493	< 2	24	1.37	< 2	< 10	64	< 0.5	< 2	1.05	40	259	2.98	< 10	< 1	0.22	< 10	4.37	0.402	0.016	0.02	< 2	3	63	0.05	< 10
191114	7.00	7	-5	< 2	7	< 5	< 2	< 0.2	< 0.5	29	403	< 1	761	< 2	23	0.39	< 2	< 10	30	< 0.5	< 2	0.34	48	165	2.81	< 10	< 1	0.07	< 10	6.98	0.121	0.008	0.03	< 2	2	18	0.02	< 10
191115	6.00	6	-5	10	6	< 5	10	< 0.2	< 0.5	511	444	< 1	108	< 2	56	1.55	< 2	< 10	40	< 0.5	< 2	1.57	44	255	6.02	< 10	< 1	0.25	< 10	1.02	0.481	0.022	0.93	< 2	20	31	0.24	< 10
191116	0.00	-4	-5	< 2	< 4	< 5	< 2	< 0.2	< 0.5	126	553	2	259	< 2	42	0.47	< 2	< 10	49	< 0.5	< 2	0.86	45	212	4.9	< 10	< 1	0.31	< 10	2.87	0.136	0.036	0.04	< 2	4	25	0.2	< 10
191117	0.00	-4	-5	< 2	< 4	< 5	< 2	< 0.2	< 0.5	132	477	< 1	256	< 2	42	0.61	< 2	< 10	110	< 0.5	< 2	0.99	44	174	4.85	< 10	< 1	0.45	< 10	2.91	0.145	0.041	0.07	< 2	4	27	0.23	< 10
191118	4.00	4	-5	6	4	< 5	6	< 0.2	< 0.5	130	274	3	55	< 2	27	1.09	< 2	< 10	27	< 0.5	< 2	1.06	18	181	2.98	< 10	< 1	0.1	< 10	0.57	0.411	0.038	0.24	< 2	11	14	0.26	< 10
191119	0.00	-4	-5	< 2	< 4	< 5	< 2	< 0.2	< 0.5	115	556	< 1	291	< 2	40	0.48	< 2	< 10	64	< 0.5	< 2	0.85	46	183	4.59	< 10	< 1	0.35	< 10	3.22	0.111	0.033	0.06	< 2	3	24	0.2	< 10
191120	4.00	4	-5	< 2	4	< 5	< 2	< 0.2	< 0.5	60	394	3	325	< 2	28	1.47	< 2	< 10	63	< 0.5	< 2	1.29	36	234	3.24	< 10	< 1	0.25	< 10	2.93	0.421	0.025	0.04	< 2	3	72	0.11	< 10
191121	14.00	9	5	< 2	9	5	< 2	< 0.2	< 0.5	14	583	< 1	1100	< 2	28	0.28	< 2	< 10	28	< 0.5	< 2	0.23	70	161	3.91	< 10	< 1	0.06	< 10	11.2	0.075	0.007	0.02	< 2	2	12	0.02	< 10
191122	5.00	-4	5	< 2	< 4	5	< 2	< 0.2	< 0.5	39	655	1	583	< 2	17	0.59	< 2	< 10	63	< 0.5	< 2	1.11	51	308	3.96	< 10	< 1	0.22	< 10	6.69	0.126	0.019	0.03	< 2	5	22	0.05	< 10
193001	0.00	-4	-5	< 2	< 4	< 5	< 2	< 0.2	< 0.5	34	240	< 1	35	< 2	33	1.17	< 2	< 10	154	< 0.5	< 2	0.92	15	31	2.7	< 10	< 1	0.22	< 10	0.73	0.415	0.049	0.04	< 2	6	73	0.15	< 10
193002	0.00	-4	-5	< 2	< 4	< 5	< 2	< 0.2	< 0.5	39	234	3	31	< 2	29	1.26	< 2	< 10	99	< 0.5	< 2	1.05	13	110	2.96	< 10	< 1	0.17	< 10	0.7	0.433	0.061	0.02	< 2	6	76	0.16	< 10
193003	6.00	-4	6	< 2	< 4	6	< 2	< 0.2	< 0.5	33	542	< 1	790	< 2	33	0.94	< 2	< 10	80	< 0.5	< 2	0.69	57	184	3.89	< 10	< 1	0.19	< 10	7.24	0.269	0.018	0.04	< 2	3	42	0.07	< 10
193004	15.00	8	7	< 2	8	7	< 2	< 0.2	< 0.5	4	186	2	26	4	20	2.21	< 2	< 10	22	0.8	< 2	3.11	6	72	0.55	< 10	< 1	0.02	< 10	0.29	0.389	0.003	0.06	< 2	4	45	0.17	< 10
193005	0.00	-4	-5	< 2	< 4	< 5	< 2	< 0.2	< 0.5	38	340	< 1	379	< 2	23	1	< 2	< 10	55	< 0.5	< 2	0.73	34	133	2.65	< 10	< 1	0.2	< 10	3.08	0.269	0.02	0.03	< 2	2	43	0.07	< 10
193006	#N/A	#N/A	#N/A	#N/A	N/A	N/A	N/A	N/A	N/A	N/A	N/A	N/A	N/A	N/A	N/A	N/A	N/A	N/A	N/A	N/A	N/A	N/A	N/A	N/A	N/A	N/A	N/A	N/A	N/A	N/A	N/A	N/A	N/A	N/A	N/A	N/A	N/A	N/A
193007	0.00	-4	-5	< 2	< 4	< 5	< 2	< 0.2	< 0.5	21	378	2	580	< 2	22	0.7	< 2	< 10	44	< 0.5	< 2	0.58	41	262	2.61	< 10	< 1	0.1	< 10	5.33	0.214	0.011	0.02	< 2	2	32	0.04	< 10
193008	15.00	9	6	3	9	6	3	< 0.2	< 0.5	271	202	< 1	95	< 2	19	1.71	< 2	< 10	36	< 0.5	< 2	1.57	28	142	3.27	< 10	< 1	0.09	< 10	0.56	0.524	0.02	0.29	< 2	9	30	0.12	< 10
193009	9.00	4	5	< 2	4	5	< 2	< 0.2	< 0.5	47	337	3	308	< 2	24	1.79	< 2	< 10	78	< 0.5	< 2	1.49	32	280	2.93	< 10	< 1	0.24	< 10	2.67	0.533	0.025	0.03	< 2	4	80	0.1	< 10
193010	0.00	-4	-5	< 2	< 4	< 5	< 2	< 0.2	< 0.5	41	316	< 1	394	< 2	19	1.27	< 2	< 10	121	< 0.5	< 2	0.88	37	264	2.92	< 10	< 1	0.35	< 10	3.23	0.31	0.025	0.03	< 2	3	45	0.09	< 10
193011	0.00	-4	-5	< 2	< 4	< 5	< 2	< 0.2	< 0.5	32	357	2	435	< 2	24	1	< 2	< 10	66	< 0.5	< 2	0.84	36	245	2.73	< 10	< 1	0.16	< 10	3.85	0.315	0.017	0.02	< 2	2	49	0.07	< 10
193012	5.00	5	-5	< 2	5	< 5	< 2	< 0.2	< 0.5	40	382	2	397	< 2	27	1.4	< 2	< 10	62	< 0.5	< 2	1.13	36	243	2.89	< 10	< 1	0.18	< 10	3.52	0.4	0.017	0.03	< 2	3	66	0.07	< 10
193013	0.00	-4	-5	< 2	< 4	< 5	< 2	< 0.2	< 0.5	32	206	< 1	328	< 2	16	2.22	< 2	< 10	112	< 0.5	< 2	1.24	34	469	2.9	< 10	< 1	0.53	< 10	3.31	0.433	0.012	0.02	< 2	4	81	0.07	< 10
193014	0.00	-4	-5	< 2	< 4	< 5	< 2	< 0.2	< 0.5	33	376	< 1	381	< 2	26	1.67	< 2	< 10	59	< 0.5	< 2	1.37	35	234	2.78	< 10	< 1	0.18	< 10	3.43	0.491	0.018	0.02	< 2	3	77	0.07	< 10
193015	5.00	-4	5	< 2	< 4	5	< 2	< 0.2	< 0.5	39	491	2	559	< 2	32	1.51	< 2	< 10	68	< 0.5	< 2	1.25	48	322	3.61	< 10	< 1	0.21	< 10	5.04	0.432	0.019	0.03	< 2	4	66	0.08	< 10
193016	0.00	-4	-5	< 2	< 4	< 5	< 2	< 0.2	1.6	118	1490	< 1	108	4	145	2.65	< 2	< 10	116	< 0.5	< 2	2.64	26	236	3.33	< 10	< 1	0.13	< 10	0.68	0.691	0.015	0.03	< 2	10	36	0.18	< 10
193017	0.00	-4	-5	< 2	< 4	< 5	< 2	< 0.2	< 0.5	47	330	3	230	< 2	24	2.48	< 2	< 10	68	< 0.5	< 2	2.05	27	230	2.79	< 10	< 1	0.2	< 10	2.12	0.724	0.028	0.03	< 2	4	114	0.1	< 10
193018	0.00	-4	-5	< 2	< 4	< 5	< 2	< 0.2	< 0.5	46	1040	< 1	1770	< 2	51	0.76	< 2	< 10	11	< 0.5	< 2	0.93	125	995	7.33	< 10	< 1	0.34	< 10	13.4	0.239	0.009	0.1	< 2	6	7	0.09	< 10
193019	13.00	7	6	< 2	7	6	< 2	< 0.2	< 0.5	95	320	< 1	207	< 2	30	1.01	< 2	< 10	120	< 0.5	< 2	1.23	34	293	3.43	< 10	< 1	0.34	< 10	1.81	0.301	0.031	0.05	< 2	7	27	0.19	< 10
193020	0.00	-4	-5	< 2	< 4	< 5	< 2	< 0.2	< 0.5	147	462	2	183	< 2	47	0.77	< 2	< 10	92	< 0.5	< 2	1.15	40	171	4.93	< 10	< 1	0.51	12	2.23	0.191	0.044	0.07	< 2	5	36	0.23	< 10
193021	0.00	-4	-5	< 2	< 4	< 5	< 2	< 0.2	< 0.5	147	458	< 1	230	< 2	39	0.67	< 2	< 10	104	< 0.5	< 2	0.98	44	201	4.84	< 10	< 1	0.47	< 10	2.51	0.153	0.039	0.04	< 2	4	25	0.2	< 10
193022	26.00	13	13	3	13	13	3	< 0.2	< 0.5	91	187	2	107	< 2	14	1.19	< 2	< 10	32	< 0.5	< 2	1.27	26	289	3.37	< 10	< 1	0.09	< 10	0.77	0.409	0.015	0.36	< 2	10	18	0.1	< 10
193023	0.00	-4	-5	< 2	< 4	< 5	< 2	< 0.2	< 0.5	119	485	< 1	226	< 2	39	0.53	< 2	< 10	47	< 0.5	< 2	0.83	43	168	4.62	< 10	< 1	0.32	< 10	2.51	0.144	0.036	0.05	< 2	4	23	0.19	< 10
193024	12.00	6	6	< 2	6	6	< 2	< 0.2	< 0.5	26	171	2	203	< 2	13	1.33	< 2	< 10	121	< 0.5	< 2	0.93	19	290	1.65	< 10	< 1	0.42	< 10	2.1	0.323	0.016	0.02	< 2	3	50	0.06	< 10
193025	9.00	4	5	< 2	4	5	< 2	< 0.2	< 0.5	50	320	< 1	256	< 2	25	2.22	< 2	< 10	70	< 0.5	< 2	1.73	28	129	2.92	< 10	< 1	0.21	< 10	2.07	0.633	0.031	0.03	< 2	3	103	0.1	< 10
193026	26.00	11	15	< 2	11	15	< 2	< 0.2	< 0.5	2	172	2	197	< 2	9	2.11	< 2	< 10	69	< 0.5	< 2	1.89	14	644	1.46	< 10	< 1	0.15	< 10	2	0.214	0.005	< 0.01	< 2	11	6	0.07	< 10
193027	0.00	-4	-5	< 2	< 4	< 5	< 2	< 0.2	< 0.5	120	554	< 1	239	< 2	39	0.46	< 2	< 10	41	< 0.5	< 2	1.06	44	173	4.75	< 10	< 1	0.26	< 10	2.7	0.148	0.036	0.04	< 2	4	29	0.19	< 10
193028	11.00	5	6	< 2	5	6	< 2	< 0.2	< 0.5	53	342	2	257	< 2	25	1.66	< 2	< 10	63	< 0.5	< 2	1.4	31	172	3.18	< 10	< 1	0.21	10	2.28	0.503	0.028	0.06	< 2	3	78	0.09	< 10
193040	0.00	-4	-5	< 2	N/A	N/A	N/A	N/A	N/A	N/A	N/A	N/A	N/A	N/A	N/A	N/A	N/A	N/A	N/A	N/A	N/A	N/A	N/A	N/A	N/A	N/A	N/A	N/A	N/A	N/A	N/A	N/A	N/A	N/A	N/A	N/A	N/A	N/A
193041	0.00	-4	-5	< 2	N/A	N/A	N/A	N/A	N/A	N/A	N/A	N/A	N/A	N/A	N/A	N/A	N/A	N/A	N/A	N/A	N/A	N/A	N/A	N/A	N/A	N/A	N/A	N/A	N/A	N/A	N/A	N/A	N/A	N/A	N/A	N/A	N/A	N/A
193042	0.00	-4	-5	< 2	N/A	N/A	N/A	N/A	N/A	N/A	N/A	N/A	N/A	N/A	N/A	N/A	N/A	N/A	N/A	N/A	N/A	N/A	N/A	N/A	N/A	N/A	N/A	N/A	N/A	N/A	N/A	N/A	N/A	N/A	N/A	N/A	N/A	N/A
193043	0.00	-4	-5	< 2	N/A	N/A	N/A	N/A	N/A	N/A	N/A	N/A	N/A	N/A	N/A	N/A	N/A	N/A	N/A	N/A	N/A	N/A	N/A	N/A	N/A	N/A	N/A	N/A	N/A	N/A	N/A	N/A	N/A	N/A	N/A	N/A	N/A	N/A
193044	0.00	-4	-5	< 2	N/A	N/A	N/A	N/A	N/A	N/A	N/A	N/A	N/A	N/A	N/A	N/A	N/A	N/A	N/A	N/A	N/A	N/A	N/A	N/A	N/A	N/A	N/A	N/A	N/A	N/A	N/A	N/A	N/A	N/A	N/A	N/A	N/A	N/A
193045	0.00	-4	-5	< 2	N/A	N/A	N/A	N/A	N/A	N/A	N/A	N/A	N/A	N/A	N/A	N/A	N/A	N/A	N/A	N/A	N/A	N/A	N/A	N/A	N/A	N/A	N/A	N/A	N/A	N/A	N/A	N/A	N/A	N/A	N/A	N/A	N/A	N/A
193046	0.00	-4	-5	< 2	N/A	N/A	N/A	N/A	N/A	N/A	N/A	N/A	N/A	N/A	N/A	N/A	N/A	N/A	N/A	N/A	N/A	N/A	N/A	N/A	N/A	N/A	N/A	N/A	N/A	N/A	N/A	N/A	N/A	N/A	N/A	N/A	N/A	N/A
193047	0.00	-4	-5	< 2	N/A	N/A	N/A	N/A	N/A	N/A	N/A	N/A	N/A	N/A	N/A	N/A	N/A	N/A	N/A	N/A	N/A	N/A	N/A	N/A	N/A	N/A	N/A	N/A	N/A	N/A	N/A	N/A	N/A	N/A	N/A	N/A	N/A	N/A
193048	0.00	-4	-5	< 2	N/A	N/A	N/A	N/A	N/A	N/A	N/A	N/A	N/A	N/A	N/A	N/A	N/A	N/A	N/A	N/A	N/A	N/A	N/A	N/A	N/A	N/A	N/A	N/A	N/A	N/A	N/A	N/A	N/A	N/A	N/A	N/A	N/A	N/A
193049	0.00	-4	-5	< 2	N/A	N/A	N/A	N/A	N/A	N/A	N/A	N/A	N/A	N/A	N/A	N/A	N/A	N/A	N/A	N/A	N/A	N/A	N/A	N/A	N/A	N/A	N/A	N/A	N/A	N/A	N/A	N/A	N/A	N/A	N/A	N/A	N/A	N/A
193050	0.00	-4	-5	< 2	N/A	N/A	N/A	N/A	N/A	N/A	N/A	N/A	N/A	N/A	N/A	N/A	N/A	N/A	N/A	N/A	N/A	N/A	N/A	N/A	N/A	N/A	N/A	N/A	N/A	N/A	N/A	N/A	N/A	N/A	N/A	N/A	N/A	N/A
12901	740.00	597	143	74	1	-0.5	1660	508	3	4810	8	32	0.74	-2	-10	49	-0.5	-2	0.48	180	214	6.08	-10	-1	0.13	-10	7.45	0.203	0.018	1.71	-2	2	30	0.05	-10	-10	36	-10
12902	30.00	20	10	4	-0.2	-0.5	649	246	1	412	-2	51	2.28	-2	-10	15	-0.5	-2	2.3	54	455	3.96	-10	-1	0.07	-10	1.36	0.687	0.036	0.86	-2	13	22	0.2	-10	-10	128	-10
177501	50.00	7	43	-2	-0.2	-0.5	38	428	-1	1400	6	28	1.96	-2	-10	95	-0.5	-2	0.32	65	509	3.51	-10	-1	0.07	12	11.8	0.097	0.046	0.01	-2	4	21	0.12	-10	-10	65	-10
177502	22.00	7	15	-2	-0.2	-0.5	103	502	-1	1160	4	41	1.94	-2	-10	107	-0.5	-2	0.36	73	400	4.42	-10	-1	0.08	16	9.12	0.104	0.04	0.01	-2	4	22	0.14	-10	-10	94	-10
177503	15.00	8	7	4	1.1	-0.5	891	190	1	442	-2	85	1.45	-2	-10	34	-0.5	-2	0.06	107	627	11	10	-1	1.43	-10	2.29	0.067	0.019	6.63	-2	10	3	0.22	-10	-10	166	-10
181501	38.00	15	23	4	-0.2	-0.5	164	648	-1	788	3	53	2.17	-2	-10	87	-0.5	-2	0.71	77	245	6.12	10	-1	0.12	27	4.86	0.236	0.084	0.03	-2	4	42	0.2	-10	-10	192	-10
181502	32.00	14	18	4	-0.2	-0.5	126	716	1	1110	3	54	1.46	-2	-10	84	-0.5	-2	0.65	90	357	6.08	-10	-1	0.24	30	8.01	0.221	0.081	0.04	-2	4	35	0.21	-10	-10	146	-10
181503	7.00	7	-5	10	-0.2	-0.5	286	608	-1	870	5	61	1.2	-2	-10	97	-0.5	-2	1.14	72	413	5.14	-10	-1	0.17	21	5.23	0.129	0.211	0.04	-2	7	22	0.12	-10	-10	102	-10
181504	0.00	-4	-5	3	-0.2	-0.5	140	270	5	156	2	26	2.15	-2	-10	49	-0.5	-2	1.47	32	176	2.09	-10	-1	0.07	11	1.02	0.447	0.109	0.02	-2	6	110	0.07	-10	-10	44	-10
181505	0.00	-4	-5	-2	-0.2	-0.5	100	370	-1	141	2	58	1.85	-2	-10	106	-0.5	-2	0.85	31	103	2.77	-10	-1	0.22	15	1.9	0.18	0.062	0.01	-2	6	33	0.09	-10	-10	40	-10
181751	0.00	-4	-5	-2	-0.2	-0.5	3	621	2	1190	-2	6	0.29	-2	-10	-10	-0.5	-2	0.65	63	338	4.21	-10	-1	-0.01	-10	11.8	0.087	0.006	-0.01	-2	4	6	0.03	-10	-10	21	-10
181752	0.00	-4	-5	-2	-0.2	-0.5	63	331	3	47	-2	26	1.34	-2	-10	40	-0.5	-2	1.57	27	265	5.66	-10	-1	0.15	-10	1.09	0.466	0.038	-0.01	-2	18	25	0.24	-10	-10	286	-10
181753	0.00	-4	-5	-2	-0.2	-0.5	30	450	3	35	13	45	1.28	-2	-10	31	-0.5	-2	0.73	15	135	1.94	-10	-1	0.21	-10	0.99	0.145	0.029	-0.01	-2	4	63	0.12	-10	-10	38	-10
181754	5.00	5	-5	-2	-0.2	-0.5	5	607	-1	1420	-2	33	0.71	-2	-10	14	-0.5	-2	0.39	89	937	4.61	-10	-1	0.06	-10	12.4	0.076	0.003	0.02	-2	4	4	0.02	-10	-10	32	-10
181755	15.00	7	8	-2	-0.2	-0.5	172	269	-1	47	-2	17	3.96	-2	-10	14	-0.5	-2	3.46	19	207	3.92	10	-1	0.04	-10	1.27	1.01	0.017	0.04	-2	14	54	0.15	-10	-10	167	-10
181756	282.00	266	16	32	0.4	-0.5	634	337	3	3300	6	21	0.89	-2	-10	84	-0.5	-2	0.49	129	289	4.47	-10	-1	0.2	-10	4.67	0.211	0.013	1.27	-2	2	29	0.05	-10	-10	38	-10
183001	0.00	-4	-5	-2	-0.2	-0.5	12	579	-1	546	-2	6	0.58	-2	-10	-10	-0.5	-2	1.18	57	434	4.29	-10	-1	-0.01	-10	8.03	0.093	0.007	-0.01	-2	6	6	0.04	-10	-10	45	-10
183002	0.00	-4	-5	-2	-0.2	-0.5	178	623	-1	42	4	55	2.42	-2	-10	161	-0.5	-2	2.4	29	42	5.59	10	-1	0.29	10	1.34	0.473	0.058	0.06	-2	13	67	0.27	-10	-10	239	-10
183251	31.00	12	19	3	-0.2	-0.5	122	693	2	1010	5	59	1.53	-2	-10	111	-0.5	-2	0.61	89	327	6.22	-10	-1	0.24	29	7.06	0.185	0.079	0.03	-2	4	31	0.22	-10	-10	154	-10
183252	44.00	18	26	5	-0.2	-0.5	155	641	-1	1130	4	52	1.73	-2	-10	95	-0.5	-2	0.71	90	309	5.63	10	-1	0.24	37	6.91	0.222	0.102	0.03	-2	4	36	0.23	-10	-10	160	-10
183253	26.00	11	15	2	-0.2	-0.5	105	607	5	833	5	52	1.67	-2	-10	78	-0.5	-2	0.84	74	361	5.6	-10	-1	0.17	16	5.66	0.308	0.044	0.03	-2	4	52	0.21	-10	-10	146	-10
183254	0.00	-4	-5	2	-0.2	-0.5	123	280	-1	148	2	27	1.85	-2	-10	35	-0.5	-2	1.46	27	66	2.01	-10	-1	0.08	12	0.91	0.384	0.185	0.01	-2	5	95	0.05	-10	-10	35	-10
183255	0.00	-4	-5	-2	-0.2	-0.5	199	278	4	195	3	43	2.72	-2	-10	71	-0.5	-2	1.71	31	187	2.34	-10	-1	0.14	-10	1.73	0.548	0.037	0.02	-2	7	136	0.07	-10	-10	45	-10
183256	0.00	-4	-5	-2	-0.2	-0.5	186	214	-1	49	7	44	1.66	4	-10	419	-0.5	-2	0.54	13	80	4.37	-10	-1	0.29	100	1.12	0.192	0.066	0.04	-2	5	27	0.15	-10	-10	68	-10
183257	899.00	710	189	37	0.8	-0.5	999	336	2	1210	10	24	1.86	-2	-10	70	-0.5	-2	0.51	46	399	7.36	-10	-1	0.11	-10	4.6	0.225	0.03	0.13	-2	3	33	0.1	-10	-10	84	-10
191101	0.00	-4	-5	-2	-0.2	-0.5	25	262	2	445	-2	15	1.86	-2	-10	87	-0.5	-2	0.79	40	430	2.94	-10	-1	0.27	-10	4.45	0.332	0.012	0.02	-2	2	49	0.04	-10	-10	31	-10
191102	5.00	5	-5	-2	-0.2	-0.5	34	374	-1	469	-2	25	1.24	-2	-10	47	-0.5	-2	0.93	39	186	2.87	-10	-1	0.18	-10	3.85	0.353	0.018	0.02	-2	2	56	0.06	-10	-10	38	-10
191103	0.00	-4	-5	4	-0.2	-0.5	181	235	11	127	3	42	4.72	-2	-10	31	0.6	-2	4.51	42	298	3.72	10	-1	0.05	-10	0.35	0.948	0.035	1.31	-2	5	119	0.15	-10	-10	73	-10
191104	0.00	-4	-5	-2	-0.2	-0.5	31	307	-1	357	-2	20	0.92	-2	-10	57	-0.5	-2	0.76	30	217	2.4	-10	-1	0.15	-10	3.24	0.285	0.017	0.02	-2	2	44	0.06	-10	-10	36	-10
191105	6.00	6	-5	-2	-0.2	-0.5	34	348	3	408	-2	23	1.77	-2	-10	58	-0.5	-2	1.38	35	262	2.7	-10	-1	0.2	-10	3.5	0.512	0.016	0.03	-2	3	83	0.06	-10	-10	37	-10
191106	10.00	5	5	-2	-0.2	-0.5	38	373	-1	423	-2	23	1.65	-2	-10	86	-0.5	-2	1.29	38	251	3.06	-10	-1	0.27	-10	3.66	0.467	0.019	0.03	-2	3	73	0.08	-10	-10	48	-10
191107	20.00	12	8	-2	-0.2	-0.5	28	325	3	427	-2	22	1.67	-2	-10	49	-0.5	-2	1.28	35	245	2.55	-10	-1	0.15	-10	3.56	0.507	0.014	0.02	-2	2	83	0.05	-10	-10	30	-10
191108	16.00	9	7	-2	-0.2	-0.5	36	386	-1	419	-2	25	1.17	-2	-10	50	-0.5	-2	1.01	38	192	3.13	-10	-1	0.13	-10	3.69	0.364	0.016	0.03	-2	3	58	0.06	-10	-10	45	-10
191109	0.00	-4	-5	-2	-0.2	-0.5	37	316	3	312	-2	21	1.72	-2	-10	56	-0.5	-2	1.37	29	317	2.49	-10	-1	0.23	-10	2.8	0.493	0.025	0.03	-2	3	84	0.09	-10	-10	60	-10
191110	0.00	-4	-5	-2	-0.2	-0.5	23	344	-1	484	-2	21	0.67	-2	-10	51	-0.5	-2	0.57	37	181	2.61	-10	-1	0.11	-10	4.32	0.212	0.013	0.02	-2	2	30	0.05	-10	-10	31	-10

191111	12.00	6	6	-2	-0.2	-0.5	41	368	2	341	-2	25	1.79	-2	-10	56	-0.5	-2	1.55	33	311	2.84	-10	-1	0.19	-10	3.25	0.535	0.019	0.03	-2	4	82	0.07	-10	-10	51	-10
191112	0.00	-4	-5	-2	-0.2	-0.5	33	395	-1	495	-2	27	1.43	-2	-10	71	-0.5	-2	1.16	41	259	3.04	-10	-1	0.19	-10	4.44	0.429	0.015	0.02	-2	3	66	0.06	-10	-10	35	-10
191113	0.00	-4	-5	-2	-0.2	-0.5	31	374	2	493	-2	24	1.37	-2	-10	64	-0.5	-2	1.05	40	259	2.98	-10	-1	0.22	-10	4.37	0.402	0.016	0.02	-2	3	63	0.05	-10	-10	35	-10
191114	7.00	7	-5	-2	-0.2	-0.5	29	403	-1	761	-2	23	0.39	-2	-10	30	-0.5	-2	0.34	48	165	2.81	-10	-1	0.07	-10	6.98	0.121	0.008	0.03	-2	2	18	0.02	-10	-10	15	-10
191115	6.00	6	-5	10	-0.2	-0.5	511	444	-1	108	-2	56	1.55	-2	-10	40	-0.5	-2	1.57	44	255	6.02	-10	-1	0.25	-10	1.02	0.481	0.022	0.93	-2	20	31	0.24	-10	-10	239	-10
191116	0.00	-4	-5	-2	-0.2	-0.5	126	553	2	259	-2	42	0.47	-2	-10	49	-0.5	-2	0.86	45	212	4.9	-10	-1	0.31	-10	2.87	0.136	0.036	0.04	-2	4	25	0.2	-10	-10	115	-10
191117	0.00	-4	-5	-2	-0.2	-0.5	132	477	-1	256	-2	42	0.61	-2	-10	110	-0.5	-2	0.99	44	174	4.85	-10	-1	0.45	-10	2.91	0.145	0.041	0.07	-2	4	27	0.23	-10	-10	128	-10
191118	4.00	4	-5	6	-0.2	-0.5	130	274	3	55	-2	27	1.09	-2	-10	27	-0.5	-2	1.06	18	181	2.98	-10	-1	0.1	-10	0.57	0.411	0.038	0.24	-2	11	14	0.26	-10	-10	150	-10
191119	0.00	-4	-5	-2	-0.2	-0.5	115	556	-1	291	-2	40	0.48	-2	-10	64	-0.5	-2	0.85	46	183	4.59	-10	-1	0.35	-10	3.22	0.111	0.033	0.06	-2	3	24	0.2	-10	-10	108	-10
191120	4.00	4	-5	-2	-0.2	-0.5	60	394	3	325	-2	28	1.47	-2	-10	63	-0.5	-2	1.29	36	234	3.24	-10	-1	0.25	-10	2.93	0.421	0.025	0.04	-2	3	72	0.11	-10	-10	66	-10
191121	14.00	9	5	-2	-0.2	-0.5	14	583	-1	1100	-2	28	0.28	-2	-10	28	-0.5	-2	0.23	70	161	3.91	-10	-1	0.06	-10	11.2	0.075	0.007	0.02	-2	2	12	0.02	-10	-10	9	-10
191122	5.00	-4	5	-2	-0.2	-0.5	39	655	1	583	-2	17	0.59	-2	-10	63	-0.5	-2	1.11	51	308	3.96	-10	-1	0.22	-10	6.69	0.126	0.019	0.03	-2	5	22	0.05	-10	-10	45	-10
193001	0.00	-4	-5	-2	-0.2	-0.5	34	240	-1	35	-2	33	1.17	-2	-10	154	-0.5	-2	0.92	15	31	2.7	-10	-1	0.22	-10	0.73	0.415	0.049	0.04	-2	6	73	0.15	-10	-10	96	-10
193002	0.00	-4	-5	-2	-0.2	-0.5	39	234	3	31	-2	29	1.26	-2	-10	99	-0.5	-2	1.05	13	110	2.96	-10	-1	0.17	-10	0.7	0.433	0.061	0.02	-2	6	76	0.16	-10	-10	111	-10
193003	6.00	-4	6	-2	-0.2	-0.5	33	542	-1	790	-2	33	0.94	-2	-10	80	-0.5	-2	0.69	57	184	3.89	-10	-1	0.19	-10	7.24	0.269	0.018	0.04	-2	3	42	0.07	-10	-10	37	-10
193004	15.00	8	7	-2	-0.2	-0.5	4	186	2	26	4	20	2.21	-2	-10	22	0.8	-2	3.11	6	72	0.55	-10	-1	0.02	-10	0.29	0.389	0.003	0.06	-2	4	45	0.17	-10	-10	22	-10
193005	0.00	-4	-5	-2	-0.2	-0.5	38	340	-1	379	-2	23	1	-2	-10	55	-0.5	-2	0.73	34	133	2.65	-10	-1	0.2	-10	3.08	0.269	0.02	0.03	-2	2	43	0.07	-10	-10	45	-10
193007	0.00	-4	-5	-2	-0.2	-0.5	21	378	2	580	-2	22	0.7	-2	-10	44	-0.5	-2	0.58	41	262	2.61	-10	-1	0.1	-10	5.33	0.214	0.011	0.02	-2	2	32	0.04	-10	-10	23	-10
193008	15.00	9	6	3	-0.2	-0.5	271	202	-1	95	-2	19	1.71	-2	-10	36	-0.5	-2	1.57	28	142	3.27	-10	-1	0.09	-10	0.56	0.524	0.02	0.29	-2	9	30	0.12	-10	-10	141	-10
193009	9.00	4	5	-2	-0.2	-0.5	47	337	3	308	-2	24	1.79	-2	-10	78	-0.5	-2	1.49	32	280	2.93	-10	-1	0.24	-10	2.67	0.533	0.025	0.03	-2	4	80	0.1	-10	-10	69	-10
193010	0.00	-4	-5	-2	-0.2	-0.5	41	316	-1	394	-2	19	1.27	-2	-10	121	-0.5	-2	0.88	37	264	2.92	-10	-1	0.35	-10	3.23	0.31	0.025	0.03	-2	3	45	0.09	-10	-10	57	-10
193011	0.00	-4	-5	-2	-0.2	-0.5	32	357	2	435	-2	24	1	-2	-10	66	-0.5	-2	0.84	36	245	2.73	-10	-1	0.16	-10	3.85	0.315	0.017	0.02	-2	2	49	0.07	-10	-10	39	-10
193012	5.00	5	-5	-2	-0.2	-0.5	40	382	2	397	-2	27	1.4	-2	-10	62	-0.5	-2	1.13	36	243	2.89	-10	-1	0.18	-10	3.52	0.4	0.017	0.03	-2	3	66	0.07	-10	-10	43	-10
193013	0.00	-4	-5	-2	-0.2	-0.5	32	206	-1	328	-2	16	2.22	-2	-10	112	-0.5	-2	1.24	34	469	2.9	-10	-1	0.53	-10	3.31	0.433	0.012	0.02	-2	4	81	0.07	-10	-10	62	-10
193014	0.00	-4	-5	-2	-0.2	-0.5	33	376	-1	381	-2	26	1.67	-2	-10	59	-0.5	-2	1.37	35	234	2.78	-10	-1	0.18	-10	3.43	0.491	0.018	0.02	-2	3	77	0.07	-10	-10	46	-10
193015	5.00	-4	5	-2	-0.2	-0.5	39	491	2	559	-2	32	1.51	-2	-10	68	-0.5	-2	1.25	48	322	3.61	-10	-1	0.21	-10	5.04	0.432	0.019	0.03	-2	4	66	0.08	-10	-10	48	-10
193016	0.00	-4	-5	-2	-0.2	1.6	118	1490	-1	108	4	145	2.65	-2	-10	116	-0.5	-2	2.64	26	236	3.33	-10	-1	0.13	-10	0.68	0.691	0.015	0.03	-2	10	36	0.18	-10	-10	159	-10
193017	0.00	-4	-5	-2	-0.2	-0.5	47	330	3	230	-2	24	2.48	-2	-10	68	-0.5	-2	2.05	27	230	2.79	-10	-1	0.2	-10	2.12	0.724	0.028	0.03	-2	4	114	0.1	-10	-10	73	-10
193018	0.00	-4	-5	-2	-0.2	-0.5	46	1040	-1	1770	-2	51	0.76	-2	-10	11	-0.5	-2	0.93	125	995	7.33	-10	-1	0.34	-10	13.4	0.239	0.009	0.1	-2	6	7	0.09	-10	-10	57	-10
193019	13.00	7	6	-2	-0.2	-0.5	95	320	-1	207	-2	30	1.01	-2	-10	120	-0.5	-2	1.23	34	293	3.43	-10	-1	0.34	-10	1.81	0.301	0.031	0.05	-2	7	27	0.19	-10	-10	126	-10
193020	0.00	-4	-5	-2	-0.2	-0.5	147	462	2	183	-2	47	0.77	-2	-10	92	-0.5	-2	1.15	40	171	4.93	-10	-1	0.51	12	2.23	0.191	0.044	0.07	-2	5	36	0.23	-10	-10	144	-10
193021	0.00	-4	-5	-2	-0.2	-0.5	147	458	-1	230	-2	39	0.67	-2	-10	104	-0.5	-2	0.98	44	201	4.84	-10	-1	0.47	-10	2.51	0.153	0.039	0.04	-2	4	25	0.2	-10	-10	122	-10
193022	26.00	13	13	3	-0.2	-0.5	91	187	2	107	-2	14	1.19	-2	-10	32	-0.5	-2	1.27	26	289	3.37	-10	-1	0.09	-10	0.77	0.409	0.015	0.36	-2	10	18	0.1	-10	-10	104	-10
193023	0.00	-4	-5	-2	-0.2	-0.5	119	485	-1	226	-2	39	0.53	-2	-10	47	-0.5	-2	0.83	43	168	4.62	-10	-1	0.32	-10	2.51	0.144	0.036	0.05	-2	4	23	0.19	-10	-10	114	-10
193024	12.00	6	6	-2	-0.2	-0.5	26	171	2	203	-2	13	1.33	-2	-10	121	-0.5	-2	0.93	19	290	1.65	-10	-1	0.42	-10	2.1	0.323	0.016	0.02	-2	3	50	0.06	-10	-10	38	-10
193025	9.00	4	5	-2	-0.2	-0.5	50	320	-1	256	-2	25	2.22	-2	-10	70	-0.5	-2	1.73	28	129	2.92	-10	-1	0.21	-10	2.07	0.633	0.031	0.03	-2	3	103	0.1	-10	-10	79	-10
193026	26.00	11	15	-2	-0.2	-0.5	2	172	2	197	-2	9	2.11	-2	-10	69	-0.5	-2	1.89	14	644	1.46	-10	-1	0.15	-10	2	0.214	0.005	-0.01	-2	11	6	0.07	-10	-10	68	-10
193027	0.00	-4	-5	-2	-0.2	-0.5	120	554	-1	239	-2	39	0.46	-2	-10	41	-0.5	-2	1.06	44	173	4.75	-10	-1	0.26	-10	2.7	0.148	0.036	0.04	-2	4	29	0.19	-10	-10	104	-10
193028	11.00	5	6	-2	-0.2	-0.5	53	342	2	257	-2	25	1.66	-2	-10	63	-0.5	-2	1.4	31	172	3.18	-10	-1	0.21	10	2.28	0.503	0.028	0.06	-2	3	78	0.09	-10	-10	81	-10
195001	31.00	17	14	6	-0.2	-0.5	2050	299	11	143	10	36	1.43	-2	-10	-10	-0.5	-2	2.2	32	330	7.36	-10	-1	0.02	13	2.44	0.425	0.124	1.2	-2	33	17	0.19	-10	-10	264	-10
195002	0.00	-4	-5	4	-0.2	-0.5	829	1010	290	149	6	65	3.15	-2	11	19	-0.5	-2	3.49	42	241	8.8	10	-1	0.06	-10	0.95	0.636	0.022	0.56	-2	16	45	0.22	-10	-10	208	-10
195003	0.00	-4	-5	13	-0.2	-0.5	1070	161	1	73	-2	13	2.48	-2	-10	54	-0.5	-2	2.2	56	34	5.18	10	-1	0.1	-10	0.66	0.635	0.011	0.82	-2	16	162	0.11	-10	-10	115	-10
195004	0.00	-4	-5	-2	-0.2	-0.5	52	408	2	72	7	32	2.15	-2	-10	108	-0.5	-2	1.88	22	125	2.39	-10	-1	0.49	-10	1.95	0.531	0.015	0.06	-2	8	93	0.07	-10	-10	40	-10
195005	0.00	-4	-5	2	-0.2	-0.5	250	154	-1	17	-2	15	1.39	-2	-10	55	-0.5	-2	1.72	17	39	3.4	-10	-1	0.06	11	0.5	0.46	0.138	0.32	-2	7	85	0.16	-10	-10	159	-10
195006	0.00	-4	-5	-2	-0.2	-0.5	2	707	3	1470	-2	17	0.15	-2	-10	-10	-0.5	-2	0.34	69	194	3.95	-10	-1	-0.01	-10	15.2	0.036	0.003	-0.01	-2	2	3	-0.01	-10	-10	10	-10
195007	4.00	4	-5	-2	-0.2	-0.5	12	514	-1	954	-2	12	0.5	-2	-10	-10	-0.5	-2	0.97	56	473	3.58	-10	-1	0.02	-10	8.38	0.123	0.004	0.03	-2	5	14	0.03	-10	-10	34	-10
195065	0.00	-4	-5	20	0.2	-0.5	913	103	-1	186	-2	32	0.64	-2	-10	116	-0.5	-2	0.22	46	81	2.56	-10	-1	0.2	-10	0.38	0.199	0.002	0.65	-2	2	26	0.13	-10	-10	61	-10
195066	15.00	6	9	-2	-0.2	-0.5	57	488	-1	358	-2	20	0.95	-2	-10	42	-0.5	-2	1.09	40	132	3.63	-10	-1	0.19	-10	3.24	0.265	0.026	0.03	-2	4	43	0.06	-10	-10	59	-10
195067	1055.00	860	195	103	2.1	-0.5	3100	483	-1	8190	4	33	0.58	-2	-10	49	-0.5	-2	0.39	223	201	6.6	-10	-1	0.17	-10	6.07	0.155	0.017	2.66	-2	2	24	0.05	-10	-10	40	-10
195068	538.00	438	100	44	1.2	-0.5	1560	347	-1	3730	2	23	0.59	-2	-10	50	-0.5	-2	0.42	117	168	4.27	-10	-1	0.15	-10	4.45	0.157	0.018	1.16	-2	2	26	0.05	-10	-10	40	-10
195301	0.00	-4	-5	-2	-0.2	-0.5	59	1150	1	53	9	61	1.94	3	-10	214	-0.5	-2	2.39	69	123	5.54	10	-1	0.23	74	1.58	0.35	0.391	0.04	-2	10	164	0.15	-10	-10	160	-10
195302	43.00	16	27	4	-0.2	-0.5	150	700	3	999	5	56	1.57	-2	-10	124	-0.5	-2	0.66	87	334	6.2	10	-1	0.26	31	6.67	0.194	0.093	0.05	-2	5	32	0.25	-10	-10	180	-10
195303	11.00	5	6	-2	-0.2	-0.5	56	801	-1	1670	-2	27	0.4	-2	-10	12	-0.5	-2	0.24	100	254	4.6	-10	-1	0.01	-10	16.3	0.052	0.011	0.02	-2	4	3	0.02	-10	-10	18	-10
195304	0.00	-4	-5	-2	-0.2	-0.5	238	539	2	223	-2	50	2.67	-2	-10	71	-0.5	-2	1.35	42	221	3.86	-10	-1	0.08	-10	2.16	0.41	0.047	0.03	-2	8	116	0.11	-10	-10	75	-10
195305	0.00	-4	-5	3	-0.2	-0.5	113	461	-1	270	3	41	2.12	-2	-10	85	-0.5	-2	1.39	37	189	2.75	-10	-1	0.09	-10	1.95	0.393	0.038	0.06	-2	7	105	0.09	-10	-10	60	-10
195306	4.00	4	-5	20	-0.2	-0.5	157	1070	14	121	14	87	2.15	-2	-10	96	-0.5	-2	1.14	69	476	5.45	-10	-1	0.38	19	1.44	0.232	0.069	0.05	-2	11	54	0.19	-10	-10	211	-10
195307	0.00	-4	-5	5	-0.2	-0.5	227	390	-1	189	2	42	1.94	-2	-10	58	-0.5	-2	1.44	48	73	3.35	-10	-1	0.14	13	1.48	0.302	0.169	0.02	-2	7	65	0.1	-10	-10	61	-10
195308	0.00	-4	-5	5	-0.2	-0.5	239	346	3	225	3	46	2.37	-2	-10	75	-0.5	-2	1.23	49	117	3.18	-10	-1	0.13	13	1.59	0.378	0.088	0.02	-2	6	111	0.09	-10	-10	57	-10
195309	0.00	-4	-5	-2	-0.2	-0.5	41	478	-1	79	7	60	2.15	-2	-10	132	-0.5	-2	1.72	28	188	3.88	-10	-1	0.24	25	1.72	0.408	0.082	0.02	-2	9	98	0.18	-10	-10	107	-10

Appendix 2

- Fire assays.
- Major and trace element concentrations.

Final Report
Activation Laboratories

Element:	Pd	Pt	Au	Ag	Cd	Cu	Mn	Mo	Ni	Pb	Zn	Al	As	B	Ba	Be	Bi	Ca	Co	Cr	Fe	Ga	Hg	K	La	Mg	Na	P	S	Sb	Sc	Sr	Ti	Tl	U	V	W
Units:	ppb	ppb	ppb	ppm	ppm	ppm	ppm	ppm	ppm	ppm	ppm	%	ppm	ppm	ppm	ppm	ppm	%	ppm	ppm	%	ppm	ppm	%	ppm	%	%	%	%	ppm	ppm	ppm	%	ppm	ppm	ppm	ppm
Detection Limit:	4	5	2	0.2	0.5	1	5	1	1	2	2	0.01	2	10	10	0.5	2	0.01	1	1	0.01	10	1	0.01	10	0.01	0.001	0.001	0.01	2	1	1	0.01	10	10	1	10
Reference Method:	FA-MS	FA-MS	FA-MS	AR-ICP	AR-ICP	AR-ICP	AR-ICP	AR-ICP	AR-ICP	AR-ICP	AR-ICP	AR-ICP	AR-ICP	AR-ICP	AR-ICP	AR-ICP	AR-ICP	AR-ICP	AR-ICP	AR-ICP	AR-ICP	AR-ICP	AR-ICP	AR-ICP	AR-ICP	AR-ICP	AR-ICP	AR-ICP	AR-ICP	AR-ICP	AR-ICP	AR-ICP	AR-ICP	AR-ICP	AR-ICP	AR-ICP	AR-ICP
Client I.D.																																					
FF SSC 181501	15	23	4	< 0.2	< 0.5	164	648	< 1	788	3	53	2.17	< 2	< 10	87	< 0.5	< 2	0.71	77	245	6.12	10	< 1	0.12	27	4.86	0.236	0.084	0.03	< 2	4	42	0.2	< 10	< 10	192	< 10
FF SSC 181502	14	18	4	< 0.2	< 0.5	126	716	1	1110	3	54	1.46	< 2	< 10	84	< 0.5	< 2	0.65	90	357	6.08	< 10	< 1	0.24	30	8.01	0.221	0.081	0.04	< 2	4	35	0.21	< 10	< 10	146	< 10
FF SSC 181503	7	< 5	10	< 0.2	< 0.5	286	608	< 1	870	5	61	1.2	< 2	< 10	97	< 0.5	< 2	1.14	72	413	5.14	< 10	< 1	0.17	21	5.23	0.129	0.211	0.04	< 2	7	22	0.12	< 10	< 10	102	< 10
FF SSC 181504	< 4	< 5	3	< 0.2	< 0.5	140	270	5	156	2	26	2.15	< 2	< 10	49	< 0.5	< 2	1.47	32	176	2.09	< 10	< 1	0.07	11	1.02	0.447	0.109	0.02	< 2	6	110	0.07	< 10	< 10	44	< 10
FF SSC 181505	< 4	< 5	< 2	< 0.2	< 0.5	100	370	< 1	141	2	58	1.85	< 2	< 10	106	< 0.5	< 2	0.85	31	103	2.77	< 10	< 1	0.22	15	1.9	0.18	0.062	0.01	< 2	6	33	0.09	< 10	< 10	40	< 10
FF RGB 181751	< 4	< 5	< 2	< 0.2	< 0.5	3	621	2	1190	< 2	6	0.29	< 2	< 10	< 10	< 0.5	< 2	0.65	63	338	4.21	< 10	< 1	< 0.01	< 10	11.8	0.087	0.006	< 0.01	< 2	4	6	0.03	< 10	< 10	21	< 10
FF RGB 181752	< 4	< 5	< 2	< 0.2	< 0.5	63	331	3	47	< 2	26	1.34	< 2	< 10	40	< 0.5	< 2	1.57	27	265	5.66	< 10	< 1	0.15	< 10	1.09	0.466	0.038	< 0.01	< 2	18	25	0.24	< 10	< 10	286	< 10
FF RCP 181753	< 4	< 5	< 2	< 0.2	< 0.5	30	450	3	35	13	45	1.28	< 2	< 10	31	< 0.5	< 2	0.73	15	135	1.94	< 10	< 1	0.21	< 10	0.99	0.145	0.029	< 0.01	< 2	4	63	0.12	< 10	< 10	38	< 10
FF RGB 181754	5	< 5	< 2	< 0.2	< 0.5	5	607	< 1	1420	< 2	33	0.71	< 2	< 10	14	< 0.5	< 2	0.39	89	937	4.61	< 10	< 1	0.06	< 10	12.4	0.076	0.003	0.02	< 2	4	4	0.02	< 10	< 10	32	< 10
FF RGB 181755	7	8	< 2	< 0.2	< 0.5	172	269	< 1	47	< 2	17	3.96	< 2	< 10	14	< 0.5	< 2	3.46	19	207	3.92	10	< 1	0.04	< 10	1.27	1.01	0.017	0.04	< 2	14	54	0.15	< 10	< 10	167	< 10
FF RGB 181756	266	16	32	0.4	< 0.5	634	337	3	3300	6	21	0.89	< 2	< 10	84	< 0.5	< 2	0.49	129	289	4.47	< 10	< 1	0.2	< 10	4.67	0.211	0.013	1.27	< 2	2	29	0.05	< 10	< 10	38	< 10
FF RGB 183001	< 4	< 5	< 2	< 0.2	< 0.5	12	579	< 1	546	< 2	6	0.58	< 2	< 10	< 10	< 0.5	< 2	1.18	57	434	4.29	< 10	< 1	< 0.01	< 10	8.03	0.093	0.007	< 0.01	< 2	6	6	0.04	< 10	< 10	45	< 10
FF RGB 183002	< 4	< 5	< 2	< 0.2	< 0.5	178	623	< 1	42	4	55	2.42	< 2	< 10	161	< 0.5	< 2	2.4	29	42	5.59	10	< 1	0.29	10	1.34	0.473	0.058	0.06	< 2	13	67	0.27	< 10	< 10	239	< 10
FF RGB 12901	597	143	74	1	< 0.5	1660	508	3	4810	8	32	0.74	< 2	< 10	49	< 0.5	< 2	0.48	180	214	6.08	< 10	< 1	0.13	< 10	7.45	0.203	0.018	1.71	< 2	2	30	0.05	< 10	< 10	36	< 10
FF RGB 12902	20	10	4	< 0.2	< 0.5	649	246	1	412	< 2	51	2.28	< 2	< 10	15	< 0.5	< 2	2.3	54	455	3.96	< 10	< 1	0.07	< 10	1.36	0.687	0.036	0.86	< 2	13	22	0.2	< 10	< 10	128	< 10
FF SSC 183251	12	19	3	< 0.2	< 0.5	122	693	2	1010	5	59	1.53	< 2	< 10	111	< 0.5	< 2	0.61	89	327	6.22	< 10	< 1	0.24	29	7.06	0.185	0.079	0.03	< 2	4	31	0.22	< 10	< 10	154	< 10
FF SSC 183252	18	26	5	< 0.2	< 0.5	155	641	< 1	1130	4	52	1.73	< 2	< 10	95	< 0.5	< 2	0.71	90	309	5.63	10	< 1	0.24	37	6.91	0.222	0.102	0.03	< 2	4	36	0.23	< 10	< 10	160	< 10
FF SSC 183253	11	15	2	< 0.2	< 0.5	105	607	5	833	5	52	1.67	< 2	< 10	78	< 0.5	< 2	0.84	74	361	5.6	< 10	< 1	0.17	16	5.66	0.308	0.044	0.03	< 2	4	52	0.21	< 10	< 10	146	< 10
FF SSC 183254	< 4	< 5	2	< 0.2	< 0.5	123	280	< 1	148	2	27	1.85	< 2	< 10	35	< 0.5	< 2	1.46	27	66	2.01	< 10	< 1	0.08	12	0.91	0.384	0.185	0.01	< 2	5	95	0.05	< 10	< 10	35	< 10
FF SSC 183255	< 4	< 5	< 2	< 0.2	< 0.5	199	278	4	195	3	43	2.72	< 2	< 10	71	< 0.5	< 2	1.71	31	187	2.34	< 10	< 1	0.14	< 10	1.73	0.548	0.037	0.02	< 2	7	136	0.07	< 10	< 10	45	< 10
FF SSC 183256	< 4	< 5	< 2	< 0.2	< 0.5	186	214	< 1	49	7	44	1.66	4	< 10	419	< 0.5	< 2	0.54	13	80	4.37	< 10	< 1	0.29	100	1.12	0.192	0.066	0.04	< 2	5	27	0.15	< 10	< 10	68	< 10
FF SSC 183257	710	189	37	0.8	< 0.5	999	336	2	1210	10	24	1.86	< 2	< 10	70	< 0.5	< 2	0.51	46	399	7.36	< 10	< 1	0.11	< 10	4.6	0.225	0.03	0.13	< 2	3	33	0.1	< 10	< 10	84	< 10
FF RGB 191101	< 4	< 5	< 2	< 0.2	< 0.5	25	262	2	445	< 2	15	1.86	< 2	< 10	87	< 0.5	< 2	0.79	40	430	2.94	< 10	< 1	0.27	< 10	4.45	0.332	0.012	0.02	< 2	2	49	0.04	< 10	< 10	31	< 10
FF RGB 191102	5	< 5	< 2	< 0.2	< 0.5	34	374	< 1	469	< 2	25	1.24	< 2	< 10	47	< 0.5	< 2	0.93	39	186	2.87	< 10	< 1	0.18	< 10	3.85	0.353	0.018	0.02	< 2	2	56	0.06	< 10	< 10	38	< 10
FF RGB 191103	< 4	< 5	4	< 0.2	< 0.5	181	235	11	127	3	42	4.72	< 2	< 10	31	0.6	< 2	4.51	42	298	3.72	10	< 1	0.05	< 10	0.35	0.948	0.035	1.31	< 2	5	119	0.15	< 10	< 10	73	< 10
FF RGB 191104	< 4	< 5	< 2	< 0.2	< 0.5	31	307	< 1	357	< 2	20	0.92	< 2	< 10	57	< 0.5	< 2	0.76	30	217	2.4	< 10	< 1	0.15	< 10	3.24	0.285	0.017	0.02	< 2	2	44	0.06	< 10	< 10	36	< 10
FF RGB 191105	6	< 5	< 2	< 0.2	< 0.5	34	348	3	408	< 2	23	1.77	< 2	< 10	58	< 0.5	< 2	1.38	35	262	2.7	< 10	< 1	0.2	< 10	3.5	0.512	0.016	0.03	< 2	3	83	0.06	< 10	< 10	37	< 10
FF RGB 191106	5	5	< 2	< 0.2	< 0.5	38	373	< 1	423	< 2	23	1.65	< 2	< 10	86	< 0.5	< 2	1.29	38	251	3.06	< 10	< 1	0.27	< 10	3.66	0.467	0.019	0.03	< 2	3	73	0.08	< 10	< 10	48	< 10
FF RGB 191107	12	8	< 2	< 0.2	< 0.5	28	325	3	427	< 2	22	1.67	< 2	< 10	49	< 0.5	< 2	1.28	35	245	2.55	< 10	< 1	0.15	< 10	3.56	0.507	0.014	0.02	< 2	2	83	0.05	< 10	< 10	30	< 10
FF RGB 191108	9	7	< 2	< 0.2	< 0.5	36	386	< 1	419	< 2	25	1.17	< 2	< 10	50	< 0.5	< 2	1.01	38	192	3.13	< 10	< 1	0.13	< 10	3.69	0.364	0.016	0.03	< 2	3	58	0.06	< 10	< 10	45	< 10
FF RGB 191109	< 4	< 5	< 2	< 0.2	< 0.5	37	316	3	312	< 2	21	1.72	< 2	< 10	56	< 0.5	< 2	1.37	29	317	2.49	< 10	< 1	0.23	< 10	2.8	0.493	0.025	0.03	< 2	3	84	0.09	< 10	< 10	60	< 10
FF RGB 191110	< 4	< 5	< 2	< 0.2	< 0.5	23	344	< 1	484	< 2	21	0.67	< 2	< 10	51	< 0.5	< 2	0.57	37	181	2.61	< 10	< 1	0.11	< 10	4.32	0.212	0.013	0.02	< 2	2	30	0.05	< 10	< 10	31	< 10
FF RGB 191111	6	6	< 2	< 0.2	< 0.5	41	368	2	341	< 2	25	1.79	< 2	< 10	56	< 0.5	< 2	1.55	33	311	2.84	< 10	< 1	0.19	< 10	3.25	0.535	0.019	0.03	< 2	4	82	0.07	< 10	< 10	51	< 10
FF RGB 191112	< 4	< 5	< 2	< 0.2	< 0.5	33	395	< 1	495	< 2	27	1.43	< 2	< 10	71	< 0.5	< 2	1.16	41	259	3.04	< 10	< 1	0.19	< 10	4.44	0.429	0.015	0.02	< 2	3	66	0.06	< 10	< 10	35	< 10
FF RGB 191113	< 4	< 5	< 2	< 0.2	< 0.5	31	374	2	493	< 2	24	1.37	< 2	< 10	64	< 0.5	< 2	1.05	40	259	2.98	< 10	< 1	0.22	< 10	4.37	0.402	0.016	0.02	< 2	3	63	0.05	< 10	< 10	35	< 10
FF RGB 191114	7	< 5	< 2	< 0.2	< 0.5	29	403	< 1	761	< 2	23	0.39	< 2	< 10	30	< 0.5	< 2	0.34	48	165	2.81	< 10	< 1	0.07	< 10	6.98	0.121	0.008	0.03	< 2	2	18	0.02	< 10	< 10	15	< 10
FF RGB 191115	6	< 5	10	< 0.2	< 0.5	511	444	< 1	108	< 2	56	1.55	< 2	< 10	40	< 0.5	< 2	1.57	44	255	6.02	< 10	< 1	0.25	< 10	1.02	0.481	0.022	0.93	< 2	20	31	0.24	< 10	< 10	239	< 10
FF RGB 191116	< 4	< 5	< 2	< 0.2	< 0.5	126	553	2	259	< 2	42	0.47	< 2	< 10	49	< 0.5	< 2	0.86	45	212	4.9	< 10	< 1	0.31	< 10	2.87	0.136	0.036	0.04	< 2	4	25	0.2	< 10	< 10	115	< 10
FF RGB 191117	< 4	< 5	< 2	< 0.2	< 0.5	132	477	< 1	256	< 2	42	0.61	< 2	< 10	110	< 0.5	< 2	0.99	44	174	4.85	< 10	< 1	0.45	< 10	2.91	0.145	0.041	0.07	< 2	4	27	0.23	< 10	< 10	128	< 10
FF RGB 191118	4	< 5	6	< 0.2	< 0.5	130	274	3	55	< 2	27	1.09	< 2	< 10	27	< 0.5	< 2	1.06	18	181	2.98	< 10	< 1	0.1	< 10	0.57	0.411	0.038	0.24	< 2	11	14	0.26	< 10	< 10	150	< 10
FF RGB 191119	< 4	< 5	< 2	< 0.2	< 0.5	115	556	< 1	291	< 2	40	0.48	< 2	< 10	64	< 0.5	< 2	0.85	46	183	4.59	< 10	< 1	0.35	< 10	3.22	0.111	0.033	0.06	< 2	3	24	0.2	< 10	< 10	108	< 10
FF RGB 191120	4	< 5	< 2	< 0.2	< 0.5	60	394	3	325	< 2	28	1.47	< 2	< 10	63	< 0.5	< 2	1.29	36	234	3.24	< 10	< 1	0.25	< 10	2.93	0.421	0.025	0.04	< 2	3	72	0.11	< 10	< 10	66	< 10
FF RGB 191121	9	5	< 2	< 0.2	< 0.5	14	583	< 1	1100	< 2	28	0.28	< 2	< 10	28	< 0.5	< 2	0.23	70	161	3.91	< 10	< 1	0.06	< 10	11.2	0.075	0.007	0.02	< 2	2	12	0.02	< 10	< 10	9	< 10
FF RGB 191122	< 4	5	< 2	< 0.2	< 0.5	39	655	1	583	< 2	17	0.59	< 2	< 10	63	< 0.5	< 2	1.11	51	308	3.96	< 10	< 1	0.22	< 10	6.69	0.126	0.019	0.03	< 2	5	22	0.05	< 10	< 10	45	< 10
FF RGB 193001	< 4	< 5	< 2	< 0.2	< 0.5	34	240	< 1	35	< 2	33	1.17	< 2	< 10	154	< 0.5	< 2	0.92	15	31	2.7	< 10	< 1	0.22	< 10	0.73	0.415	0.049	0.04	< 2	6	73	0.15	< 10	< 10	96	< 10
FF RGB 193002	< 4	< 5	< 2	< 0.2	< 0.5	39	234	3	31	< 2	29	1.26	< 2	< 10	99	< 0.5	< 2	1.05	13	110	2.96	< 10	< 1	0.17	< 10	0.7	0.433	0.061	0.02	< 2	6	76	0.16	< 10	< 10	111	< 10
FF RGB 193003	< 4	6	< 2	< 0.2	< 0.5	33	542	< 1	790	< 2	33	0.94	< 2	< 10	80	< 0.5	< 2	0.69	57	184	3.89	< 10	< 1	0.19	< 10	7.24	0.269	0.018	0.04	< 2	3	42	0.07	< 10	< 10	37	< 10
FF RGB 193004	8	7	< 2	< 0.2	< 0.5	4	186	2	26	4	20	2.21	< 2	< 10	22	0.8	< 2	3.11	6	72	0.55	< 10	< 1	0.02	< 10	0.29	0.389	0.003	0.06	< 2	4	45	0.17	< 10	< 10	22	< 10
FF RGB 193005	< 4	< 5	< 2	< 0.2	< 0.5	38	340	< 1	379	< 2	23	1	< 2	< 10	55	< 0.5	< 2	0.73	34	133	2.65	< 10	< 1	0.2	< 10	3.08	0.269	0.02	0.03	< 2	2	43	0.07	< 10	< 10	45	< 10
FF RGB 193007	< 4	< 5	< 2	< 0.2	< 0.5	21	378	2	580	< 2	22	0.7	< 2	< 10	44	< 0.5	< 2	0.58	41	262	2.61	< 10	< 1	0.1	< 10	5.33	0.214	0.011	0.02	< 2	2	32	0.04	< 10	< 10	23	< 10
FF RGB 193008	9	6	3	< 0.2	< 0.5	271	202	< 1	95	< 2	19	1.71	< 2	< 10	36	< 0.5	< 2	1.57	28	142	3.27	< 10	< 1	0.09	< 10	0.56	0.524	0.02	0.29	< 2	9	30	0.12	< 10	< 10	141	< 10
FF RGB 193009	4	5	< 2	< 0.2	< 0.5	47	337	3	308	< 2	24	1.79	< 2	< 10	78	< 0.5	< 2	1.49	32	280	2.93	< 10	< 1	0.24	< 10	2.67	0.533	0.025	0.03	< 2	4	80	0.1	< 10	< 10	69	< 10
FF RGB 193010	< 4	< 5	< 2	< 0.2	< 0.5	41	316	< 1	394	< 2	19	1.27	< 2	< 10	121	< 0.5	< 2	0.88	37	264	2.92	< 10	< 1	0.35	< 10	3.23	0.31	0.025	0.03	< 2	3	45	0.09	< 10	< 10	57	< 10
FF RGB 193011	< 4	< 5	< 2	< 0.2	< 0.5	32	357	2	435	< 2	24	1	< 2	< 10	66	< 0.5	< 2	0.84	36	245	2.73	< 10	< 1	0.16	< 10	3.85	0.315	0.017	0.02	< 2	2	49	0.07	< 10	< 10	39	< 10
FF RGB 193012	5	< 5	< 2	< 0.2	< 0.5	40	382	2	397	< 2	27	1.4	< 2	< 10	62	< 0.5	< 2	1.13	36	243	2.89	< 10	< 1	0.18	< 10	3.52	0.4	0.017	0.03	< 2	3	66	0.07	< 10	< 10	43	< 10
FF RGB 193013	< 4	< 5	< 2	< 0.2	< 0.5	32	206	< 1	328	< 2	16	2.22	< 2	< 10	112	< 0.5	< 2	1.24	34	469	2.9	< 10	< 1	0.53	< 10	3.31	0.433	0.012	0.02	< 2	4	81	0.07	< 10	< 10	62	< 10
FF RGB 193014	< 4	< 5	< 2	< 0.2	< 0.5	33	376	< 1	381	< 2	26	1.67	< 2	< 10	59	< 0.5	< 2	1.37	35	234	2.78	< 10	< 1	0.18	< 10	3.43	0.491	0.018	0.02	< 2	3	77	0.07	< 10	< 10	46	< 10
FF RGB 193015	< 4	5	< 2	< 0.2	< 0.5	39	491	2	559	< 2	32	1.51	< 2	< 10	68	< 0.5	< 2	1.25	48	322	3.61	< 10	< 1	0.21	< 10	5.04	0.432	0.019	0.03	< 2	4	66	0.08	< 10	< 10	48	< 10
FF RGB 193016	< 4	< 5	< 2	< 0.2	1.6	118	1490	< 1	108	4	145	2.65	< 2	< 10	116	< 0.5	< 2	2.64	26	236	3.33	< 10	< 1	0.13	< 10	0.68	0.691	0.015	0.03	< 2	10	36	0.18	< 10	< 10	159	< 10
FF RGB 193017	< 4	< 5	< 2	< 0.2	< 0.5	47	330	3	230	< 2	24	2.48	< 2	< 10	68	< 0.5	< 2	2.05	27	230	2.79	< 10	< 1	0.2	< 10	2.12	0.724	0.028	0.03	< 2	4	114	0.1	< 10	< 10	73	< 10
FF RGB 193018	< 4	< 5	< 2	< 0.2	< 0.5	46	1040	< 1	1770	< 2	51	0.76	< 2	< 10	11	< 0.5	< 2	0.93	125	995	7.33	< 10	< 1	0.34	< 10	13.4	0.239	0.009	0.1	< 2	6	7	0.09	< 10	< 10	57	< 10
FF RGB 193019	7	6	< 2	< 0.2	< 0.5	95	320	< 1	207	< 2	30	1.01	< 2	< 10	120	< 0.5	< 2	1.23	34	293	3.43	< 10	< 1	0.34	< 10	1.81	0.301	0.031	0.05	< 2	7	27	0.19	< 10	< 10	126	< 10
FF RGB 193020	< 4	< 5	< 2	< 0.2	< 0.5	147	462	2	183	< 2	47	0.77	< 2	< 10	92	< 0.5	< 2	1.15	40	171	4.93	< 10	< 1	0.51	12	2.23	0.191	0.044	0.07	< 2	5	36	0.23	< 10	< 10	144	< 10
FF RGB 193021	< 4	< 5	< 2	< 0.2	< 0.5	147	458	< 1	230	< 2	39	0.67	< 2	< 10	104	< 0.5	< 2	0.98	44	201	4.84	< 10	< 1	0.47	< 10	2.51	0.153	0.039	0.04	< 2	4	25	0.2	< 10	< 10	122	< 10
FF RGB 193022	13	13	3	< 0.2	< 0.5	91	187	2	107	< 2	14	1.19	< 2	< 10	32	< 0.5	< 2	1.27	26	289	3.37	< 10	< 1	0.09	< 10	0.77	0.409	0.015	0.36	< 2	10	18	0.1	< 10	< 10	104	< 10
FF RGB 193023	< 4	< 5	< 2	< 0.2	< 0.5	119	485	< 1	226	< 2	39	0.53	< 2	< 10	47	< 0.5	< 2	0.83	43	168	4.62	< 10	< 1	0.32	< 10	2.51	0.144	0.036	0.05	< 2	4	23	0.19	< 10	< 10	114	< 10
FF RGB 193024	6	6	< 2	< 0.2	< 0.5	26	171	2	203	< 2	13	1.33	< 2	< 10	121	< 0.5	< 2	0.93	19	290	1.65	< 10	< 1	0.42	< 10	2.1	0.323	0.016	0.02	< 2	3	50	0.06	< 10	< 10	38	< 10
FF RGB 193025	4	5	< 2	< 0.2	< 0.5	50	320	< 1	256	< 2	25	2.22	< 2	< 10	70	< 0.5	< 2	1.73	28	129	2.92	< 10	< 1	0.21	< 10	2.07	0.633	0.031	0.03	< 2	3	103	0.1	< 10	< 10	79	< 10
FF RGB 193026	11	15	< 2	< 0.2	< 0.5	2	172	2	197	< 2	9	2.11	< 2	< 10	69	< 0.5	< 2	1.89	14	644	1.46	< 10	< 1	0.15	< 10	2	0.214	0.005	< 0.01	< 2	11	6	0.07	< 10	< 10	68	< 10
FF RGB 193027	< 4	< 5	< 2	< 0.2	< 0.5	120	554	< 1	239	< 2	39	0.46	< 2	< 10	41	< 0.5	< 2	1.06	44	173	4.75	< 10	< 1	0.26	< 10	2.7	0.148	0.036	0.04	< 2	4	29	0.19	< 10	< 10	104	< 10
FF RGB 193028	5	6	< 2	< 0.2	< 0.5	53	342	2	257	< 2	25	1.66	< 2	< 10	63	< 0.5	< 2	1.4	31	172	3.18	< 10	< 1	0.21	10	2.28	0.503	0.028	0.06	< 2	3	78	0.09	< 10	< 10	81	< 10
FF RGB 195001	17	14	6	< 0.2	< 0.5	2050	299	11	143	10	36	1.43	< 2	< 10	< 10	< 0.5	< 2	2.2	32	330	7.36	< 10	< 1	0.02	13	2.44	0.425	0.124	1.2	< 2	33	17	0.19	< 10	< 10	264	< 10
FF RGB 195002	< 4	< 5	4	< 0.2	< 0.5	829	1010	290	149	6	65	3.15	< 2	11	19	< 0.5	< 2	3.49	42	241	8.8	10	< 1	0.06	< 10	0.95	0.636	0.022	0.56	< 2	16	45	0.22	< 10	< 10	208	< 10
FF SSC 195003	< 4	< 5	13	< 0.2	< 0.5	1070	161	1	73	< 2	13	2.48	< 2	< 10	54	< 0.5	< 2	2.2	56	34	5.18	10	< 1	0.1	< 10	0.66	0.635	0.011	0.82	< 2	16	162	0.11	< 10	< 10	115	< 10
FF RTR 195004	< 4	< 5	< 2	< 0.2	< 0.5	52	408	2	72	7	32	2.15	< 2	< 10	108	< 0.5	< 2	1.88	22	125	2.39	< 10	< 1	0.49	< 10	1.95	0.531	0.015	0.06	< 2	8	93	0.07	< 10	< 10	40	< 10
FF RGB 195005	< 4	< 5	2	< 0.2	< 0.5	250	154	< 1	17	< 2	15	1.39	< 2	< 10	55	< 0.5	< 2	1.72	17	39	3.4	< 10	< 1	0.06	11	0.5	0.46	0.138	0.32	< 2	7	85	0.16	< 10	< 10	159	< 10
FF RGB 195006	< 4	< 5	< 2	< 0.2	< 0.5	2	707	3	1470	< 2	17	0.15	< 2	< 10	< 10	< 0.5	< 2	0.34	69	194	3.95	< 10	< 1	< 0.01	< 10	15.2	0.036	0.003	< 0.01	< 2	2	3	< 0.01	< 10	< 10	10	< 10
FF RGC 195007	4	< 5	< 2	< 0.2	< 0.5	12	514	< 1	954	< 2	12	0.5	< 2	< 10	< 10	< 0.5	< 2	0.97	56	473	3.58	< 10	< 1	0.02	< 10	8.38	0.123	0.004	0.03	< 2	5	14	0.03	< 10	< 10	34	< 10
FF SSC 195301	< 4	< 5	< 2	< 0.2	< 0.5	59	1150	1	53	9	61	1.94	3	< 10	214	< 0.5	< 2	2.39	69	123	5.54	10	< 1	0.23	74	1.58	0.35	0.391	0.04	< 2	10	164	0.15	< 10	< 10	160	< 10
FF SSC 195302	16	27	4	< 0.2	< 0.5	150	700	3	999	5	56	1.57	< 2	< 10	124	< 0.5	< 2	0.66	87	334	6.2	10	< 1	0.26	31	6.67	0.194	0.093	0.05	< 2	5	32	0.25	< 10	< 10	180	< 10
FF SSC 195303	5	6	< 2	< 0.2	< 0.5	56	801	< 1	1670	< 2	27	0.4	< 2	< 10	12	< 0.5	< 2	0.24	100	254	4.6	< 10	< 1	0.01	< 10	16.3	0.052	0.011	0.02	< 2	4	3	0.02	< 10	< 10	18	< 10
FF SSC 195304	< 4	< 5	< 2	< 0.2	< 0.5	238	539	2	223	< 2	50	2.67	< 2	< 10	71	< 0.5	< 2	1.35	42	221	3.86	< 10	< 1	0.08	< 10	2.16	0.41	0.047	0.03	< 2	8	116	0.11	< 10	< 10	75	< 10
FF SSC 195305	< 4	< 5	3	< 0.2	< 0.5	113	461	< 1	270	3	41	2.12	< 2	< 10	85	< 0.5	< 2	1.39	37	189	2.75	< 10	< 1	0.09	< 10	1.95	0.393	0.038	0.06	< 2	7	105	0.09	< 10	< 10	60	< 10
FF SSS 195306	4	< 5	20	< 0.2	< 0.5	157	1070	14	121	14	87	2.15	< 2	< 10	96	< 0.5	< 2	1.14	69	476	5.45	< 10	< 1	0.38	19	1.44	0.232	0.069	0.05	< 2	11	54	0.19	< 10	< 10	211	< 10

Report: G08-0002

QC Results
Activation Laboratories

Element:	Pd	Pt	Au	Ag	Cd	Cu	Mn	Mo	Ni	Pb	Zn	Al	As	B	Ba	Be	Bi	Ca	Co	Cr	Fe	Ga	Hg	K	La	Mg	Na	P	S	Sb	Sc	Sr	Ti	Tl	U	V	W
Units:	ppb	ppb	ppb	ppm	ppm	ppm	ppm	ppm	ppm	ppm	ppm	%	ppm	ppm	ppm	ppm	ppm	%	ppm	ppm	%	ppm	ppm	%	ppm	%	%	%	%	ppm	ppm	ppm	%	ppm	ppm	ppm	ppm
Detection Limit:	4	5	2	0.2	0.5	1	5	1	1	2	2	0.01	2	10	10	0.5	2	0.01	1	1	0.01	10	1	0.01	10	0.01	0.001	0.001	0.01	2	1	1	0.01	10	10	1	10
Reference Method:	FA-MS	FA-MS	FA-MS	AR-ICP	AR-ICP	AR-ICP	AR-ICP	AR-ICP	AR-ICP	AR-ICP	AR-ICP	AR-ICP	AR-ICP	AR-ICP	AR-ICP	AR-ICP	AR-ICP	AR-ICP	AR-ICP	AR-ICP	AR-ICP	AR-ICP	AR-ICP	AR-ICP	AR-ICP	AR-ICP	AR-ICP	AR-ICP	AR-ICP	AR-ICP	AR-ICP	AR-ICP	AR-ICP	AR-ICP	AR-ICP	AR-ICP	AR-ICP
Client I.D.																																					
Method Blank	< 4	< 5	< 2																																		
Method Blank	< 4	< 5	< 2																																		
Method Blank	< 4	< 5	< 2																																		
Method Blank	< 4	< 5	< 2																																		
Method Blank	< 4	< 5	< 2																																		
CDN-PGMS-11 Meas	415	126	215																																		
CDN-PGMS-11 Cert	405	107	219																																		
CDN-PGMS-8 Meas	1490	447	838																																		
CDN-PGMS-8 Cert	1500	440	820																																		
CDN-PGMS-11 Meas	420	123	213																																		
CDN-PGMS-11 Cert	405	107	219																																		
CDN-PGMS-8 Meas	1510	457	706																																		
CDN-PGMS-8 Cert	1500	440	820																																		
CDN-PGMS-11 Meas	392	112	250																																		
CDN-PGMS-11 Cert	405	107	219																																		
FF 181755 Rep Orig	8	8	< 2																																		
FF 183255 Rep Orig	< 4	< 5	3																																		
FF 191108 Rep Orig	9	7	< 2																																		
FF 181755 Rep Dup	7	8	< 2																																		
FF 183255 Rep Dup	< 4	< 5	< 2																																		
FF 191108 Rep Dup	9	6	< 2																																		
FF 193001 Rep Orig	< 4	< 5	< 2																																		
FF 193012 Rep Orig	5	< 5	< 2																																		
FF 193022 Rep Orig	13	13	3																																		
FF 193001 Rep Dup	< 4	< 5	< 2																																		
FF 193012 Rep Dup	5	< 5	< 2																																		
FF 193022 Rep Dup	13	12	4																																		
Method Blank				< 0.2	< 0.5	< 1	< 5	< 1	< 1	< 2	< 2	< 0.01	< 2	< 10	< 10	< 0.5	< 2	< 0.01	< 1	< 1	< 0.01	< 10	< 1	< 0.01	< 10	< 0.01	0.012	< 0.001	< 0.01	< 2	< 1	< 1	< 0.01	< 10	< 10	< 1	< 10
Method Blank				< 0.2	< 0.5	< 1	< 5	< 1	2	< 2	< 2	< 0.01	< 2	< 10	< 10	< 0.5	< 2	< 0.01	< 1	< 1	< 0.01	< 10	< 1	< 0.01	< 10	< 0.01	0.011	< 0.001	< 0.01	< 2	< 1	< 1	< 0.01	< 10	< 10	< 1	< 10
GXR-6 Meas				< 0.2	< 0.5	61	991	2	22	95	124	5.64	244	< 10	1010	0.8	< 2	0.15	14	78	5.13	20	< 1	0.96	12	0.37	0.077	0.032	0.01	2	23	34	0.1	< 10	< 10	174	< 10
GXR-6 Cert				1	1	66	1010	2	27	100	118	17.7	330	9.8	1300	1	0.3	0.18	14	96	5.58	40	0.07	1.9	14	0.61	0.1	0.035	0.02	4	28	35		2.2	1.5	186	1.9
GXR-2 Meas				17.7	4.2	77	1020	< 1	16	703	522	2.76	16	21	1240	1	< 2	0.69	9	24	1.8	10	3	0.57	23	0.48	0.167	0.052	0.03	35	5	92	0.08	< 10	< 10	46	< 10
GXR-2 Cert				17	4.1	76	1010	2	21	690	530	16.5	25	42	2240	1.7	0.7	0.93	9	36	1.86	40	3	1.4	26	0.85	0.556	0.1	0.03	49	7	160		1	2.9	52	1.9
GXR-1 Meas				29.2	1.9	1080	781	17	37	679	667	0.28	385	12	341	0.7	1580	0.74	7	5	21.5	< 10	4	0.02	< 10	0.11	0.052	0.038	0.21	77	1	164	< 0.01	< 10	40	73	139
GXR-1 Cert				31	3.3	1110	852	18	41	730	760	3.5	427	15	750	1	1380	0.96	8	10	23.6	10	4	0.05	7.5	0.22	0.052	0.065	0.26	120	2	275		0.39	35	80	164
GXR-4 Meas				3.2	< 0.5	6380	135	331	38	44	70	2.29	105	13	123	1.4	15	0.84	15	57	2.91	10	< 1	1.5	55	1.63	0.139	0.119	1.85	2	7	76	0.11	< 10	< 10	80	13
GXR-4 Cert				4	0.9	6520	155	310	42	52	73	7.2	98	4.5	1640	1.9	19	1	15	64	3.09	20	0.1	4.01	65	1.66	0.564	0.12	1.77	5	8	220		3.2	6.2	87	31
FF 183002 Rep Orig				< 0.2	< 0.5	179	629	< 1	42	3	55	2.41	< 2	< 10	160	< 0.5	< 2	2.42	30	42	5.66	10	< 1	0.29	11	1.34	0.474	0.058	0.06	< 2	13	66	0.27	< 10	< 10	240	< 10
FF 183002 Rep Dup				< 0.2	< 0.5	177	616	< 1	42	4	55	2.43	< 2	< 10	161	< 0.5	< 2	2.38	29	42	5.52	10	< 1	0.29	10	1.33	0.472	0.058	0.06	< 2	13	67	0.26	< 10	< 10	238	< 10
FF 191105 Rep Orig				< 0.2	< 0.5	34	347	3	407	< 2	23	1.76	< 2	< 10	58	< 0.5	< 2	1.37	35	257	2.67	< 10	< 1	0.2	< 10	3.5	0.504	0.016	0.03	< 2	2	82	0.06	< 10	< 10	37	< 10
FF 191105 Rep Dup				< 0.2	< 0.5	35	350	3	408	< 2	23	1.79	< 2	< 10	59	< 0.5	< 2	1.4	35	268	2.72	< 10	< 1	0.2	< 10	3.5	0.521	0.016	0.03	< 2	3	83	0.06	< 10	< 10	37	< 10
FF 191118 Rep Orig				< 0.2	< 0.5	131	278	3	55	< 2	27	1.12	< 2	< 10	27	< 0.5	< 2	1.09	18	181	3	< 10	< 1	0.1	< 10	0.58	0.426	0.038	0.24	< 2	11	14	0.27	< 10	< 10	151	< 10
FF 191118 Rep Dup				< 0.2	< 0.5	129	270	3	55	< 2	27	1.06	< 2	< 10	26	< 0.5	< 2	1.03	18	180	2.95	< 10	< 1	0.1	< 10	0.55	0.395	0.038	0.24	< 2	11	13	0.26	< 10	< 10	150	< 10
FF 193011 Rep Orig				< 0.2	< 0.5	30	340	2	411	< 2	23	0.96	< 2	< 10	62	< 0.5	< 2	0.79	34	229	2.59	< 10	< 1	0.15	< 10	3.64	0.295	0.016	0.02	< 2	2	45	0.06	< 10	< 10	37	< 10
FF 193011 Rep Dup				< 0.2	< 0.5	33	375	2	458	< 2	25	1.11	< 2	< 10	70	< 0.5	< 2	0.9	38	261	2.86	< 10	< 1	0.17	< 10	4.06	0.334	0.018	0.03	< 2	3	52	0.07	< 10	< 10	41	< 10
FF 193024 Rep Orig				< 0.2	< 0.5	26	171	2	203	< 2	13	1.32	< 2	< 10	121	< 0.5	< 2	0.93	19	289	1.65	< 10	< 1	0.42	< 10	2.1	0.322	0.016	0.02	< 2	3	50	0.06	< 10	< 10	38	< 10
FF 193024 Rep Dup				< 0.2	< 0.5	26	171	2	203	< 2	13	1.34	< 2	< 10	122	< 0.5	< 2	0.93	19	290	1.64	< 10	< 1	0.42	< 10	2.11	0.323	0.016	0.02	< 2	3	50	0.06	< 10	< 10	39	< 10
FF 195303 Rep Orig				< 0.2	< 0.5	54	777	< 1	1630	< 2	26	0.38	< 2	< 10	12	< 0.5	< 2	0.23	98	243	4.41	< 10	< 1	0.01	< 10	16.1	0.049	0.011	0.02	< 2	3	3	0.02	< 10	< 10	17	< 10
FF 195303 Rep Dup				< 0.2	< 0.5	58	825	< 1	1720	< 2	28	0.42	< 2	< 10	12	< 0.5	< 2	0.25	106	265	4.78	< 10	< 1	0.01	< 10	16.6	0.055	0.012	0.02	< 2	4	3	0.02	< 10	< 10	18	< 10

Report: G08-0081

Final Report
Activation Laboratories

Element:	Pd	Pt	Au
Units:	ppb	ppb	ppb
Detection Limit:	4	5	2
Reference Method:	FA-MS	FA-MS	FA-MS
Client I.D.			
FF RGB 193040	< 4	< 5	< 2
FF RGB 193041	< 4	< 5	< 2
FF RGB 193042	< 4	< 5	< 2
FF RGB 193043	< 4	< 5	< 2
FF RGB 193044	< 4	< 5	< 2
FF RGB 193045	< 4	< 5	< 2
FF RGB 193046	< 4	< 5	< 2
FF RGB 193047	< 4	< 5	< 2
FF RGB 193048	< 4	< 5	< 2
FF RGB 193049	< 4	< 5	< 2
FF RGB 193050	< 4	< 5	< 2
FF RGB 88218	< 4	< 5	< 2
FF RGB 88219	< 4	6	< 2
FF RGB 88220	< 4	6	< 2
FF RGB 88221	6	17	< 2
FF RGB 88222	< 4	< 5	< 2
FF RGB 88223	< 4	< 5	< 2
FF RGB 88224	< 4	7	< 2
FF RGB 88225	< 4	< 5	< 2
FF RGB 88226	< 4	< 5	< 2

Report: G08-0081

QC Results
Activation Laboratories

Element:	Pd	Pt	Au
Units:	ppb	ppb	ppb
Detection Limit:	4	5	2
Reference Method:	FA-MS	FA-MS	FA-MS
Client I.D.			
Method Blank	< 4	< 5	< 2
Method Blank	< 4	< 5	< 2
Method Blank	< 4	< 5	< 2
Method Blank	< 4	< 5	< 2
Method Blank	< 4	< 5	< 2
Method Blank	< 4	< 5	< 2
Method Blank	< 4	< 5	< 2
Method Blank	< 4	< 5	< 2
Method Blank	< 4	< 5	< 2
Method Blank	< 4	< 5	< 2
Method Blank	< 4	< 5	< 2
Method Blank	< 4	< 5	< 2
Method Blank	< 4	< 5	< 2
Method Blank	< 4	< 5	< 2
Method Blank	< 4	< 5	< 2
Method Blank	< 4	< 5	< 2
CDN-PGMS-9 Meas	2760	736	1210
CDN-PGMS-9 Cert	2600	710	1040
CDN-GS-P3 Meas	< 4	< 5	335
CDN-GS-P3 Cert			300
CDN-PGMS-9 Meas	2710	715	1040
CDN-PGMS-9 Cert	2600	710	1040
CDN-GS-P3 Meas	< 4	< 5	325
CDN-GS-P3 Cert			300
CDN-PGMS-9 Meas	2720	760	1140
CDN-PGMS-9 Cert	2600	710	1040
CDN-GS-P3 Meas	< 4	< 5	308
CDN-GS-P3 Cert			300
CDN-PGMS-9 Meas	2680	686	1030
CDN-PGMS-9 Cert	2600	710	1040
CDN-GS-P3 Meas	< 4	< 5	311
CDN-GS-P3 Cert			300
CDN-PGMS-9 Meas	2610	725	1070
CDN-PGMS-9 Cert	2600	710	1040
CDN-GS-P3 Meas	< 4	< 5	343
CDN-GS-P3 Cert			300
CDN-PGMS-9 Meas	2620	727	1120
CDN-PGMS-9 Cert	2600	710	1040
CDN-GS-P3 Meas	< 4	< 5	368
CDN-GS-P3 Cert			300
CDN-PGMS-9 Meas	2590	740	1080
CDN-PGMS-9 Cert	2600	710	1040
CDN-GS-P3 Meas	< 4	< 5	309
CDN-GS-P3 Cert			300
CDN-PGMS-9 Meas	2730	751	1080
CDN-PGMS-9 Cert	2600	710	1040
CDN-GS-P3 Meas	< 4	< 5	312
CDN-GS-P3 Cert			300
FF RGB 193049 Rep Orig	< 4	< 5	< 2
FF RGB 88226 Rep Orig	< 4	< 5	< 2
FF RGB 193049 Rep Dup	< 4	< 5	< 2
FF RGB 88226 Rep Dup	< 4	< 5	< 2

Appendix 3

Geochemical analyses performed at Cardiff University.

Cardiff University analyses

Lithology	→	DOL dyke	BN dyke	DUN	PDT	PDT	AMPH	DUN	PDT	NOR	NOR	NOR	NOR	
Area	→	F'vand N	F'vand N	F'vand W	F'vand W	F'vand W	Miaggoq	Miaggoq	Miaggoq	Miaggoq	Miaggoq	Miaggoq	Miaggoq	
Sample ID	→	**191119**	**191106**	**101005**	**101006**	**101010**	**101421**	**193050**	**088225**	**088223**	**088224**	**101422**	**193047**	
SiO2	wt%	50.45	50.07	39.51	44.05	51.59	48.57	42.71	41.72	50.35	51.07	49.28	48.08	**SiO2**
TiO2	wt%	0.83	0.30	0.03	0.04	0.06	0.81	0.08	0.03	0.57	0.10	0.51	1.31	**TiO2**
Al2O3	wt%	7.40	8.98	1.99	2.29	4.34	15.33	4.17	2.54	16.41	10.07	16.74	13.38	**Al2O3**
Fe2O3	wt%	12.48	9.70	12.58	11.17	9.50	14.54	13.72	9.19	10.54	10.56	6.27	12.39	**Fe2O3**
MnO	wt%	0.18	0.14	0.14	0.11	0.17	0.20	0.20	0.12	0.19	0.16	0.17	0.26	**MnO**
MgO	wt%	15.26	21.44	45.07	40.21	30.97	6.23	33.52	45.04	11.41	23.87	14.98	15.80	**MgO**
CaO	wt%	10.64	5.85	0.61	1.13	3.02	8.63	1.50	0.92	7.67	3.94	9.85	4.88	**CaO**
Na2O	wt%	2.19	1.65	0.07	0.12	0.42	3.34	0.14	0.09	1.69	0.39	1.77	2.04	**Na2O**
K2O	wt%	0.67	0.41	0.01	0.02	0.13	0.24	0.02	0.05	0.09	0.18	0.31	0.21	**K2O**
P2O5	wt%	0.09	0.05	0.01	0.01	0.01	0.07	0.00	0.01	0.01	0.00	0.00	0.00	**P2O5**
LOI	wt%	0.36	0.57	0.26	0.16	0.28	0.44	3.85	-0.01	-0.01	0.04	0.70	0.77	**LOI**
Total	wt%	100.56	99.16	100.28	99.31	100.48	98.41	99.91	99.71	98.92	100.39	100.58	99.13	**Total**
Sc	ppm	30.0	22.6	9.2	14.0	34.1	48.6	15.7	10.6	44.5	30.4	39.8	54.8	**Sc**
V	ppm	207.5	109.2	60.2	64.0	90.7	284.5	83.2	64.5	146.7	113.9	34.2	39.8	**V**
Cr	ppm	1755.0	2575.9	7328.9	7625.9	3755.4	444.9	3774.0	10818.8	575.3	1573.1	323.8	672.1	**Cr**
Co	ppm	65.3	61.1	113.0	88.2	63.4	63.7	81.7	90.3	36.3	54.0	33.7	42.4	**Co**
Ni	ppm	342.1	572.5	947.5	699.9	248.2	142.7	830.1	1545.0	723.2	281.0	213.4	150.2	**Ni**
Cu	ppm	83.4	55.0	54.2	47.5	44.8	86.0	57.0	40.1	45.1	45.9	35.8	54.7	**Cu**
Zn	ppm	86.3	79.9	79.5	111.9	66.1	102.0	100.1	86.2	69.4	61.9	70.0	81.4	**Zn**
Ga	ppm	11.4	10.2	3.2	4.3	4.7	16.3	5.1	3.5	14.8	8.8	8.9	8.3	**Ga**
Rb	ppm	18.3	11.5	0.3	0.4	4.2	0.8	0.6	2.0	0.9	7.8	11.9	10.4	**Rb**
Sr	ppm	294.9	162.5	1.1	2.2	22.8	74.0	1.3	1.2	81.6	30.4	90.1	45.0	**Sr**
Y	ppm	13.3	7.3	2.3	2.9	4.1	18.0	2.1	1.5	12.5	2.2	5.3	1.7	**Y**
Zr	ppm	83.6	44.0	8.1	4.8	10.7	36.6	8.0	6.7	54.8	11.8	41.5	38.0	**Zr**
Nb	ppm	4.35	1.57	0.27	0.29	0.41	1.66	0.39	0.27	1.91	0.29	0.67	0.77	**Nb**
Mo	ppm	0.16	0.17	1.71	1.23	1.23	0.85	0.31	0.32	0.18	0.14	0.92	0.03	**Mo**
Sn	ppm	7.23	11.89	8.31	5.96	18.89	7.20	11.16	6.53	6.00	5.34	6.68	10.03	**Sn**
Cs	ppm	0.39	0.29	0.03	0.03	0.06	0.03	0.06	0.06	0.03	0.07	0.22	0.26	**Cs**
Ba	ppm	229.5	180.7	8.0	7.6	82.2	67.9	5.7	8.4	122.2	35.7	57.2	42.8	**Ba**
La	ppm	10.44	7.24	0.48	1.04	2.00	2.99	0.40	0.13	1.60	0.50	1.87	1.36	**La**
Ce	ppm	23.67	14.69	1.14	2.25	3.97	5.98	0.76	0.41	3.15	0.88	4.61	1.84	**Ce**
Pr	ppm	3.26	1.82	0.15	0.28	0.45	0.84	0.09	0.06	0.45	0.10	0.75	0.19	**Pr**
Nd	ppm	13.22	6.70	0.53	0.97	1.44	4.05	0.37	0.27	2.11	0.34	3.15	0.62	**Nd**
Sm	ppm	2.98	1.35	0.12	0.18	0.27	1.61	0.11	0.11	0.71	0.10	0.79	0.13	**Sm**
Eu	ppm	0.91	0.43	0.03	0.05	0.15	0.46	0.06	0.04	0.35	0.10	0.26	0.29	**Eu**
Gd	ppm	2.72	1.26	0.08	0.14	0.25	2.14	0.12	0.11	0.97	0.11	0.80	0.13	**Gd**
Tb	ppm	0.39	0.19	0.02	0.03	0.05	0.39	0.03	0.02	0.20	0.03	0.13	0.03	**Tb**
Dy	ppm	2.28	1.20	0.20	0.33	0.46	2.73	0.24	0.24	1.57	0.28	0.86	0.24	**Dy**
Ho	ppm	0.39	0.23	0.05	0.08	0.11	0.54	0.06	0.05	0.35	0.07	0.17	0.06	**Ho**
Er	ppm	1.08	0.69	0.20	0.35	0.41	1.67	0.24	0.17	1.24	0.27	0.54	0.24	**Er**
Tm	ppm	0.17	0.11	0.04	0.08	0.08	0.28	0.05	0.03	0.23	0.06	0.10	0.05	**Tm**
Yb	ppm	1.00	0.73	0.31	0.55	0.63	1.82	0.42	0.21	1.66	0.43	0.68	0.45	**Yb**
Lu	ppm	0.15	0.12	0.05	0.10	0.11	0.30	0.08	0.04	0.29	0.08	0.12	0.08	**Lu**
Hf	ppm	1.82	1.02	0.14	0.05	0.12	1.01	0.20	0.06	1.44	0.26	1.10	1.19	**Hf**
Ta	ppm	0.25	0.08	0.02	0.02	0.02	0.09	0.03	0.02	0.12	0.02	0.07	0.05	**Ta**
Th	ppm	1.24	0.94	0.08	0.17	0.61	0.09	0.09	0.06	0.15	0.04	0.43	0.02	**Th**
U	ppm	0.13	0.04	0.02	0.03	0.05	0.03	0.03	0.05	0.06	0.00	0.17	0.03	**U**

Normalised after Sun & McDonough (1989)

	191119	**191106**	**101005**	**101006**	**101010**	**101421**	**193050**	**088225**	**088223**	**088224**	**101422**	**193047**	
Ba	34.77	27.38	1.22	1.15	12.46	10.30	0.87	1.28	18.52	5.41	8.66	6.48	**Ba**
Rb	30.44	19.10	0.54	0.64	6.94	1.35	1.01	3.38	1.47	13.03	19.79	17.40	**Rb**
Th	15.63	11.76	1.07	2.09	7.64	1.13	1.12	0.80	1.89	0.55	5.38	0.20	**Th**
K	23.00	14.19	0.51	0.81	4.62	8.37	0.57	1.81	3.03	6.38	10.57	7.27	**K**
Nb	6.61	2.39	0.42	0.45	0.62	2.53	0.59	0.41	2.91	0.44	1.01	1.17	**Nb**
Ta	6.72	2.27	0.42	0.42	0.65	2.40	0.84	0.43	3.20	0.43	1.78	1.41	**Ta**
La	16.11	11.17	0.75	1.61	3.09	4.61	0.61	0.20	2.47	0.78	2.88	2.10	**La**
Ce	14.13	8.77	0.68	1.34	2.37	3.57	0.45	0.25	1.88	0.53	2.75	1.10	**Ce**
Sr	14.82	8.17	0.05	0.11	1.15	3.72	0.06	0.06	4.10	1.53	4.53	2.26	**Sr**
Nd	10.57	5.36	0.42	0.77	1.16	3.24	0.29	0.22	1.69	0.27	2.52	0.50	**Nd**
P	4.57	2.42	0.25	0.25	0.25	3.16	0.10	0.37	0.48	0.24	0.19	-0.05	**P**
Sm	7.33	3.32	0.30	0.44	0.66	3.97	0.27	0.27	1.75	0.26	1.96	0.32	**Sm**
Zr	7.96	4.19	0.77	0.45	1.02	3.48	0.76	0.64	5.22	1.12	3.95	3.62	**Zr**
Hf	6.45	3.60	0.51	0.16	0.42	3.56	0.70	0.20	5.09	0.91	3.89	4.19	**Hf**
Ti	4.12	1.48	0.12	0.22	0.31	4.01	0.42	0.17	2.83	0.49	2.55	6.51	**Ti**
Tb	3.98	1.90	0.18	0.32	0.52	3.98	0.28	0.25	1.99	0.27	1.31	0.27	**Tb**
Y	3.09	1.71	0.54	0.68	0.94	4.19	0.48	0.36	2.90	0.51	1.24	0.41	**Y**
Tm	2.43	1.63	0.60	1.11	1.22	4.06	0.77	0.45	3.41	0.82	1.42	0.77	**Tm**
Yb	2.27	1.66	0.70	1.24	1.42	4.12	0.96	0.48	3.77	0.98	1.54	1.03	**Yb**

Cardiff University analyses

			La	Ce	Pr	Nd	Sm	Eu	Gd	Tb	Dy	Ho	Er	Tm	Yb	Lu	Eu/Eu*
JB1a	*Standard*		122.07	81.75	59.51	42.58	26.01	20.61	18.42	14.79	12.72	10.27	10.11	10.26	10.14	10.36	0.93
NIM-G	*Standard*		346.98	275.95	170.13	109.94	70.14	4.53	53.50	52.44	53.22	48.60	54.74	61.97	64.29	64.68	0.07
191119	Fiskevandet	DOL dyke	33.67	29.30	26.71	22.03	15.26	12.32	10.50	8.31	7.09	5.43	5.13	5.10	4.79	4.65	0.96
191106	Fiskevandet	BN dyke	23.35	18.19	14.92	11.16	6.91	5.86	4.87	3.97	3.71	3.20	3.28	3.41	3.51	3.63	0.99
101005	Fiskevandet	DUN	1.56	1.41	1.20	0.88	0.62	0.35	0.32	0.38	0.62	0.72	0.95	1.25	1.48	1.58	0.74
101006	Fiskevandet	PDT	3.36	2.78	2.29	1.61	0.91	0.64	0.55	0.67	1.03	1.16	1.67	2.33	2.62	3.09	0.87
101010	Fiskevandet	PDT	6.46	4.92	3.72	2.41	1.37	1.98	0.97	1.08	1.42	1.50	1.95	2.57	2.99	3.40	1.69
101421	Miaggoq	AMPH	9.63	7.39	6.85	6.74	8.27	6.28	8.28	8.32	8.48	7.46	7.97	8.51	8.69	9.44	0.76
193050	Miaggoq	DUN	1.28	0.93	0.76	0.61	0.57	0.77	0.46	0.59	0.76	0.82	1.14	1.62	2.02	2.52	1.50
088225	Miaggoq	PDT	0.43	0.51	0.51	0.46	0.56	0.50	0.42	0.53	0.73	0.71	0.80	0.95	1.00	1.15	1.03
088223	Miaggoq	NOR	5.16	3.90	3.71	3.52	3.64	4.70	3.74	4.16	4.89	4.85	5.91	7.15	7.95	8.98	1.28
088224	Miaggoq	NOR	1.62	1.09	0.83	0.57	0.53	1.32	0.41	0.57	0.87	0.97	1.28	1.72	2.07	2.60	2.82
101422	Miaggoq	NOR	6.03	5.71	6.15	5.26	4.08	3.48	3.08	2.73	2.68	2.33	2.56	2.97	3.24	3.67	0.97
193047	Miaggoq	NOR	4.40	2.28	1.53	1.04	0.67	3.89	0.50	0.57	0.73	0.84	1.14	1.61	2.17	2.59	6.66